

Photosynthetic Free Energy Transduction
Modelling Electrochemical Events

Fotosynthetische vrije energie omzetting
Modelbeschrijvingen van elektrochemische verschijnselen



BIBLIOTHEEK
LANDBOUWUNIVERSITEIT
WAGeningen

Promotor: Dr. W. J. Vredenberg
hoogleraar in de plantenfysiologie,
met bijzondere aandacht voor de fysische aspecten

NN08201,1195

Olaf van Kooten

Photosynthetic Free Energy Transduction

Modelling Electrochemical Events

Proefschrift

ter verkrijging van de graad van
doctor in de landbouwwetenschappen,

op gezag van de rector magnificus,

dr. C. C. Oosterlee,

in het openbaar te verdedigen

op vrijdag 22 januari 1988

des namiddags te vier uur in de aula

van de Landbouwuniversiteit te Wageningen

ISN 266 093

This work was supported by the Netherlands Biophysics Foundation (Stichting voor Biofysica) financed by the Netherlands Organization for the Advancement of Pure Research (Z.W.O.) and by a grant from the Agricultural University Wageningen. It was performed at the Department of Plant Physiological Research, Agricultural University Wageningen, the Netherlands.

Stellingen bij het proefschrift van O. van Kooten

1. De protonen, die betrokken zijn bij de onderdrukking van de reactie II component van het electrochrome P_{515} signaal, volgen een andere route door het ATPase dan de protonen die de energie overdracht verzorgen bij de ATP synthese of hydrolyse.
 Peters et al. (1985) *J. Bioenerg. Biomembr.* 17, 207-216
 Dit proefschrift, hoofdstuk 6
2. De verklaring, die Hope en Matthews geven voor de trage component van het P_{515} signaal, is zowel gebaseerd op een foutieve interpretatie van de Q-cyclus als op het niet korrekt rekening houden met het effect van lokale ladingen.
 Hope, A. B. en Matthews, D. B. (1987) *Aust. J. Plant Physiol.* 14, 29-46
3. De veronderstelling, dat een ijs-achtige („ice-like”) water structuur aan het oppervlak van het membraan aanleiding geeft tot een versneld proton transport, duidt zowel op een gebrek aan inzicht in de structuur van het membraanoppervlak als op een gebrek aan kennis van proton diffusie in ijs.
 Kell, D. B. (1979) *Biochim. Biophys. Acta* 549, 55-99
 Van Kooten, O. (1984) *Trends. Biochem. Sci.* 9, 221-222
4. De uitspraak, dat een hoge concentratie geïmmobiliseerde buffergroepen geen aanleiding kan geven tot een verlaagde lokale pH, is niet gebaseerd op een rigoureuze afleiding van het effect van dit soort buffers op de proton concentraties.
 Westerhoff, H. V. (1983) *Dissertatie Universiteit van Amsterdam*, pp. 257-258
 Dit proefschrift
5. Het verschijnsel, dat bij membraan gebonden energieomzetting, waarbij slechts „enkele” protonen in het spel zijn, de tweede hoofdwet schijnbaar overtreden kan worden, impliceert dat traditionele metingen van potentialen m.b.v. kleurstoffen en/of zwakke zuren tot foutieve resultaten en conclusies leiden.
 Westerhoff, H. V. en Chen, Y. (1985) *Proc. Nat. Acad. Sci. USA* 82, 3222-3226
6. Het feit, dat in de transactie-theorie de ineenstorting van de quantummechanische golf functie niet wordt bewerkstelligd door de waarnemer, zoals in de Koppenhaagse interpretatie, maar juist door de waargenomen objecten zelf, kan met recht beschouwd worden als een Copernicaanse omwenteling.
 Cramer, J. G. (1986) *Rev. Mod. Phys.* 58, 647-687
7. De bepaling van de F_0 -waarde (instantane chlorofyl fluorescentie) na een sterke actinische belichting zonder daarbij gebruik te maken van een ver-rood belichting leidt tot een aanzienlijke overschatting van F_0 .
 Bilger, W. en Schreiber, U. (1986) *Photosynth. Res.* 10, 303-308
8. De toepassing van gemoduleerde chlorofyl fluorescentie, zoals beschreven door Schreiber et al., gecombineerd met model simulaties van het fotosynthese proces, biedt ruime mogelijkheden voor non-invasieve diagnostiek binnen het landbouwkundig en stress fysiologisch onderzoek.
 Schreiber, U., Schliwa, U. en Bilger, W. (1986) *Photosynth. Res.* 10, 51-62

9. Recente metingen, die de complexe interacties aantonen tussen het electronen transport, de CO₂ fixatie en de sucrose synthese, zijn een duidelijke indicatie van het belang van een gedegen kennis van de processen op thylakoid niveau voor het begrip van de plantaardige fotosynthese. .
Stitt, M. (1987) in: Progr. Photosynth. Res. (Biggins J. ed.) Vol. III, pp. 685-692
10. De werkelijkheidszin van de uitspraak „Het gebruik van een microelectrode bij bioenergetisch onderzoek kan vergeleken worden met het injecteren van een kat met een honkbalknuppel”, is gelijk aan die van de uitspraak „Het isoleren van chloroplasten kan vergeleken worden met het wassen van een porseleinen servies in een betonmolen”.
Racker, E. (1976) in: A New Look at Mechanisms in Bioenergetics. p. 62, Academic Press, New York
11. De behoefte aan anti-tactische ballistische raket raketten (ATBM) in Europa wordt niet ingegeven door militaire maar door economische overwegingen, waarbij de in principe verliesgevende kontrakten van de Strategic Defense Initiative Organisation (SDIO) aan Europese bedrijven weer winstgevend gemaakt kunnen worden.
F. A. S. (1987) Public Interest Report Vol. 40 (4), p. 10
A. H. Cordesman (1987) International Defense Review, Vol. 4, p. 414
Van Kooten, O. (1987) Proc. Int. Symp. „Europ. Secur. Non-Off. Defence”, Varna
12. De vraag van politici om eenduidige oplossingen vanuit de wetenschap, zoals nu weer gebeurt in het kader van de verzuringsproblematiek, duidt enerzijds op een negentiende-eeuws vertrouwen in de wetenschap en anderzijds op een gebrek aan politieke daadkracht.
13. Het gemak, waarmee sommige volwassenen hun macht over kinderen uitoefenen, verklaart mede waarom voor veel mensen macht een onweerstaanbare aantrekkingskracht heeft.
14. Het begrip junior in de naam „Junior Pugwash Nederland” zegt iets over de frisheid van de ideeën, die leven bij de vereniging waaruit deze voortgekomen is.
15. Een „zorgzame samenleving” en een zich „terugtrekkende overheid” roepen associaties op aan een tekening van Albert Hahn, waarin deze de taakverdeling tussen kerk en kapitaal verbeeldt. Echter nu is het de overheid in plaats van de pastoor die „ze” dom houdt en de schim van het financieringstekort in plaats van de kapitalist die „ze” arm houdt.

It is the author's wish that no agency should ever derive military benefit from the publication of this dissertation. Authors who cite this work in support of their own are requested to qualify similarly the availability of their results.

vi Photosynthetic Free Energy Transduction

Contents

Preface	ix
Voorwoord	xi
List of abbreviations and symbols	xiii
1. Introduction	1
1.1. Photosynthesis	1
1.1.1. PSII	1
1.1.2. PSI	4
1.1.3. The Cytochrome b/f Complex	5
1.1.4. The Light Harvesting Complex	6
1.1.5. The Proton ATP Synthase (CF_1-CF_0).	7
1.2. History	8
1.3. Outline of the Study	10
2. Materials and Methods	13
2.1. Microelectrode Measurements	13
2.1.1. Measurement Procedure	13
2.1.1.1. Illumination.	13
2.1.1.2. Impalement.	15
2.1.1.3. Registration	15
2.1.2. Cultivation of <i>Peperomia metallica</i>	15
2.2. P_{515} Measurements	16
2.2.1. Cultivation of <i>Spinacea oleracea</i> L.	16
2.2.2. Isolation and Characterization of Chloroplasts	17
2.2.3. Instrumentation	18
2.2.3.1. The Spectrophotometer	18
2.2.3.2. The Flash Lamp	18
2.2.3.3. Electronics	18
2.2.3.4. Process Control and Data Acquisition	18
2.2.3.5. Data Handling and Analysis	19
2.3. Model calculations	19
2.3.1. Free-Energy Transduction	19
2.3.2. A P_{515} Model	19
2.3.3. Proton Diffusion in the Lumen	19
3. Modelling Photosynthetic Free Energy Transduction	21
3.1. Introduction	21
3.2. Basic Assumptions	21
3.2.1. Electron Transport	22
3.2.2. The Backpressure	23
3.2.3. Passive Dissipation of $\Delta\tilde{\mu}_1$	23
3.2.4. Buffering Capacity	23
3.2.5. The ATPase	23
3.2.6. Surface and Donnan Potential	24
3.3. The Model	24
3.3.1. The Light Driven Proton Pumps	25
3.3.1.1. Backpressure	26
3.3.2. The Passive Dissipation of $\Delta\tilde{\mu}_{H^+}$	27

3.3.3. The Buffering Capacity of the Lumen	30
3.3.4. The ATPase Dependent Proton Flux	33
3.4. Conclusions	35
4. Applications of the Model	37
4.1. Introduction	37
4.2. The Donnan Potential	37
4.2.1. Calculating the Donnan Potential	39
4.2.2. The Effect of the Donnan Potential	39
4.3. The Effects of Uncouplers	42
4.3.1. (F)CCCP	42
4.3.2. Ammonia	43
4.3.3. Nigericin	45
4.3.4. A23187	47
4.3.5. Valinomycin	47
4.4. Fluorescence	49
4.4.1. Photochemical Quenching (q_Q)	49
4.4.2. Energy Dependent Quenching (q_E)	51
4.5. Conclusions	53
5. Measuring Changes in the Transmembrane Electric Potential	55
5.1. Introduction	55
5.2. Microelectrode Measurements	55
5.2.1. The "classical" Signal	56
5.2.2. The "new" Signal	57
5.3. P_{515} Measurements	60
5.3.1. Kinetics of the Flash-Induced Response	61
5.3.1.1. Reaction I	62
5.3.1.2. Reaction II	63
5.3.2. The Q-cycle	63
5.3.2.1. Cytochrome b_{563}	65
5.4. Comparing the Microelectrode to the P_{515} Measurements	66
5.5. Conclusions	67
6. The Secondary Slow Rise in the Flash-Induced Electric Potential Change	69
6.1. Introduction	69
6.1.1. The Q- or b-cycle	70
6.1.2. "Localized" Chemiosmosis	70
6.2. The Q-cycle	71
6.2.1. Cytochrome b_{563}	72
6.2.2. The Decay Rates	72
6.2.3. The Theory	72
6.2.4. The Addition of Reductant	74
6.3. A Model for Reaction II	75
6.4. Resistance to Lateral Diffusion	78
6.4.1. Diffusion in a Plane	78
6.4.1.1. Boundary Conditions	79
6.4.1.2. Fick's Second Law	79
6.4.1.3. Mobile Buffers	80
6.4.1.4. Immobile Buffers	80
6.4.2. Retarded Diffusion and the Electric Potential	81
6.4.2.1. Destruction Upon Impalement	82
6.5. Conclusions	83

viii Photosynthetic Free Energy Transduction

7. General Discussion	85
7.1. Introduction	85
7.2. The Electric Potential and the Nature of Coupling	86
7.2.1. Microelectrode Measurements	86
7.2.1.1. The "classical" Response	86
7.2.1.1.1. The Structural Reason	87
7.2.1.1.2. The Catalytic Reason	88
7.2.1.2. The "new" Response	89
7.2.2. P_{515} Measurements	90
7.2.2.1. Reaction I and II	90
7.3. Simulating the Electric Potential	91
7.3.1. Redox State of the Simulated ATPase	91
7.3.2. The Capabilities of the Model	92
7.3.3. The Future of the Model	92
7.4. Conclusions	93
Summary	95
Samenvatting	97
References	101
Curriculum Vitae	111

Preface

Writing a preface to this dissertation gives me the opportunity to express my gratitude to all the people who have freely given me part of their valuable time. It has been a great joy for me to work on this subject. This was not only caused by the intellectual satisfaction of acquiring knowledge, but also by the vast number of people I have met and worked with. I would like to thank all of these people by name, but then I would risk omitting a few by sheer poor memory. Also it would raise the printing cost of the manuscript to unaffordable high levels. But I feel a few of the people who have been of crucial importance to the realization of this thesis must be mentioned here. I shall mention my Dutch colleagues in the next paragraph entitled "Voorwoord", which is the Dutch translation of the word Preface. But two of them I must also mention here since they have stimulated me to the extreme to make all these international contacts. First my promotor Wim Vredenberg who had hired me for the job and who was capable of nudging me in the right direction every time I appeared to ride off on a side-issue. He has always persuaded me to go to international conferences and symposia and helped me to make contact. Somehow he also managed to get the money for these trips. I thank you Wim for stimulating and guiding me through this exciting field of photosynthesis research. Another Dutch colleague who has been crucial for a host of international contacts is Hans Westerhoff. He introduced me to an international summer school in Szeged, Hungary. There I have met many fellow scientists, who have become dear friends of mine. Hans you have been an example for me and you have shown me that it is possible to deliver first class work and retain a broad view on many subjects in science. You have stimulated me to express my ideas on "localized" chemiosmosis in public. Our discussions were lively and always revitalized me.

A few of the persons from abroad which have been very helpful in the coming about of this thesis are: Gyözo Garab, with whom discussions concerning the slow phase of $P_{5,15}$ could be heard all the way down the corridor. Steve Theg, who introduced me to the technique of neutral red measurements. Ulrich Schreiber, who taught me the value of a well built spectrophotometer and who kindly shared his enormous knowledge and enthusiasm with me. Wolfgang Junge, whose commentary to an early version of a manuscript spurred me on to develop my mathematical model to the level it is presented here. Dick Dille, who visualized the concept of localized coupling for me and was a major stimulating force behind the work performed in collaboration with Rob Peters. And many more whom I have met but do not mention here, I want to thank you all for helping me and thereby becoming part of a wonderful experience.

One person I must still mention, although we have never met in person, is Alexander Bulychev. Having performed electrophysiological experiments with chloroplasts myself I cannot help but

x Photosynthetic Free Energy Transduction

admire the work he and his co-workers have published about on so many occasions. Most people do not have any idea what it takes to perform these experiments. Alexander without your work this thesis would not have come about.

Voorwoord

Graag wil ik van deze gelegenheid gebruik maken om al diegenen te bedanken, die mij geholpen hebben bij het tot stand komen van dit proefschrift. In de eerste plaats wil ik mijn promotor, prof. W.J. Vredenberg bedanken. Beste Wim, jou beschrijving van het onderzoek tijdens mijn sollicitatie gesprek op de vakgroep Plantenfysiologisch Onderzoek herinner ik mij nog levendig. Het was niet alleen mijn eerste kennismaking met fotosynthese, het maakte mij ook meteen bijzonder enthousiast voor dit onderzoek. Dat heeft altijd centraal gestaan in jouw begeleiding. Jij wist het pure plezier van het onderzoeken over te brengen. Daarnaast gunde je mij een zeer hoge mate van vrijheid in mijn onderzoek, waarvan ik de waarde pas aan het einde van deze periode echt onderkende. Tevens wist jij op bijna onmerkbaar wijze voorwaarden te scheppen, waardoor mijn onderzoek zich tot de huidige vorm kon ontwikkelen. Ik ben je bijzonder erkentelijk voor de fijne samenwerking en hoop en verwacht dat deze nog een tijd zal voortduren.

De samenwerking met Rob Peters heeft niet alleen geleid tot acht gezamenlijke publikaties maar ook tot een warme vriendschap. Samen met Jan Snel vormden wij een onderzoek trio, dat gezamenlijke experimenten uitvoerden en apparatuur ontwikkelden. Beste Jan en Rob, ik geloof dat onze samenwerking en vriendschap uniek genoemd mag worden. Af en toe denk ik met heimwee terug aan die periode, waarin we ons bijna zorgeloos konden overgeven aan het fotosynthese onderzoek.

Ook de studenten die hun doctoraal onderzoek onder mijn begeleiding wilden uitvoeren ben ik bijzonder dankbaar. Zij droegen in belangrijke mate bij aan het tot stand komen van het onderzoek. Met Ton Gloudemans heb ik het eerste jaar van mijn onderzoek samengewerkt. Samen hebben wij het vak geleerd van Rembrandt Zeegers en Wim Tonk. Het plezier en enthousiasme leidde ook nog tot een gezamenlijke publikatie. Ook de roerige samenwerking met Frans Leermakers leidde tot een publikatie. Naast de bijzonder knappe microelectrode experimenten heb je mij veel geleerd over de structuur van membranen Frans. Ik herinner onze diskussies over de modellen die zich net zo dynamisch ontwikkelden als het membraan zelf. Hierbij zal ik het derde compartiment niet snel vergeten. Het doorzettingsvermogen van Henk Granzier was voor mij een voorbeeld. Hij moest en zou het effect van fytochroom m.b.v. de microelectrode aantonen. Hoewel dit uiteindelijk een onmogelijke opdracht bleek te zijn, heeft hij alles geprobeerd en ontloopte hij zich als een zeer bekwaam electrofysioloog. Fijne herinneringen heb ik over gehouden aan de samenwerking met Hans Harms en Chiel Fernig, ook hun onderzoek heeft bijgedragen aan mijn werk.

Wim Tonk heeft een bijzondere plaats in dit hele onderzoek. Toen ik begon heeft hij mij het prikken met de microelectrode bijgebracht, het meten van P_{515} en een beetje magie van het onderzoek. Alle apparatuur was grotendeels door hem ontworpen

en/of zelf gemaakt. Helaas werd het leven voor jou er niet gemakkelijker op bij mijn komst Wim. Toch heb jij je altijd voor 100% ingezet om mij zo goed mogelijk te kunnen laten werken. Daarvoor ben ik je erg dankbaar. Ook je inzet voor de studenten was van onschatbare waarde, wat door weinigen onderkent werd maar wat in ieder geval af te leiden is aan de hechte vriendschappen, die je er aan overhield. Naast de samenwerking in het onderzoek, heb je mij ook ingewijd in het nuttigen van de Trippel. Ik hoop dat we beiden nog lang kunnen voort zetten.

Van het technisch personeel wil ik vooral Rienk Bouma noemen, die ondanks een zekere tegenwerking toch in staat was om een electronische sluiters sturing te maken die zelfs niet stoorde op een microelectrode met een slecht afgeschermd ingangs impedantie van $10^{11} \Omega$. Voor electronisch ingewijden moet dit duidelijk zijn. Maar ook de heren Van Kreel, Looijen en Van Rinssum ben ik erkentelijk voor hun inzet en het vriendschappelijke contact. Leen Peterse wil ik bedanken voor zijn niet aflatende zorg voor de spinazie kweek. En de verzorging van al het gebruikte planten materiaal. Het tekenwerk van Alex Haasdijk en Paul van Snippenburg, tezamen met het fotografische werk van Siep Massalt is altijd van groot belang geweest bij de vele keren dat ik mijn onderzoek moest presenteren. Zo ook in dit proefschrift, waaraan hun inspanningen een belangrijke bijdrage hebben geleverd. Gert van Eck (van het rekencentrum) heeft mij ingewijd in de fijne kneepjes van het gestructureerd programmeren. Zonder zijn wijze lessen in de praktijk zou ik al lang verdronken zijn in onontwarbare listings. Daarnaast wil ik alle andere medewerkers van het laboratorium voor plantenfysiologisch onderzoek, wiens naam ik niet genoemd heb, ook bedanken voor alle dingen die zij voor mij gedaan hebben. Het feit dat ik ze niet bij naam noem duidt niet op een lagere rangorde van interesse, maar meer op de financiële noodzaak om de kosten van de drukker in de hand te houden.

Er zijn nog een groot aantal mensen, die niet aan de vakgroep verbonden zijn en ook op een bijzondere wijze hebben bijgedragen aan het tot stand komen van dit proefschrift door mij te helpen ontwikkelen als mens en als wetenschapper. Deze mensen zou ik zeker niet allen bij naam kunnen noemen uit puur ruimte gebrek. Mijn buitenlandse kollega's heb ik in het engelstalige voorwoord bedankt. Van mijn Nederlandse kollega's moet ik in ieder geval Hans Westerhoff, Ad Schapendonk, Ruud Kraaijenhof, Jan Greve en Johan Blok noemen. Voor de ruimte en rust, mij geboden om dit proefschrift te schrijven, ben ik Ineke Deckers dankbaar. Voor mijn ontwikkeling als mens, een niet kwantificeerbaar ingrediënt voor het tot stand komen van dit werk, ben ik dank verschuldigd aan mijn ouders en aan Monique. Samen met hun ben ik geworden tot wat ik ben. Hoewel mijn kinderen zich nu met volle overgave hebben gestort op mijn heropvoeding.

List of abbreviations and symbols

A	thylakoid membrane surface area (cm^2)
ADP	adenosine-5'-diphosphate
ATP	adenosine-5'-triphosphate
ATPase	thylakoid membrane H^+ -ATP synthase complex
B_i	concentration of buffer group i ($\text{mol}\cdot\text{cm}^{-3}$)
BSA	Bovine Serum Albumin
$c(r,t)$	time dependent concentration profile in a plane
c	Laplace transform $c(r,t)$
$c_{\text{H}^+}^{\text{in}}$	internal (luminal) proton concentration ($\text{mol}\cdot\text{cm}^{-3}$)
$c_{\text{H}^+}^{\text{out}}$	external (stromal) proton concentration
$c_{\text{K}^+}^{\text{in}}$	internal potassium concentration
$c_{\text{K}^+}^{\text{out}}$	external potassium concentration
$c_{\text{Cl}^-}^{\text{in}}$	internal chloride concentration
$c_{\text{Cl}^-}^{\text{out}}$	external chloride concentration
$c_{\text{Mg}^{2+}}^{\text{in}}$	internal magnesium concentration
$c_{\text{Mg}^{2+}}^{\text{out}}$	external magnesium concentration
CCCP	carbonyl cyanide p-chlorophenylhydrazone
C_{elch}	number of electron transport chains per unit area (cm^{-2})
CF_0	chloroplast ATPase coupling factor 0
CF_1	chloroplast ATPase coupling factor 1
Chl	chlorophyll
Cm	thylakoid membrane electric capacitance ($\text{F}\cdot\text{cm}^{-2}$)
$\text{Cm}_{\text{I I}}$	internal thylakoid membrane electric capacitance
C_p	localized membrane proton capacitance
cyt	cytochrome
cyt b/f	plastoquinone-plastocyanin oxidoreductase complex
DBMB	dibromothymoquinone = 2,5-dibromo-3-methyl-6-isopropyl- p-benzoquinone
DCCD	N,N'-dicyclohexylcarbodiimide
DCMU	3-(3,4-di-chlorophenyl)-1,1-dimethylurea
DMSO	dimethylsulfoxide
DQ	duroquinone
DQH_2	durohydroquinone
DTE	1,4-dithioerythritol
Ea	number of activated ATPases
EDTA	ethylenediaminetetraacetic acid
Em	thylakoid transmembrane (Galvani) potential difference $\phi^{\text{in}} - \phi^{\text{out}}$ (V)
Et	total number of ATPases
$E_1(z)$	Exponential integral (see Abramowitz and Stegun 1972)
F	Faraday constant ($\text{C}\cdot\text{mol}^{-1}$)
FCCP	carbonyl cyanide p-trifluoromethoxyphenylhydrazone
Fd	ferredoxin
Fv	variable chlorophyll fluorescence intensity

xiv Photosynthetic Free Energy Transduction

HEPES	4-(2-hydroxyethyl)-1-piperazineethanesulfonic acid
$I_0(z)$	zero order modified Bessel function
i	as a subscript can imply any ion
$J_{H^+}^{PSI}$	light-induced proton flux density from PSI ($\text{mol}\cdot\text{cm}^{-2}\cdot\text{s}^{-1}$)
$J_{H^+}^{PSII}$	light-induced proton flux density from PSII
$J_{H^+}^b$	basal (leak) membrane proton flux density
$J_{H^+}^{ATP}$	ATPase controlled proton flux density
J_{Cl^-}	chloride flux density
J_{K^+}	potassium flux density
$J_{Mg^{2+}}$	magnesium flux density
k_1	maximum turnover rate of PSI (s^{-1})
k_2	maximum turnover rate of PSII
$K_0(z)$	zero order modified Bessel function
K_E^0	equilibrium constant of the ATPase-proton activation reaction (Gräber et al. 1984)
K_i	dissociation constant of buffer group i
k_f	energy dependent Chl a fluorescence quenching constant
LHC	light harvesting pigment complex
n	maximum number of electrons contained in the redox chain between PSII and PSI
n_{rd}	number of electrons actually present in the redox chain between PSII and PSI
n_{ox}	number of oxidized equivalents present in the redox chain between PSII and PSI
NADP ⁺	oxidized nicotinamide-adenine dinucleotide phosphate
NADPH	reduced nicotinamide-adenine dinucleotide phosphate
OEC	Oxygen Evolving Complex
P_{515}	pigment complex with a maximum electrochromic absorbance change at 518 nm
P_{680}	reaction centre of photosystem II
P_{700}	reaction centre of photosystem I
p	Laplace number
Pc	plastocyanin
P	anorganic phosphate PO_4^{3-}
P_i	permeability coefficient of ion species i
pK_i	negative logarithm of K_i
$p.m.f.$	proton motive force
PQ	plastoquinone
PQH ₂	plastohydroquinone
PSI	photosystem I
PSII	photosystem II
q_E	energy dependent quenching
q_Q	photochemical quenching
r	distance from the origin, i.e. $r^2 = x^2 + y^2$
R	universal gas constant ($\text{J}\cdot\text{mol}^{-1}\cdot\text{K}^{-1}$)
R_m	total membrane ionic resistance ($\Omega\cdot\text{cm}^2$)
R_{1d}	apparent resistance to lateral movement of charges in the membrane
R_p	resistance for dissipation of membrane stabilized protons
T	absolute temperature (K)
V	thylakoid membrane enclosed volume (cm^3)
v/v_{max}	relative rate of ATP synthesis
Z	conversion factor $2.3RT/F$
z_i	valence of ion i

α	coefficient of coupling
β	buffering capacity parameter for the lumen
$\Delta\tilde{\mu}_{H^+}$	electrochemical transmembrane proton potential difference ($J \cdot mol^{-1}$)
$\Delta\tilde{\mu}_{Cl^-}$	electrochemical chloride potential difference
$\Delta\tilde{\mu}_{K^+}$	electrochemical potassium potential difference
$\Delta\tilde{\mu}_{Mg^{2+}}$	electrochemical magnesium potential difference
ΔG_{ATP}	Gibbs free-energy (free-enthalpy) of ATP hydrolysis reaction ($J \cdot mol^{-1}$)
Δp	proton motive force (V) (Mitchell and Moyle 1968)
ΔpH	$pH_{lumen} - pH_{stroma}$
Φ	electric (Galvani) potential (V)
σ	surface charge density ($C \cdot cm^{-2}$)
ρ	volume charge density ($C \cdot cm^{-3}$)

xvi Photosynthetic Free Energy Transduction

*The Mind-ground holds the seeds
Which sprout when falls the all-pervading rain.
The wisdom flower of instantaneous awakening
Cannot fail to bear the Bodhi-fruit.*

Hui Neng

Ter nagedachtenis aan: Mia van Kooten
Erna van den Kolk
en Jacob Gouda

Zij leerden mij dat de zorgvuldigheid
waarmee wij met elkaar omgaan
uiteindelijk het enige van belang is.

1. Introduction

In this chapter we will introduce the concept of free energy transduction in photosynthesis. We will explain that part of photosynthesis on which the research, reported on in this thesis, was performed. It is also intended to describe the history of the experiments and concepts leading to the work presented here.

1.1. Photosynthesis

When a quantum of light passes a pigment in a plant, the time span within which they can interact (i.e. "see" each other) is less than 10^{-15} s. Considering the crude oil and natural gas reserves in our world today it is awesome to realize that a process exists, which is capable of stabilizing the energy present in this very short encounter over a period larger by more than 30 orders of magnitude, i.e. $\approx 3 \cdot 10^{+15}$ s. This process is called photosynthesis and it is the capacity of certain biological organisms to transform the energy of light into the more stable energetic chemical bonds, necessary to sustain life as we know it on this planet. Such a transformation of energy of one form (electromagnetic radiation energy, e.g. sunlight) into another form (chemical bonding energy, e.g. food) is known as energy transduction. The process is performed in a series of steps as depicted in fig. 1.1 for higher plant organisms. The first step being the absorption of light by the photosynthetic pigments chlorophyll a and b and by the carotenoids. In green plants mainly the blue and red part of the visual spectrum are absorbed leaving green to be scattered. Following the absorption of a photon its energy is transferred from one pigment to another until it reaches one of the specialised dimer molecules of chlorophyll a known as the reaction centers P_{680} or P_{700} of the photosystems PSII and PSI respectively (Holzwarth 1987). PSI and PSII are together with cyt b/f, LHC and the ATPase the 5 main protein complexes in the thylakoid serving the membrane bound energy transduction process. The function of these complexes will be briefly surveyed in the following sections.

1.1.1. PSII

In PSII the absorbed photon energy is used to excite an electron of P_{680} situated near the luminal side of the thylakoid

2 Photosynthetic Free Energy Transduction

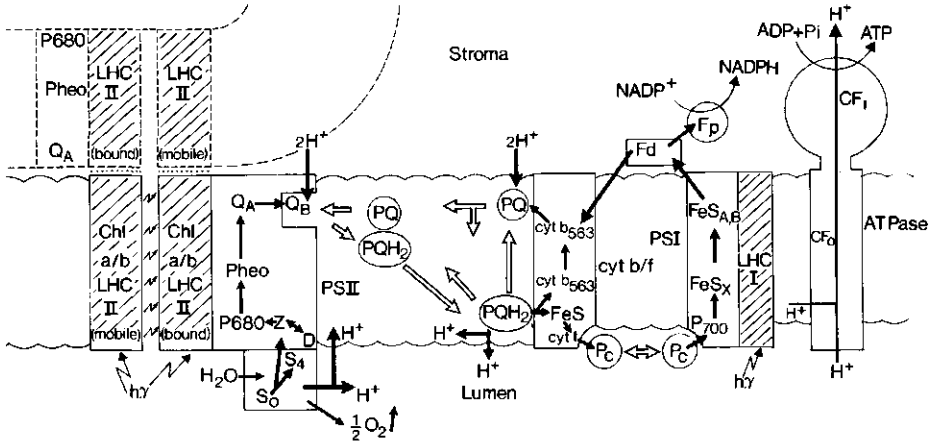


Figure 1.1. Electron transport and photosynthetic free energy transduction in the thylakoid membrane of plant chloroplasts. Light is absorbed by the pigment protein complexes LHC I and LHC II or directly by the antennae pigments of the reaction centers of PSII (P_{680}) or PSI (P_{700}). When the energy of the absorbed photon reaches the reaction centre a charge separation occurs leading to the oxidation of the reaction centre and a reduction of the acceptors of the two photosystems, i.e. Q_A in PSII and reduced ferredoxin (Fd) in PSI. The electron to reduce P_{680} comes from the oxidation of water. Water oxidation is a four step light-induced process $S_0 \Rightarrow S_4$. At the oxidation of two water molecules one oxygen molecule evolves and four protons are released either into the lumen or into a restricted areas of the membrane as proposed by Dilley (1986). The electron of Q_A^- is passed on to a two electron acceptor Q_B , which can take up two protons from the stroma when fully reduced. $Q_B H_2$ exchanges with the hydrogen carrying PQ pool and a hydrogen molecule is transferred from the stroma to the lumen and from the appressed to the non-appressed membrane regions. PQH_2 is oxidized at the cytochrome b/f complex. Protons are thereby released either into the lumen or within the membrane (see paragraph 6.3 of this thesis). One electron is transferred to P_{700} via plastocyanin, cytochrome f and the Rieske-FeS protein. Another electron is thought to reduce cytochrome b_6 and can cause a "secondary" charge separation by reducing PQ on the stroma side together with an electron from Fd. This type of cyclic electron transport is sometimes referred to as the Q-cycle (Hendler et al. 1985). Thus electrons are transferred from water to Fd and to $NADP^+$. In the process protons are transferred from the stroma to the lumen. This leads to an electrochemical proton potential $\Delta\mu_{H^+}$. The ATPase converts the energy of protons into bound energy (ATP).

membrane (see fig. 1.2). This energized electron moves to a pheophytin molecule, which is situated on the same side of the membrane (Van Gorkom 1986). The next acceptor is a quinone molecule known as Q_A situated near the stromal side of the membrane. If it is oxidized it can be reduced by the electron from pheophytin and a transmembrane charge separation has occurred as a result of this electron movement. The reduction of Q_A to a semi-quinone anion is believed to be facilitated by the presence of an iron atom Fe embedded in the protein complex near this quinone.

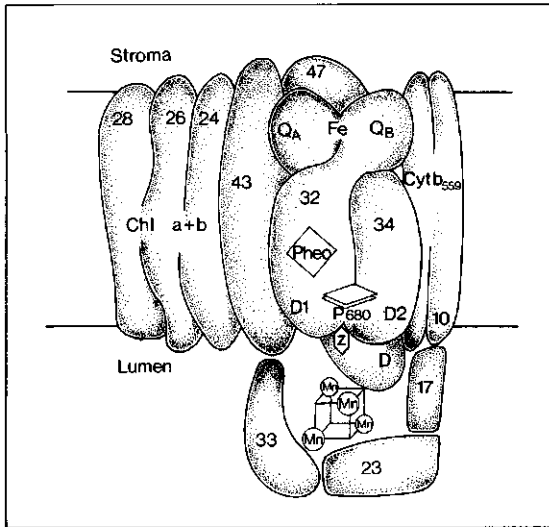


Figure 1.2. Photosystem 2 (PSII) together with the light harvesting complex (LHC II) proteins and the manganese containing oxygen evolving complex (OEC) depicted as one large complex in the thylakoid membrane. The D1-D2 proteins form a minimal configuration in which a charge separation can still occur. They contain the Chl *a* dimer known as P_{680} . One of the transitions of the primary acceptor (a pheophytin molecule) is perpendicular to the plane of the membrane. The D1-D2 complex also contains the two quinone acceptors Q_A and Q_B and a liganded iron atom, which probably mediates the electron transfer from the one electron acceptor Q_A to the two electron acceptor Q_B . Cytochrome b_{559} is thought to play a part in cyclic electron flow around PSII. The 47 kDa protein contains the primary (Z) and the secondary (D) donor for P_{680} . Together with the 43 kDa protein it is believed to bind the OEC (33, 23 and 17 kDa) to PSII. The OEC contains two tightly bound and two loosely bound manganese atoms. The LHC II is thought to consist of three different proteins (24, 26 and 28 kDa). One group is tightly bound to PSII, while three groups are believed to be mobile. The mobile units can be phosphorylated and then detach from PSII. The phosphorylated LHC II is thought to associate with LHC I, thereby changing the ratio of absorption between PSI and PSII in favour of PSI.

In the mean time the oxidized P_{680} molecule is reduced again by an electron extracted from a water molecule in the oxygen evolving complex (OEC). This extraction of electrons from water is a four step process resulting in the release of an oxygen molecule O_2 and 4 protons H^+ on the luminal side of the thylakoid membrane. On the stromal side of PSII the reduced semi-quinone anion Q_A^- can transfer its electron to a secondary acceptor Q_B . This acceptor is believed to be a plastoquinone molecule bound to a 32 kDa protein known as the Q_B binding protein or D2 (Mathis 1987). This molecule can be exchanged by oxidized PQ either in its oxidized state Q_B or in its hydrogenated state Q_BH_2 for which it needs to receive two electrons via Q_A and two protons from the stroma. As a consequence of the absorption of 4 photons and their subsequent utilization by PSII an oxygen molecule is evolved,

4 Photosynthetic Free Energy Transduction

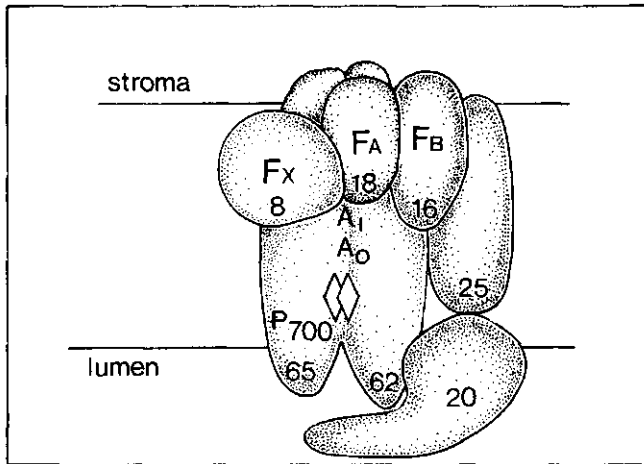


Figure 1.3. A hypothetical model of photosystem I (PSI) based on our present knowledge. The reaction centre complex consists of two large proteins (65 and 62 kDa) in which the primary charge separation between the special Chl *a* dimer P_{700} and the primary chlorophyll type acceptor A_0 takes place. The second acceptor A_1 , a molecule with properties resembling vitamin K, also resides in the reaction centre complex. Three iron sulfur centers, thought to be 4Fe-4S centers and designated as F_x (8 kDa, $E_{m,7} = -730$ mV), F_B (16 kDa, $E_{m,7} = -590$ mV) and F_A (18 kDa, $E_{m,7} = -550$ mV), appear to form a linear transport chain for the electron, which is finally donated to ferredoxin or lost to oxygen (Mehler reaction). The function of the other two proteins (25 and 20 kDa) is unknown as yet. Although it is speculated that the 20 kDa protein plays a role in the positioning of the Cu-protein plastocyanin, to facilitate electron transfer to P_{700} .

4 protons are released on the inside and absorbed on the outside of the thylakoid membrane and 4 electrons are transferred from water to two PQ molecules. The reduction level of the pool of free PQ molecules in the thylakoid membrane has thereby been increased by 2 PQH_2 molecules.

1.1.2. PSI

In PSI the process of energy transduction is similar to the process in PSII. The energy of the absorbed photon is transferred to an electron of P_{700} , which is also believed to be a dimer of chlorophyll *a* (Setif and Mathis 1986). The energized electron is transferred to the primary electron acceptor A_0 , which is presumed to be a chlorophyll *a* molecule (Nuijs et al. 1986). The electron is then transferred to the secondary acceptor presumably a quinone, vitamin K_1 (Interschick-Niebler and Lichtenthaler 1981, Schöder and Lockau 1986, Brettel et al. 1987). The electron is further transported through a chain of iron-sulfur centers F_x , F_A and F_B (Rutherford and Heathcote 1985) to its final acceptor as can be seen in fig. 1.3. The final acceptor of PSI can be O_2 (Mehler reaction) or the water soluble protein Ferredoxin (Fd). Reduced Fd can pass its electron either to the Ferredoxin-NADP⁺ oxidoreductase (FNR), in order to reduce NADP⁺ to NADPH (Witt

1979), or to the thioredoxin complex, in order to reduce a dithiol component of the ATPase for activation (Mills and Mitchell 1982, Shahak 1982), or it can pass it back into the electron transport chain either directly to the PQ-pool or indirectly via the cytochrome b/f complex for cyclic electron transport (Crowther et al. 1979, Shahak et al. 1981, Peters et al. 1984, Garab and Hind 1987).

Oxidized P_{700} can be reduced by the water soluble plastocyanin (Pc). This copper containing protein mediates electron transfer between cytochrome f and PSI (Haehnel 1984). In turn cytochrome f is reduced via the Rieske type iron-sulfur protein in a concerted reaction together with cytochrome b_{559} by electrons from PQH₂ (Joliot and Joliot 1986). The oxidation of PQH₂ is believed to be the slowest step in the electron transport chain from water to NADP⁺ (Witt 1979). Concomitant with the oxidation of PQH₂ two protons are released on the luminal side of the membrane. Depending on the occurrence of linear or cyclic electron transport the proton to electron transfer ratio H⁺/e⁻ of this step will be 1 or 2 respectively (Selak and Whitmarsh 1982, Whitmarsh et al. 1982, Jones and Whitmarsh 1985).

1.1.3. The Cytochrome b/f Complex

As is apparent from fig. 1.1 the cytochrome b/f complex plays a crucial role in the electron transfer between PSII and PSI (Anderson and Boardman 1973, Hurt and Hauska 1981, Lam and Malkin 1982). Although it has been known that the two other main complexes of the electron transfer chain PSI and PSII are laterally separated in the thylakoid membrane (Andersson and Anderson 1980) the localization of the cyt b/f complex is still controversial (Allred and Staehelin 1986). Although most reports situate this complex more or less evenly distributed between the grana and the stroma thylakoids (Åkerlund and Andersson 1983, Allred and Staehelin 1985), a recent report localizes the cyt b/f complex in the fret regions which serve as a continuum between the granal and the stromal membranes (Morrissey et al. 1987). The complex is shown in fig. 1.4 and contains two cytochrome b_{559} hemes, a cytochrome f, a Rieske type iron-sulfur protein and a functionally unidentified fifth protein of 17 kDa (Hurt and Hauska 1982). Both cyt b and cyt f can accept electrons from PQH₂, which appears to be a concerted reaction at the so called "Q_z" site (Joliot and Joliot 1986, Jones and Whitmarsh 1987b, Rich et al. 1987), with the iron-sulfur cluster as an intermediary between PQH₂ and cyt f. At the "Q_c" site it is assumed that cyt b can donate an electron to plastoquinone (Jones and Whitmarsh 1987a). Since "Q_z" is supposed to be situated near the luminal side of the membrane and "Q_c" near the stromal side, electron transfer from PQH₂ to PQ via cyt b constitutes an electrogenic step known as the Q-cycle (Mitchell 1976, Wikström et al. 1981, Rich 1984, Joliot and Joliot 1985). In the linear electron transport scheme electrons are channelled to the cyt b/f complex through intra-membrane diffusion of PQH₂ and transported to PSI by luminal diffusion of Plastocyanin (Haehnel et al. 1987). In cyclic electron transport luminal diffusion of Plastocyanin also mediates electron transport between the cyt b/f complex and PSI while Ferredoxin transports the electrons back to

6 Photosynthetic Free Energy Transduction

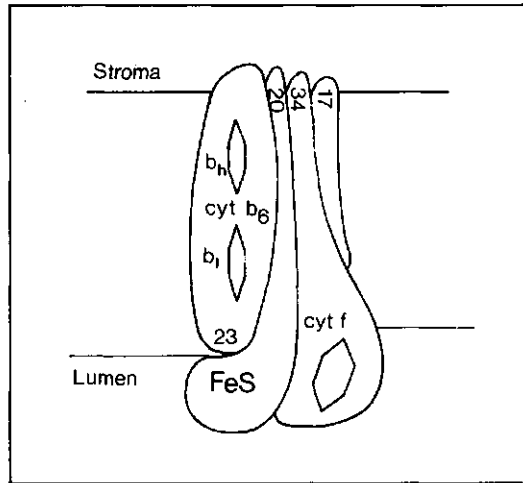


Figure 1.4. The cytochrome b/f (cyt b/f) complex containing two cyt b₅₆₃ hemes aligned above each other perpendicular to the plane of the membrane. Both the FeS centre of the "Rieske" protein and the heme of the cytochrome f molecule are situated in the lumen. Both proteins, however have an alpha helix strand passing through the membrane (Hauska 1986). The function of the 17 kDa protein is unknown as yet.

the PQ-pool (Shahak et al. 1981, Peters A.L.J. et al. 1984, Hosler and Yocum 1985).

1.1.4. The Light Harvesting Complex

This pigment-protein complex contains Chl *a* and *b*, carotenoids and proteins (Thorner 1986). Its main function is to absorb photons and transfer the energy of these photons to the pigments of the antennae complexes of the reaction centers PSI and PSII (see figs. 1.1 and 1.2). Not only is the absorption cross section of these centers enhanced by the presence of the LHC, it also prolongs the residence time of the photon's energy near the reaction centre (Van Gorkom 1983), which would otherwise be below the femtosecond range, i.e. $\leq 10^{-15}$ s. The LHC plays an important part in thylakoid membrane stacking due to its low charge density on the stromal exposed side (Barber 1980). The complex formed by PSII and the LHC (see fig. 1.2) tends to aggregate in the membrane creating local areas with a high protein to lipid ratio and a very low surface charge density. The Vander Waals force of these areas seems to overcome the electrostatic repulsion. As a result of this these membrane patches are attracted to each other and form so called appressed membrane regions within the grana stacks. The charge density of the LHC in the chloroplast is altered upon phosphorylating part of its proteins (Allen et al. 1981). The phosphorylated pigment-protein complex diffuses out of the granal regions, due to electrostatic repulsion, and attaches itself to the LHC of PSI. Thereby the energy distribution of absorbed light between PSI and PSII is shifted in favour of PSI (Barber 1982). This type of energy redistribution between PSI and PSII is different from the so called "spill-over" mechanism.

The latter mechanism occurs only at higher temperatures in vivo, when the thermal motion disrupts the aggregation of PSII complexes and a free intermingling of PSI and PSII ensues, enabling direct energy transfer (spill-over) from PSII to PSI (Weis 1985).

1.1.5. The Proton ATP Synthase (CF_1 - CF_0).

The chloroplast ATPase complex consists of a hydrophobic CF_0 part, consisting of three types of proteins I, II and the hexamer III, buried within the membrane and a hydrophilic CF_1 part, consisting of the two trimers α and β and of the subunits γ , δ and ϵ , on the stromal side of the membrane and attached to its counterpart CF_0 by electrostatic attraction (Barber 1980, Strotmann and Schumann 1983, Strotmann and Bickel-Sandkötter 1984, Strotmann et al. 1987) as can be seen in fig. 1.5. It was first proposed by Mitchell (Mitchell 1961, Mitchell 1966) that vectorial electron transport in energy transducing organelles would lead to the build-up of a proton motive force p.m.f., in analogy to the electromotive force e.m.f., which would be used by an ATP synthase complex to bind inorganic phosphate (P_i) to adenosine-5'-diphosphate (ADP) to form the energy rich adenosine-5'-triphosphate ($ADP + P_i = ATP$). This so called chemiosmotic hypothesis balances the generation of a transmembrane electrochemical proton potential difference $\Delta\mu_H^+$

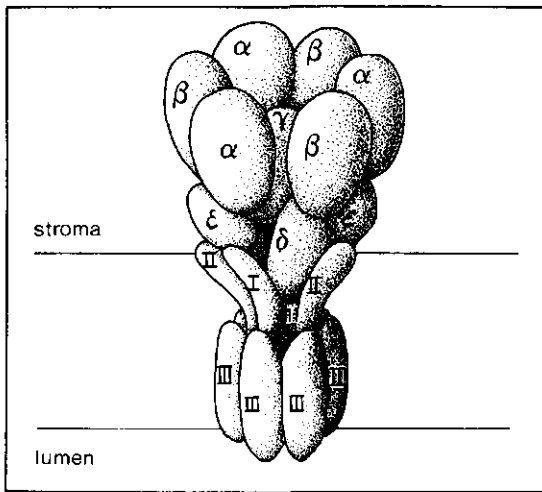


Figure 1.5. The proton ATP synthase (ATPase) complex consisting of an integral membrane part CF_0 (containing the subunits I, II and III) and a part protruding into the stroma CF_1 (containing the subunits α , β , γ , δ and ϵ). The CF_0 is considered to be the proton conductive part, in which subunit III (9 kDa) forms a hexamer with 6 $-COO^-$ residues in the centre of the membrane. This forms a hexacooperative buffer (Junge et al. 1984a). The enzymatic part of the complex (CF_1) contains a trimeric complex $\alpha_3\beta_3$, which is believed to be the catalytic site for ATP synthesis or hydrolysis. The other subunits appear to play a role in the interconnection of the two coupling factor parts CF_0 and CF_1 .

8 Photosynthetic Free Energy Transduction

with a change in the free enthalpy of ATP (ΔG_{ATP}). It presupposes a homogeneous lumen and stroma separated by a thin semi-permeable and inert membrane. Charge or concentration differences within the lumen itself should be abolished completely within the turnover time of an ATPase, which is estimated to be 2.5 ms (Gräber et al. 1984). The same restrictions hold for the stroma. Another theory was proposed by Williams (Williams 1961, Williams 1975) in which the build-up of a $\Delta\bar{\mu}_H^+$ was not considered. Instead electron transport was proposed to energize protons which were transported laterally through the membrane to the sites where their energy could be used to bind P_i to ADP. In contrast to Mitchell's hypothesis, which has been tested in experiments a multitude of times since it was proposed (Jagendorf and Uribe 1966, Junge 1977, Boyer et al. 1977, Mitchell 1979, Gräber 1982, Junge et al. 1987) Williams' hypothesis lacked the thermodynamic basis for verification. The role of the ATPase is crucial in this controversy in that it can transport energized protons from the lumen to the stroma (Gräber and Witt 1976, Gräber et al. 1977, Gräber 1980) or it connects an inner membrane compartment to the stroma (Ort et al. 1976, Baker et al. 1981, Dilley et al. 1982, Theg and Homann 1982, Ort and Melandri 1982, Theg and Junge 1983, Dilley and Schreiber 1984, Polle and Junge 1986). The fact that the integral membrane part CF_0 of the ATPase contains proton binding groups, which can act in a hexacooperative way (Junge et al. 1984a), can corroborate the above stated view. In any case it is clear that the coupling of electron transport to ATP synthesis is still a matter of debate, although the chemiosmotic hypothesis has been asserted as being correct in principle (Junge et al. 1987). It appears however that under certain conditions the coupling can shift from bulk phase $\Delta\bar{\mu}_H^+$ to a localized form of chemiosmosis (Westerhoff et al. 1983, Westerhoff et al. 1984, Westerhoff 1985, Westerhoff and Chen 1985, Beard and Dilley 1986, Beard and Dilley 1987, Theg and Dilley 1987).

1.2. History

Ever since the advent of the chemiosmotic theory (Mitchell 1961), many techniques have been used to measure the light-induced electrochemical potential across the thylakoid membrane in higher plant chloroplasts (Witt 1971, Vredenberg 1976, Junge 1977, Witt 1979, Junge and Jackson 1982, Junge et al. 1987). The common technique for measuring the electric potential changes, due to actinic light flashes of relatively short duration (≤ 1 ms), is by monitoring the electrochromic absorbance change of an intrinsic membrane pigment assembly, called P_{515} , at 515nm (Junge 1977, Witt 1979, Vredenberg 1981, Junge and Jackson 1982). This absorbance change was first observed by Duysens (Duysens 1954). However, for actinic illuminations of longer duration (≥ 10 ms), the absorbance change is obscured by scattering changes and this technique is not applicable (Deamer et al. 1967, Thorne et al. 1975, Schapendonk 1980, Coughlan and Schreiber 1984a, Coughlan and Schreiber 1984b). The only other technique available to measure the electric potential changes with a time resolution $\leq 10^{-3}$ s during prolonged actinic illumination periods, e.g. ≥ 1 s, is the open ended glass capillary microelectrode technique (Bulychev et

al. 1971, Bulychev et al. 1972, Vredenberg et al. 1973, Vredenberg and Tonk 1975, Bulychev et al. 1976, Bulychev and Vredenberg 1976, Vredenberg and Bulychev 1976, Vredenberg 1976, Bulychev et al. 1980, Remis et al. 1981, Bulychev et al. 1983, Remis et al. 1984, Bulychev 1984a, Bulychev 1984b, Van Kooten et al. 1984, Bulychev 1985, Bulychev et al. 1986, Remis et al. 1986a, Remis et al. 1986b, Van Kooten et al. 1986, Vredenberg et al. 1987, Van Kooten et al. 1987). The time-course of the electric potential during actinic illumination periods of several seconds is complex, especially after a dark adaptation period of a few minutes (Bulychev 1984a, Bulychev 1984b, Van Kooten et al. 1984, Van Kooten et al. 1986). The complexity of the signal implies an extremely high information content in the measured responses. The urge to disclose this information was the starting point for the work reported on in this thesis. We believe that a start has been made in understanding these complex signals through our modelling of photosynthetic electron transport (Van Kooten et al. 1986, Vredenberg et al. 1987, Snel et al. 1987, Van Kooten et al. 1987). Our own microelectrode experiments gave us a sense of confidence that we were working along the right direction in solving this problem. However recent experiments using an antimony pH sensitive microelectrode gave such a qualitative resemblance of the measured $\Delta\mu_{\text{H}^+}$ with our calculated results (Remis et al. 1986a, Remis et al. 1986b), that we interpret this as strong evidence for the correctness of our basic assumptions.

Beside measurements of the electric potential during actinic illumination periods of relatively long duration, potential changes caused by single turnover saturating actinic light flashes (width of the flash at half the maximum amplitude is $8 \mu\text{s}$ and wavelength $\geq 635\text{nm}$) were also studied. Ideally they should be compared to the electrochromic absorption change measurements at 515nm , which was proven to be a linear response to the electric field across the thylakoid membrane (Schapendonk and Vredenberg 1977). Here a clear discrepancy was found between the microelectrode measurements and the P_{515} results (Schapendonk et al. 1979). In most instances the microelectrode measurements showed a rather simple response (Bulychev et al. 1976, however see Bulychev and Vredenberg 1976a for a different response), which could be explained with the aid of our standard knowledge of membrane transport (Goldmann 1943, Schultz 1980). The more complex response measured by the P_{515} technique (Joliot and Delosme 1974, Slovacek and Hind 1978, Velthuys 1978, Horvath et al. 1979, Schapendonk and Vredenberg 1979) was analyzed in detail and compared to the microelectrode measurements (Schapendonk et al. 1979, Schapendonk 1980). It has been suggested that this signal could be explained by an extra charge separation in the cyt b/f complex known as the Q-cycle (Mitchell 1976, Bouges-Bocquet 1977, Crowther and Hind 1980, Velthuys 1980). A first tentative explanation involving the ATPase was given by Schapendonk (Schapendonk 1980). When we started investigating this phenomenon it became clear that the signal we measured could not be explained by a Q-cycle (Van Kooten et al. 1983). Deconvolution of the response led to an explanation involving a heterogeneity of field effects caused by localizing certain charges within the membrane (see van Kooten in Westerhoff et al. 1983). This idea together with the published results of others

10 Photosynthetic Free Energy Transduction

(Schuermans et al. 1981, Schreiber and Rienitts 1982, Schreiber and Del Valle-Tascon 1982) led to an intensive research into the origins of the P_{515} flash-induced response (Peters et al. 1983, 1984a-c, Van Kooten et al. 1984, Peters et al. 1985, 1986). Thus at the start of the study presented here two vital questions were posed:

- 1- Is it possible to interpret the more complex responses measured by the microelectrode during actinic illuminations of several seconds (Vredenberg 1976)?
- 2- Is it possible to reconcile the difference in response measured by the microelectrode and measured by the P_{515} technique when a transmembrane voltage is induced by a single turnover saturating light flash (Schapendonk et al. 1979)?

Although our research does not answer these questions fully, we believe that it has contributed to a better understanding of the underlying principles involved.

1.3. Outline of the Study

This study deals with the biological free-energy transduction of the thylakoid membrane electric potential into the synthesis of ATP at the onset of actinic illumination. Both electrophysiological (i.e. the microelectrode) and spectrophotometric (i.e. P_{515}) techniques were used to study the electric potential kinetic patterns in intact leaves, leaf sections, isolated intact chloroplasts and broken chloroplasts. ATP synthesis and hydrolysis was mainly measured by Rob Peters, using the bioluminescent firefly luciferin-luciferase assay method (Lundin et al. 1977). These results have been reported on in Peters' doctoral thesis (Peters 1986).

In chapter 3 we will explain a mathematical model of photosynthetic free-energy transduction incorporating electron transport, proton translocation, ionic distributions and ATP synthesis/hydrolysis. The model is based on the chemi-osmotic hypothesis as proposed by Mitchell (Mitchell 1961, Mitchell 1966, Mitchell and Moyle 1983).

In chapter 4 we will demonstrate the possible use of the model in testing certain assumptions about energy coupling in photosynthesis. It is here that we will also compare experimental results with our model calculations and demonstrate the validity of the chemi-osmotic theory under the conditions applied during electrophysiological experiments.

In chapter 5 we will discuss the P_{515} measurements in comparison to the microelectrode measurements. It will be made clear that a better understanding of the origins of the complex P_{515} flash-induced response leads to the disappearance of the above mentioned discrepancy between the two measuring techniques.

In chapter 6 we will treat several models explaining the P_{515} response also in the light of the work done in cooperation with Rob Peters.

In chapter 7 a general discussion concerning "localized" versus "delocalized" chemiosmosis will be held. Our results will be interpreted within the frame work of this debate.

Part of the work presented in this book has been published (Van Kooten et al. 1983, Peters et al. 1983, Westerhoff et al.

1983, Vredenberg et al. 1984, Van Kooten et al. 1984, Van Kooten 1984, Peters et al. 1984a, Peters et al. 1984b, Peters et al. 1984c, Peters et al. 1985, Van Kooten et al. 1986, Peters et al. 1986, Vredenberg et al. 1987, Snel et al. 1987, Van Kooten et al. 1987).

12 Photosynthetic Free Energy Transduction

2. Materials and Methods

2.1. Microelectrode Measurements

Micro-capillary glass electrodes were made from borosilicate glass (Clark, GC 200F-15) and pulled on a BB-CH puller (Bertrand et al. 1983). The electrodes were filled with a 1 M KCl solution. The electrode was moved with the aid of a three dimensional micromanipulator (Märzhauser, FRG) on a home made vibration damped table. The table was designed by W.J.M. Tonk and constructed at the Technical and Physical Engineering Research Service at Wageningen. The electrode tip is immersed in a solution and connected via a 1 M KCl-agar bridge and an Ag-AgCl electrode to a high impedance PICO-metric unity gain amplifier (input impedance $10^{13} \Omega$ and a bias current of less than 10^{-12} A). The connecting cable is coaxially guarded and the stray capacitance can be compensated up till 10 pF via a negative capacitance coupling circuit. The reference input of the amplifier is connected through a 1 M KCl-agar bridge and an Ag-AgCl electrode to the solution. By applying a 1 Volt square voltage pulse over a $10^9 \Omega$ resistor to the input of the amplifier one can determine the electrode resistance when it is below $10^8 \Omega$. The electrodes we used had a resistance of about $2 \cdot 10^7 \Omega$ as measured in our situation. As was shown before (Schapendonk 1980) the outer diameter of the tip of such an electrode lies well beneath $1 \mu\text{m}$. In order to understand why we have chosen certain values for our parameters in chapters 3 and 4 it is necessary to describe the measurement procedure.

2.1.1. Measurement Procedure

A thin strip of a *Peperomia metallica* leaf is cut with a sharp razor blade. It is clamped to the bottom of a cuvette filled with a medium of 15 mM sorbitol + 20 mM HEPES/KOH pH7.5. Through an inverted microscope (Wild M5) one can look at the rim of the leaf cut, which was sliced at an angle of 45° as shown in fig. 2.1. By squirting the leave rim with medium from a syringe one can remove light scattering air bubbles and residues of ruptured cells. The leave is illuminated from above by a forked flexible light guide, which enables us to simultaneously use two different light sources.

2.1.1.1. Illumination.

The actinic illumination was supplied by 150 Watt halogen lamps with the proper heat filtering or by a xenon flash lamp

14 Photosynthetic Free Energy Transduction

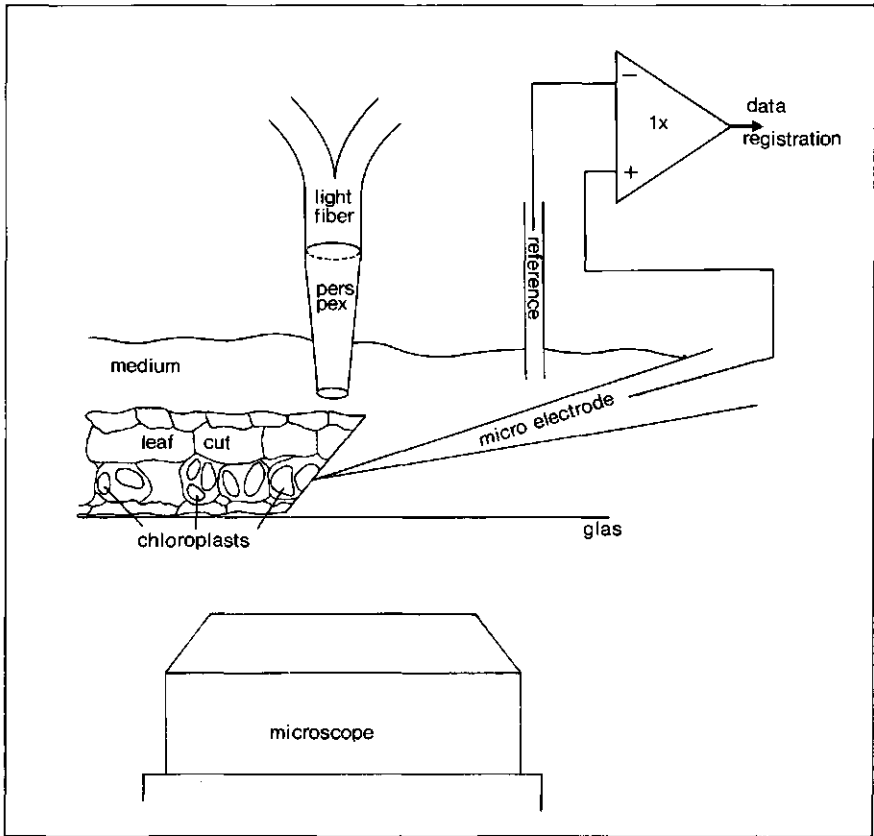


Figure 2.1. Schematic drawing of the microelectrode experiments. A leaf cut of *P. metallica* is clamped to the glass bottom of a cuvette and immersed in medium. The leaf rim is cleaned of cell rests and air bubbles. With an inverted microscope the giant chloroplasts in the cells at the edge of the leaf can be seen. The chloroplasts are illuminated with the aid of a forked light fiber, enabling the simultaneous use of two light sources. The light fiber is prolonged with a conically shaped perspex rod. This allows a close approachment of the light source to the leaf cut without introducing electric disturbances. A reference electrode consisting of Ag-AgCl in a 1 M KCl agar gel, is inserted in the medium in the vicinity of the leaf edge. The microelectrode enters the medium at a sharp angle with the aid of an electronically steered manipulator. Thus the tip of the microelectrode and the chloroplast intended to be impaled can both be seen through the microscope. The microelectrode contains 1 M KCl and is connected through an Ag-AgCl electrode to a unity gain amplifier.

(General Electric FT-230). The width of the white flash at half the maximum amplitude is $8 \mu\text{s}$. Using a 30% neutral filter gave no diminution of the chloroplast response to the flash. The light beam could be switched on and off by a fast shutter with a total rise time of 0.5 ms (Vincent Asc., 23X). The shutter was controlled by a laboratory built electronic device. With the aid of a conically shaped perspex tube of 1 cm length glued to the end of the light guide, it was possible to approach the

chloroplast to be measured within 1 mm distance with the light source without making electrical contact. To test whether the actinic light was saturating within the rise time of the shutter we combined a xenon flash with the light of the halogen lamp during opening of the shutter. It was found that the chloroplast response to the flash disappeared within 400 μ s after the shutter started opening.

2.1.1.2. Impalement.

When the leave cut and the electrode are in place one can observe a row of mesophyll cells (see fig. 2.1). Each cell contains 3 to 4 chloroplasts with a diameter of about 25 μ m. This size varies and alters by changing the growth conditions of the plant (see paragraph 2.1.2.). After choosing a manipulatory suitable chloroplast the microelectrode is manipulated into position. The final impalement occurs with the aid of a hydraulic device enabling a slow and controlled motion of the electrode. Impalement is suspected as soon as a cell potential between -100 to -250 mV is detected. During this procedure the background light has been turned on in order to make a visualization of the process possible. The intensity of this background illumination is substantial and can be considered to be near saturation for steady-state photosynthesis. The light is turned off for a short period of time and then turned on and off transiently to elicit a response from the chloroplast. When a positive signal of sufficient magnitude (≥ 10 mV) is detected the light is turned off for a longer duration to start the actual experiment. These dark adaptation periods are however not very long since an electrical contact can be broken at any moment due to mechanical vibrations. Thus we restrict ourselves usually to dark adaptation periods of several minutes, although we have had electrical contact with the proper response for several hours from time to time. That the open ended glass capillary microelectrode actually measures the thylakoid transmembrane electric potential has been substantially verified before (Bulychev et al. 1976, Vredenberg 1976, Schapendonk 1980).

Partial destruction of thylakoid membranes by impalement was checked by comparing the half-time of the decaying electric field after a xenon flash with electrochromic P_{515} measurements in intact pre-illuminated leaves (Peters et al. 1983). If the half-time of decay measured with the microelectrode was an order of magnitude faster than that measured with the P_{515} technique, which was about 60 ms at 25°C (see also Bulychev et al. 1976), the measurement was discarded.

2.1.1.3. Registration

The signals were recorded on a strip chart recorder (Linseis, FRG) or on a transient recorder (Nicolet 2090-111A). The transient recordings were relayed to a micro-computer (HP-86) for further processing.

2.1.2. Cultivation of *Peperomia metallica*

The aim of the cultivation is to grow a phenotype suitable for electrophysiological experiments. Thus the plants are grown under conditions to which they adapt by enlarging their

16 Photosynthetic Free Energy Transduction

chloroplasts. Plants are exposed to a 12 hour per day period of luminescent light (Philips, TL 33) with an intensity between 1.2 and 1.5 $W \cdot m^{-2}$. The air temperature varies between 24° and 28°C in the day and between 16° and 18°C at night. Substrate temperature varies between 20° and 24°C in the day and between 14° and 16°C at night. The relative humidity is kept at 80% during the day and rises to 90% at night. The soil is sterilized and consists of 1 part compost, 1 part peat and 2 parts river sand. The plants are top cuts which are planted in red clay pots of 5 cm diameter together with some cytokinin to induce root formation. The pots were placed in gravel and kept slightly moist. Ventilation was kept down to 1 $m \cdot s^{-1}$. The plants are usable between 3 and 4 months after planting.

2.2. P_{515} Measurements

Most of the P_{515} measurements were done with either intact spinach leaves *Spinacea oleracea* cvs. "Amsterdams Breedblad", "Nobel", "Kir" and "Bergola" or with isolated intact or broken chloroplasts therefrom. A few experiments were done with intact leaves of *Peperomia metallica*. The principles of the instrumentation used was described before (Schapendonk 1980). We have connected the measuring equipment to a computer for process control and digital data acquisition. Modifications to the spectrophotometer and the electronics (see paragraph 2.2.3.) yielded a much higher signal to noise ratio and enabled us to record P_{515} responses without the need of averaging to improve this ratio.

2.2.1. Cultivation of *Spinacea oleracea* L.

Spinach was sowed in fresh soil in trays of 60x80x20 cm. The soil consisted of a mixture of commercial soil (TKS: Torf-Kultur-Substrat) and gardener soil with the following composition: 5 parts compost + 5 parts leaf mould, 3 parts peat dust + 2 parts stable manure and 1 part sand. Both soils were mixed in a 1:1 proportion. After the seeds were put in furrows a little fungicide was added. The plants were exposed to a light period of eight hours per day. During this light period the plants were placed in a greenhouse where they received supplementary light from high pressure mercury lamps (Philips HPLR 400 Watt). This assured a minimum light intensity of 80 $W \cdot m^{-2}$ (PAR), which could rise to about 400 $W \cdot m^{-2}$ (PAR) in full sunshine. Heat radiation from the lamps was dissipated by water filters of 7 cm thickness, through which water was flowing at a minimal rate of 5 liters per hour. The temperature at the soil surface and at the leaves was about 16°C and 18°C respectively, but never exceeded 20°C. The relative humidity of the atmosphere was kept at 70%. The airflow above the leaves was minimized, because it was found that a constant breeze induced a texture change in the leaves, which made it harder to extract intact chloroplasts from them. The plants were transferred to the phytotron at night where they were kept in the dark at 16°C and 70% r.h., and returned to the greenhouse again in the morning. Whenever insecticides were used the P_{515} signal was duly influenced and the measurements were

discarded. Plants between 5 and 8 weeks old were used for chloroplast isolation.

2.2.2. Isolation and Characterization of Chloroplasts

About 30 grams of spinach leaves were harvested in the morning after the plants had received 1 to 2 hours of light necessary to assimilate sufficient reducing equivalents, but not enough to generate large starch granules. After harvesting the excised leaves were put on ice. All subsequent actions were performed at 0°C and under low intensity green light or in total darkness when possible. Our isolation method is a modified version of the one used by Cockburn and Walker (1968). After extraction of the midribs the leaves were cut into small rectangular pieces of 2x4 mm. The leaf pieces were deposited in 50 ml of grinding medium which consisted of: 0.33 M sorbitol, 10 mM Na₂P₂O₇/HCl pH 6.5, 5 mM MgCl₂ and 2 mM ascorbate. The leaf pieces were ground by an Ultra-Turrax type TP 18/10 at 20000 rpm (Janke & Kunkel KG). The Turrax was set up to give grinding pulses of 0.5 s. The ice cold suspension of leaf pieces received 4 such pulses, while the suspension was stirred thoroughly in between pulses. The ground suspension was filtered through 4 layers of perlon (mesh distance 40 μm), which had been immersed in ice cold grinding medium before the filtering. The filtered suspension was distributed between two centrifuge tubes, which were polished on the inside and contained a flat bottom. The intact organelles were spun down in 50 s at 2800 rpm (i.e. 900xg) in a Chillspin table top centrifuge. The pellets were re-suspended in 1 ml of washing medium containing: 0.33 M sorbitol, 50 mM Hepes/NaOH pH 7.5, 1 mM MnCl₂, 1 mM MgCl₂, 2 mM EDTA, 2 mM ascorbate, and 0.1 mg·ml⁻¹ BSA. Re-suspension occurred by gently shaking the tubes on ice or by brushing the pellet with a soft paint brush. When the pellets were completely re-suspended the rest of the 50 ml washing medium was added to the tubes. Chloroplasts were spun down again for 60 s at 2800 rpm. These pellets were re-suspended in 0.5 ml of stock medium containing: 0.33 M sorbitol, 50 mM Hepes/NaOH pH 7.5, 1 mM MnCl₂, 1 mM MgCl₂, 2 mM EDTA, 2 mM MgCl₂. Re-suspension was done in the same manner as in the washing step. This stock suspension contained mainly intact chloroplasts at a concentration of about 1 mg Chl·ml⁻¹ and was kept in absolute darkness on ice. This procedure yielded chloroplasts which were 90 to 95% intact as determined with ferricyanide reduction (Heber and Santarius 1970). The chlorophyll content was determined spectrophotometrically (Bruinsma 1961). If broken chloroplasts were needed an aliquot of the stock suspension was taken (between 50 and 100 μl) and suspended in 1 ml of ice cold break medium consisting of: 5 mM Hepes/NaOH pH 7.5 and 5 mM MgCl₂. After 60 s 1 ml of double concentrated medium was added: 0.66 M sorbitol, 100 mM Hepes/NaOH pH 7.5. Broken uncoupled chloroplasts, obtained by adding 12.5 mM NH₄Cl, with ferricyanide as electron acceptor revealed oxygen evolution rates at 20°C of 250 μmol O₂·(mg Chl·hr)⁻¹ or higher. The coupling ratio of these chloroplasts was routinely between 5 and 10.

2.2.3. Instrumentation

Flash-induced absorbance changes were measured in a modified Aminco-Chance absorption difference spectrophotometer described before (Schapendonk 1980).

2.2.3.1. The Spectrophotometer

This apparatus was modified further (J. Snel, thesis 1985) so that both monochromators were used at the same wavelength, casting two continuous and parallel beams on a 1x1x5 cm measurement cuvette. Thus a surface of 1x1.8 cm of the cuvette was irradiated by a monochromic parallel measuring light beam. The light intensity at 518 nm was $7 \mu\text{W}\cdot\text{m}^{-2}$ at the front of the cuvette. Directly behind the cuvette 9 mm of BG-39 filters (Schott, Jena) were placed to shield the photomultiplier from red ($\geq 665\text{nm}$) actinic flash light. Water thermostating kept the measuring cuvette at the desired temperature, which was usually 3°C except with the *P. metallica* measurements where 25°C was used. Thus a large measuring area and a short distance between photomultiplier and cuvette (1.4 cm), combined with careful avoidance of excessive vibrations led to a high signal to noise ratio. This enabled us to measure relative intensity changes $\Delta I/I \approx 10^{-3}$ on the second time scale without averaging. In early publications there was still the necessity to average the signal before a sufficient response emerged (Van Kooten et al. 1983, Vredenberg et al. 1984, Van Kooten et al. 1984).

2.2.3.2. The Flash Lamp

The xenon flash lamps (GE, FT-230) were operated at 2 kV, with an $8 \mu\text{F}$ buffer and a 10 kV trigger pulse. This resulted in a peak of white light $8 \mu\text{s}$ wide at half height of the maximum amplitude, but with a $300 \mu\text{s}$ tail below 1% of the maximum intensity. The spectrum of the flash was curtailed by 2 mm RG-665 filters (Schott, Jena) and transmitted to the sample via light guides of 10 mm diameter. The light guides were connected to the sides of the cuvette via polished perspex blocks of 1x1.8x2 cm. This enabled the light coming from the light guide to be distributed over the side of the cuvette, ensuring saturation throughout the whole suspension. The use of two flash lamps enabled us to repeat saturating flashes within a short time interval.

2.2.3.3. Electronics

The anode voltage of the photomultiplier was amplified by a differential amplifier (AN22, Tektronix), with a compensating battery voltage of -0.5 V on the negative input. The difference signal ($\approx 0 \text{ V}$) was amplified by a factor of 200 in most instances.

2.2.3.4. Process Control and Data Acquisition

The measuring process was controlled by a MINC 11/23 minicomputer (Digital Equipment Co.) running in real time mode with the necessary interfaces. Flash triggers were given by a digital I/O interface and data were acquired by a 12 bits A/D converter. The whole measurement process was timed by three crystal clocks running at 1 MHz. The necessary software was developed in cooperation with G. van Eck of the Computational Centre of the Agricultural University Wageningen.

2.2.3.5. Data Handling and Analysis

P_{515} responses could thus be measured, averaged, stored on disk and plotted (HP 7221C). The signals were fitted to a sum of exponential curves (three at most) with the aid of program using an expansion of the solution of a Fredholm integral equation of the first kind in the orthogonal eigenfunctions of the kernel (Provencher 1976). The spectral peaks of the solution are used to provide starting values for nonlinear least squares analyses of the raw data. Thus an unbiased fit of exponential curves results, with a signal to fit ratio ≈ 1 in most instances. However the mere assumption that the membrane electric potential decay process consists solely of independent first order phenomena is dubious. Combined with the fact that any continuous function can be simulated by an infinite number of exponential curves, leads us to the conclusion that we should be extremely careful in handling the results of these fits.

2.3. Model Calculations

In this thesis we present three different types of calculations.

2.3.1. Free-Energy Transduction

The most exacting and time consuming were the calculations of the transmembrane potentials and ATP synthesis based on a chemiosmotic coupling mechanism. These calculations are presented in chapters three and four. They consist mainly of numerical integration by incremental time steps. The computations were performed on a PDP11/23 minicomputer (Digital Equipment Co.) under Fortran IV programming. All variables which were subject to continuous summing at the end of each integration loop were kept in double precision (i.e. 55 bits for the mantissa, of a real variable) in order to minimize systematic errors. The incremental time step Δt varied between $0.5 \mu s$ and 50 ms depending on the magnitude of the fluxes involved.

2.3.2. A P_{515} Model

In chapter 6 a inhomogeneous second order differential equation is used to describe a possible model of reaction II in the P_{515} response. An analytical solution is found by the substitution method.

2.3.3. Proton Diffusion in the Lumen

Also in chapter 6 a diffusion model for protons in a two dimensional plane with immobilized buffering groups is given (Ott and Rys 1973, Crank 1975, Hong and Junge 1983). It consists of an analytical solution of Fick's second law with the proper boundary conditions. Actual numerical results were obtained with the aid of a programmable hand held calculator (TI59, Texas Instruments).

3. Modelling Photosynthetic Free Energy Transduction

3.1. Introduction

Ever since the advent of the chemiosmotic theory (Mitchell 1961) many experiments have been performed to verify the hypothesis (e.g. Jagendorf and Uribe 1966, Witt 1971, Junge 1977, Witt 1979, Junge et al. 1987) and many physical parameters pertaining to the coupling process have been measured (e.g. Barber 1972, Heldt et al. 1973, Walz et al. 1974, Werdan et al. 1975, Bulychev et al. 1976, Vredenberg 1976, Junge 1977, Junge et al. 1979, Rubin and Barber 1980, Junge and Jackson 1982). This has led to the acquisition of a vast amount of data. The framework within which we interpret the data is thermodynamically well defined, but lacks enough detail to check the exact influence of the magnitude of a certain parameter on all potentials and concentrations. This, together with complex responses measured with the microelectrode in giant chloroplasts of *Peperomia metallica* and of *Anthoceros* sp. (Vredenberg and Bulychev 1976, Remish et al. 1981, Bulychev 1984b), drove us to develop a mathematical description incorporating the essential variables of photosynthetic free-energy transduction. In this chapter we will explain the mathematics of the model and the choice of the values for certain physical parameters we used. Other attempts to model biological free-energy transduction were based on the use of non-equilibrium thermodynamics and the Onsager relations (Heinz 1982, Westerhoff 1983), which is inadequate to simulate the light off-on and on-off transitions we were interested in.

3.2. Basic Assumptions

The model is entirely based on the chemiosmotic hypothesis as proposed by Mitchell (Mitchell 1961, Mitchell 1966, Mitchell and Moyle 1968), in that it considers the membrane solely as a semipermeable barrier containing vectorial oriented protein complexes capable of generating a $\Delta\bar{\mu}_{H^+}$ and an ATPase capable of consuming this $\Delta\bar{\mu}_{H^+}$ and thereby convert $ADP + P_i$ into ATP. The two phases separated by the membrane are considered to be homogeneous aqueous phases. Local disturbances within such an aqueous phase are considered to equilibrate throughout the homogeneous water space well within the time frame of the maximum turn over rate of the ATPase, which is considered to be 2.5 ms (Gräber et al. 1984). In fig. 3.1 we show the main forces and

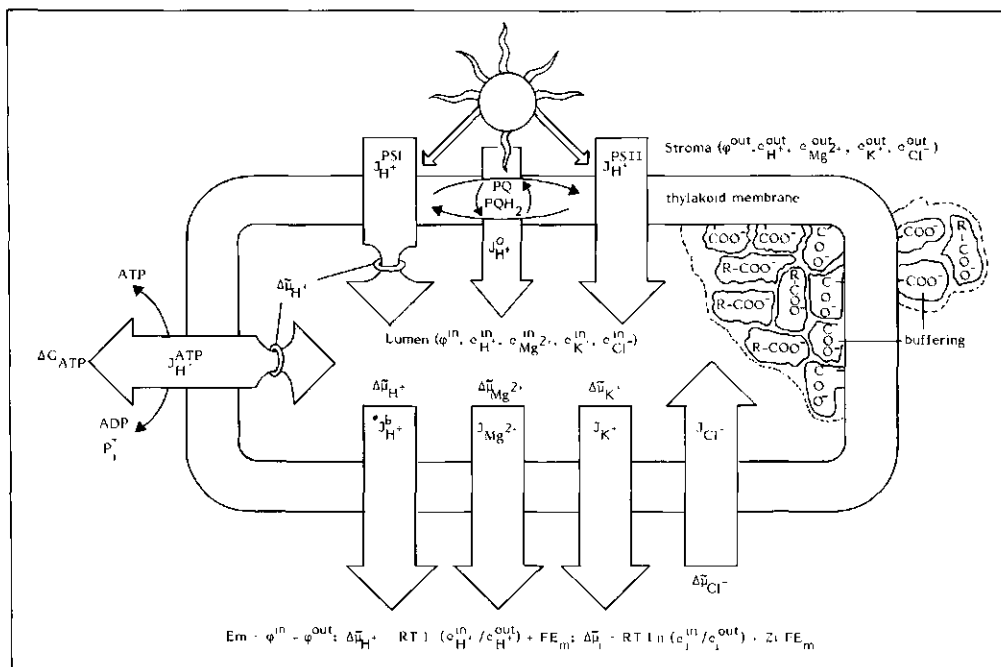


Figure 3.1. Schematic representation of the forces and fluxes involved in the photosynthetic free energy transduction as described by the model presented in this chapter. The two photosystems are described as two photon-induced proton pumps interconnected by a mobile hydrogen carrying redox pool and attenuated by the $\Delta \bar{\mu}_{H^+}$. A third proton pump, caused by redox mediated electron flow through the cyt b/f complex ($J_{H^+}^{b}$), can be included when desired in the calculations. Active dissipation of $\Delta \bar{\mu}_{H^+}$ can occur through the ATPase, controlled by the chemical free energy of phosphorylation ΔG_{ATP} and by $\Delta \bar{\mu}_{H^+}$. The activation state of the ATPase is also regulated by $\Delta \bar{\mu}_{H^+}$, as described by Gräber et al. (1984, 1987) for an oxidized ATPase. The presence of a large concentration of buffer groups is taken into account within the model. The passive dissipation of any potential build-up is caused by the ions and protons present. The main formulae pertaining to the electrochemical events are presented and the sign convention is taken from Lowe and Jones (1984).

fluxes involved in free-energy transduction of higher plant photosynthesis. The sign and symbol convention concerning chemiosmotic coupling, used throughout this thesis, is taken from Lowe and Jones (1984). This implies that the reference point is imagined outside the thylakoid (i.e. in the stroma) and the measuring point inside the thylakoid (i.e. in the lumen), thus all potentials are calculated by taking the inside value and subtracting the outside value from it.

3.2.1. Electron Transport

Photons are considered to induce a proton flux through two different types of photosystems interconnected by an electron transport chain, depicted as $PQ = PQH_2$, in fig. 3.1. Since our

experimental setup allows us to measure electric potential changes either at saturating light intensities (see paragraph 2.1.1.2.) or in darkness, only a rather crude description of electron transport is used in the model. This description suffices for the simulation of our microelectrode measurements, but it is not capable of simulating electron transport under non saturating light conditions. At present attempts are made to incorporate a complete simulation of electron transport involving all the intermediate redox components in the chain (Snel et al. 1987).

3.2.2. The Backpressure

The proton flux caused by PSI is assumed to be attenuated by the magnitude of $\Delta\bar{\mu}_{H^+}$ (Siggel 1976, Huber and Rumberg 1981). This so-called "backpressure" effect has been shown to be approximately linear with the internal pH (Huber and Rumberg 1981). We depict this backpressure in fig. 3.1 by a ring constricting the PSI proton flux. One of the main reasons for choosing $\Delta\bar{\mu}_{H^+}$ as the cause of backpressure on electron transport as opposed to just E_m or ΔpH is that the latter gave calculated results which deviated extremely from experimental results.

3.2.3. Passive Dissipation of $\Delta\bar{\mu}_i$

In chloroplasts an abundance of different anions and cations prevail (Barber 1976, Barber 1980). We have restrained ourselves to one type of anion (Cl^-) and three different cations (H^+ , K^+ and Mg^{2+}). We chose these ions because of their relative abundance in the chloroplast and because all but one permeability coefficients have been measured for thylakoids (Barber 1972, Vredenberg 1976, Schönfeld and Schickler 1984, Gräber et al. 1984, Robinson and Downtown 1984). The flux densities of the different ions were calculated with the Goldman-Hodgkin-Katz equation (Goldmann 1943) and whenever the electric membrane potential became small an approximation for this equation was used (Schultz 1980).

3.2.4. Buffering Capacity

Here only the buffering capacity of the lumen is considered, because the stroma is viewed as infinitely larger than the lumen. Thus no stromal concentration changes are possible in our calculations. The buffering capacity of the thylakoid lumen has been measured (Heldt et al. 1973, Walz et al. 1974, Junge et al. 1979). But to be able to incorporate these results in our model it was necessary to develop the pertaining equations.

3.2.5. The ATPase

A proper mathematical description of ATP syntheses and hydrolysis was not available to our knowledge when we first published a preliminary version of our model (Van Kooten et al. 1984). However soon thereafter Peter Gräber and coworkers published on this complicated matter (Gräber and Schlodder 1981, Schlodder et al. 1982, Gräber 1984, Gräber et al. 1984, Junesch and Gräber 1984, Gräber et al. 1987, Junesch and Gräber 1987).

24 Photosynthetic Free Energy Transduction

They developed a mathematical description, which is applicable in our calculations. In their concept both ΔG_{ATP} and $\Delta \bar{\mu}_{H^+}$ exert a pressure on the proton flux through the ATPase, but $\Delta \bar{\mu}_{H^+}$ alone determines the activation state of the population of ATPases present. With slight modifications we have transformed their equations into our model. This addition yielded the results which gave a qualitative agreement with the measurements. The value for ΔG_{ATP} in the chloroplast stroma were taken from measurements of Giersch et al. (1980).

3.2.6. Surface and Donnan Potential

Many elegant techniques have been used to measure the surface charge density of thylakoids (Huber and Rumberg 1981, Siggel 1981c, Mansfield et al. 1982). They invariably lead to very high negative values for the lumenal membrane side. The model presented in this chapter will not concern itself with these charge densities. However we take the Gouy-Chapmann double layer into account when we assume high cationic concentrations near the membrane. In the next chapter we do take the Donnan potential into account as was shown to be necessary (Siggel 1981a, Siggel 1981b). Then it will be clear that the high cationic concentrations can be explained with the Donnan potential.

3.3. The Model

At the onset of the calculations it is possible to choose a set of variable values as boundary conditions at $t=0$ s. Thus at a certain moment in time all concentrations and electrochemical potentials are known! The resulting flux densities at $t=0$ s can be calculated with the Goldman-Hodgkin-Katz equation. The concomitant changes in concentrations and electric potential can be derived as follows:

$$\frac{dE_m}{dt} = \frac{F}{C_m} (J_{H^+}^{PSII} + J_{H^+}^{PSI} + J_{H^+}^b + J_{H^+}^{ATP} + 2J_{Mg^{2+}} + J_{K^+} + J_{Cl^-}) \quad (3.1)$$

$$\frac{dc_{H^+}^l}{dt} = \frac{A}{V} \beta (J_{H^+}^{PSII} + J_{H^+}^{PSI} + J_{H^+}^b + J_{H^+}^{ATP}) \quad (3.2)$$

$$\frac{dc_i^s}{dt} = \frac{A}{V} J_i \quad (3.3)$$

In eq. 3.1 the sum of all fluxes, multiplied by the valency of their constituent ions, is multiplied by the ratio of the Faraday constant (F) and the membrane capacitance (C_m). This results in a time-dependent change of the electric potential E_m across the thylakoid membrane. In eq. 3.2 the sum of all proton fluxes is multiplied by the surface to volume ratio (A/V) of the thylakoid and by a buffering capacity parameter (β) for the lumen. This results in a free proton concentration change in the lumen. As was stated before the concentrations and potentials of the stroma are kept constant. Finally the changes in concentration of ion species i are simply calculated with eq. 3.3. We can assume that

eqs. 3.1-3.3 remain constant during an incremental time period Δt , provided Δt is small enough. As a result a new set of potentials, concentrations and flux densities can be calculated at the moment $t + \Delta t$. With the aid of a computer the time resolved potential changes during and after illumination for periods of many seconds can thus be calculated.

The calculation of a new set of variable values for every incremental period can be subdivided in four parts, the light driven proton pump ($J_{H^+}^{PSI} + J_{H^+}^{PSII}$), the passive dissipation of $\Delta\mu_{H^+}$, the buffering capacity of the lumen and the active ATPase-dependent proton flux $J_{H^+}^{ATP}$.

3.3.1. The Light Driven Proton Pumps

Our algorithm for light-induced proton pumping in thylakoid membranes is based on the Z-scheme of electron transport (Witt 1979). Two photosystems, i.e. PSI and PSII, each with its own apparent absorption cross section, are interconnected by a pool of mobile redox mediators. The rate limiting step for electron transport is assumed to be in the intermediary redox pool, i.e. at the site of oxidation of PQH₂ by cyt b/f (Siggel 1976, Huber and Rumberg 1981, Haehnel 1984). The turnover of a photosystem results in the translocation of a proton from the stroma to the lumen. The maximum turnover rate of PSII (k_2), when provided with a proper electron acceptor, is about 1000 s^{-1} (Witt 1979). The maximum turnover rate of PSI (k_1) is dependent on the plant species. Extremely high values $k_1=200\text{s}^{-1}$ have been found in spinach, but low values were found in the shade plant *Asarum europaeum* $k_1=20\text{s}^{-1}$ (Dietz et al. 1984). The number of photosystems per unit membrane area, expressed as Chl/ P_{700} for PSI and Chl/ Q_A for PSII, can also vary considerably between sun and obligate shade plants (Björkman 1981, Melis 1984, McCauley et al. 1984, Whitmarsh and Ort 1984). All these differences can be accounted for by expressing the number of electron transport chains per unit area (c_{e1ch}) as the number of chlorophyll molecules per cyt f molecule, i.e. $c_{e1ch}=400 \text{ Chl/cyt f}$ in sun leaves and $c_{e1ch}=1000 \text{ Chl/cyt f}$ in shade leaves (Björkman 1981).

The two turnover rates can then incorporate the differences in concentration (Q_A/P_{700}) and the differences in absorption cross section. Since we will compare our model with experiments on chloroplasts of the obligate shade plant (see paragraph 2.1.2.) *Peperomia metallica* in this chapter, we will use the following values: $c_{e1ch}=1000 \text{ Chl/cyt f} = 1.14 \cdot 10^{-13} \text{ mol } P_{700} \cdot \text{cm}^{-2}$ (based on $2 P_{700}/\text{cyt f}$ (Björkman 1981) and on $1.75 \text{ m}^2 \cdot \text{mg Chl}$ (Barber 1980), $k_1 = 100\text{s}^{-1}$, $k_2 = 1000\text{s}^{-1}$ and $n = 32/P_{700}$ (Björkman 1981). The last parameter n represents the approximate number of electron equivalents the intermediary redox chain can contain. The redox state of the intermediary electron transport chain will attenuate the proton fluxes caused by PSI and PSII as follows:

$$J_{H^+}^{PSI} = \frac{n_{rd}}{n} k_1 c_{e1ch} \quad (3.4)$$

$$J_{H^+}^{PSII} = \frac{n_{ox}}{n} k_2 c_{e1ch} \quad (3.5)$$

26 Photosynthetic Free Energy Transduction

It follows from eqs. 3.4 and 3.5 that the sum of the fractions reduced and oxidized intermediary redox equivalents must always equal 1 ($n_{r,d}/n + n_{o,x}/n = 1$). The change in time of the concentration in oxidized redox equivalents is enhanced by PSI turnovers and diminished by PSII turnovers.

$$\frac{d}{dt} (n_{o,x} c_{e,1ch}) = J_{H^+}^{PSI} - J_{H^+}^{PSII} \quad (3.6)$$

combining eqs. 3.4-3.6 yields

$$\frac{dn_{o,x}}{dt} = \frac{n_{r,d}}{n} k_1 - \frac{n_{o,x}}{n} k_2 \quad (3.7)$$

This differential equation can be solved if we assume $n_{o,x} = \chi$ at $t = 0$.

$$\frac{n_{o,x}}{n} = \frac{k_1}{k_1 + k_2} + \left(\chi - \frac{k_1}{k_1 + k_2} \right) \cdot \exp\{-(k_1 + k_2)t/n\} \quad (3.8)$$

If we define $t = 0$ as the moment saturating actinic illumination starts and $\chi = 1$, i.e. a fully oxidized intermediary redox pool, the two fluxes can be calculated as shown in fig. 3.2a.

For convenience the concomitant rise in proton motive force (p.m.f. or Δp expressed in mV) is also shown. The calculation of Δp will be explained later. It is clear from fig. 3.2a that the two fluxes reach a steady state within 0.2 s. However it is also clear that this kind of proton pumping would lead to a breakdown of the thylakoid membrane within several seconds due to a prodigious rise in Δp .

3.3.1.1. Backpressure

Extreme high levels of Δp is prevented in the thylakoid by attenuation of the turnover rate k_1 , i.e. decreasing the internal pH leads to a decreased turnover rate of PQH₂ oxidation (Siggel 1976, Huber and Rumberg 1981). The so called "backpressure" effect has been shown to be approximately linear with the pH (Huber and Rumberg 1981), which implies that it can be incorporated in k_1 as follows:

$$k_1' = \frac{k_1}{\left(1 + \alpha \cdot \frac{\Delta \bar{\mu}_{H^+}}{RT}\right)} \quad (3.9)$$

The basic assumption in eq. 3.9 is that E_m has an equivalent effect with regard to the backpressure as ΔpH . By dividing $\Delta \bar{\mu}_{H^+}$ with the gas constant (R) and the absolute temperature (T) this quotient becomes dimensionless. The parameter α expresses the coefficient of coupling. When α equals 1, eq. 3.9 implies an attenuation of k_1 by a factor of 10 when $\Delta \bar{\mu}_{H^+}$ reaches a value equivalent to $\Delta pH = -4$, a value reached after about 0.5 s of illumination in fig. 3.2a. This can be considered as a reasonable

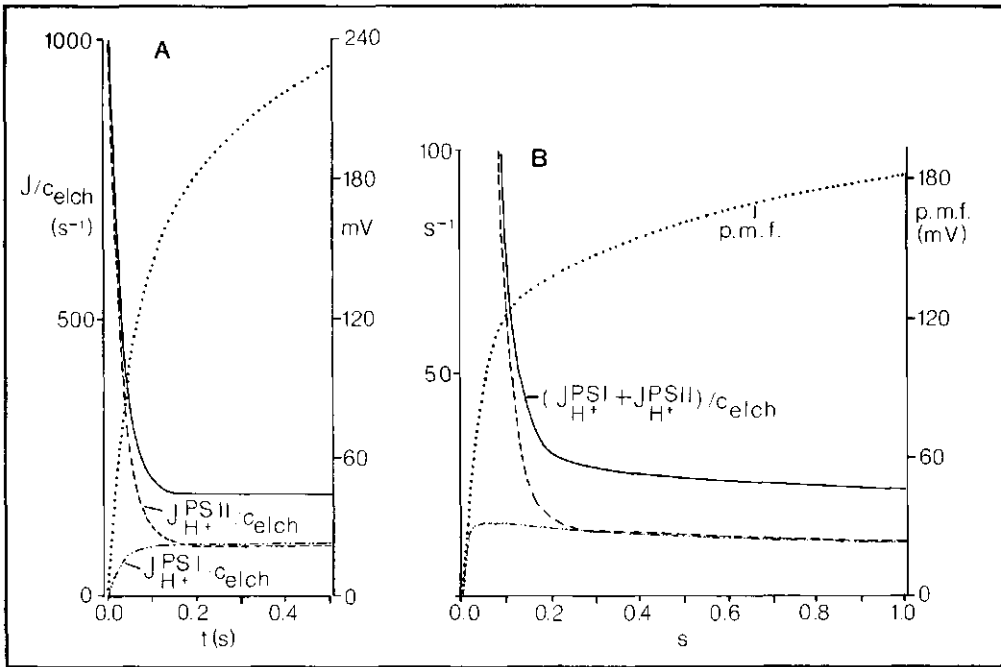


Figure 3.2. The photon-induced proton flux of both PSI and PSII calculated in a thylakoid fully permeable to all ions except protons, i.e. $P_{K^+} = P_{Mg^{2+}} = P_{Cl^-} = \infty$ and $P_{H^+} = 2 \cdot 10^{-5} \text{ cm} \cdot \text{s}^{-1}$. The concomitant rise in p.m.f. is completely based on a change in pH in the lumen. **A:** in this calculation the illumination is started at $t = 0$ and no "backpressure" of $\Delta\bar{\mu}_{H^+}$ on $J_{H^+}^{PSI}$ is assumed. **B:** equivalent to A but now a backpressure on $J_{H^+}^{PSI}$ is assumed. As a consequence it takes much longer to reach a steady state photon-induced proton flux and the p.m.f. will stay within a reasonable range. Note the difference in left hand scaling between A and B. In B the flux also starts at 1000 turnovers per electron transport chain, but the scale is started at 100 s^{-1} in order to reveal the attenuated fluxes in more detail.

value since the ratio of uncoupled to coupled electron transport under saturating continuous illumination in freshly prepared thylakoids is usually around 7 to 8 (see paragraph 2.2.2.). In fig. 3.2b the same calculation as in fig. 3.2a is shown except that eq. 3.9 is now included with $\alpha = 1$. The two flux densities become equal in magnitude after about 0.3 s of illumination. But the total magnitude $J_{H^+}^{PSI} + J_{H^+}^{PSII}$ at $t = 0.3 \text{ s}$ is much lower than in fig. 3.2a and it continues to decline as the Δp rises. If the calculation in fig. 3.2b were to be continued the proton flux would reach a steady state within 10s and the Δp stays below 250mV.

3.3.2. The Passive Dissipation of $\Delta\bar{\mu}_{H^+}$

When Δp rises due to light induced proton pumping, it can be dissipated by passive ion movements across the membrane. These

28 Photosynthetic Free Energy Transduction

passive ion fluxes can be described by the Goldman-Hodgkin-Katz equation (Goldmann 1943).

$$J_i = \frac{z_i F E_m}{RT} \cdot P_i \cdot \frac{(c_i^{out} - c_i^{in} \cdot \exp\{z_i F E_m / RT\})}{(1 - \exp\{z_i F E_m / RT\})} \quad (3.10)$$

The subscript in eq. 3.10 denotes the ion species i . The permeability coefficients (P_i) were taken from the literature ($P_{Cl^-} = 1.8 \cdot 10^{-8} \text{ cm} \cdot \text{s}^{-1}$ (Barber 1972, Vredenberg 1976), $P_{K^+} = 3.6 \cdot 10^{-8} \text{ cm} \cdot \text{s}^{-1}$ (Barber 1972, Vredenberg 1976), $P_{H^+} = 2 \cdot 10^{-5} \text{ cm} \cdot \text{s}^{-1}$ (Vredenberg 1976, Schönfeld and Schickler 1984) or $P_{H^+} = 2.5 \cdot 10^{-4} \text{ cm} \cdot \text{s}^{-1}$ (Gräber et al. 1984)). The permeability coefficient of magnesium is unknown. We assumed $P_{Mg^{2+}} = 0.5 \cdot 10^{-8} \text{ cm} \cdot \text{s}^{-1}$. The concentrations of all ions in the stroma is assumed to be constant. In reality transient concentration changes will occur, but for all ions except protons these changes will be assumed to be marginal (Vredenberg 1976) in view of the high concentrations already present in the stroma (Robinson and Downton 1984). The pH of the stroma may rise by less than 1 pH unit during illumination (Heldt et al. 1973). This rise is related to a light-induced extrusion of protons across the chloroplast envelope (Werdan et al. 1975). Since the stromal pH rises from 7.03 in the dark to 7.91 in the light (Robinson 1985), with kinetics unknown to us, we keep $\text{pH}^{out} = 7.5$ and constant. For the other ion concentrations it is known that chloroplasts in leaves contain between 40 and 200 mM K^+ (Robinson and Downton 1984) and between 20 to 40 mM Mg^{2+} (Barber 1976). However the thylakoid membrane has a large negative surface charge density, $\sigma^{in} = -3.67 \text{ } \mu\text{C} \cdot \text{cm}^{-2}$ and $\sigma^{out} = -2.06 \text{ } \mu\text{C} \cdot \text{cm}^{-2}$ at an external pH 7.5 (Mansfield et al. 1982). This leads to a surplus of positive ions in the Gouy-Chapmann double layer adjacent to the membrane surface (McLaughlin 1977). Calculations of the space charge density result in a surplus positive charge concentration of at least 0.2M in a layer of 10nm thickness adjacent to the membrane (Rubin and Barber 1980). When potassium and magnesium are present in equal concentrations in the stroma, the surplus charge near the membrane will predominantly be formed by the divalent cation (Barber 1980). These considerations have led us to choose our concentrations as follows: $c_{Mg^{2+}}^{out} = 0.1\text{M}$, $c_{K^+}^{out} = 20\text{mM}$ and $c_{Cl^-}^{out} = 20\text{mM}$. The concentrations were so chosen that E_m , according to the calculation of a passive discharge of the membrane after a flash, will decay with a halftime of 60 ms (Bulychev et al. 1976 and see paragraph 2.1.1.2.).

When eq. 3.10 is used it must be replaced by an approximation whenever the exponential functions ($\exp\{z_i F E_m / RT\}$) approach the value of 1, i.e. when E_m approaches the value of 0. The following approximation was used whenever $|E_m| \leq 0.5\text{mV}$ (Schultz 1980):

$$J_i = P_i \cdot (c_i^{out} \cdot \exp\{-z_i F E_m / RT\} - c_i^{in} \cdot \exp\{z_i F E_m / RT\}) \quad (3.11)$$

By using the equations and values of the physical parameters given one can calculate the time resolved potential and flux density changes in a system consisting of light driven proton pumps and the passive dissipation by protons and three other ions. The results of such a calculation are given in fig. 3.3.

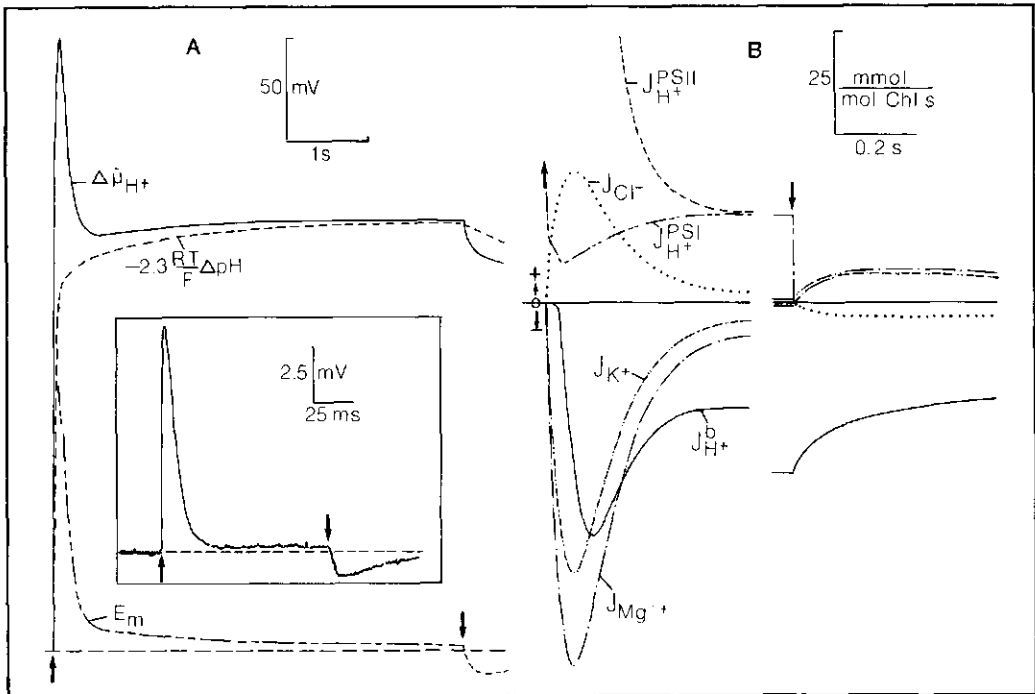


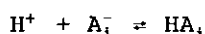
Figure 3.3. A: calculation of the three potentials influencing the proton flux in a thylakoid. The upward arrows indicate the start and the downward arrows the end of actinic illumination. The inset shows an E_m profile measured in a *P. metallica* chloroplast immersed in a medium with DCCD (≈ 1 mM). The apparent similarity between the measured E_m profile and the calculated one is probably explained by the lack of buffer in the lumen. B: the fluxes of all ions and protons are given on an enlarged time scale. The non-protonic passive fluxes are the major ones when E_m is large. After 0.3 s the passive proton flux J_{H^+} is the major flux and this remains so even after the illumination period.

The time resolved changes in E_m , $-2.3(RT/F)\Delta pH$ and Δp are shown. The values of parameters not mentioned so far are $T=293.16K$, $C_m=1 \mu F \cdot cm^{-2}$ (Vredenberg and Tonk 1975) and $A/V=2.9 \cdot 10^6 cm^{-1}$ (equivalent to $5 \mu l \cdot mg^{-1} Chl$). The buffering parameter β used in eq. 3.2 was taken as 1, which explains the steep rise in Δp . The state of the intermediate redox pool at $t=0$ was not taken as fully oxidized, since *cyt f*, *Pc* and P_{700} normally stay reduced in the dark, i.e. $\chi = 0.867$ (Velthuys 1980, Haehnel 1984). The value of the turnover rate of PSII was halved compared to the calculations shown in fig. 3.2. This was done to prevent E_m from reaching a prodigious peak value in the simulated first 200ms. In fig. 3.3b all the time courses of the changes in flux densities are shown on an enlarged time scale. It is clear that the main passive fluxes are those of the cations (not the protons) and the anion in the first 200ms of simulated time. After that period the passive proton flux becomes predominant (see also Peters et al. 1985). Before the light is turned off the system has reached a true steady state in that the passive proton flux density is

equal in magnitude but opposite in sign to the sum of the light induced flux densities, i.e. $J_{H^+}^{PSI} + J_{H^+}^{PSII} + J_{H^+}^b = 0$. After the light is turned off the passive proton flux remains the main dissipative flux for many seconds. The time course of E_m in fig. 3.3a resembles experimental results from microelectrode measurements in *Peperomia metallica* chloroplasts *in situ* immersed in a medium with a high concentration of DCCD, i.e. more than 1 mM (see inset fig. 3.3a). DCCD is known to inhibit the ATPase at low concentrations, ≤ 50 nM (Peters et al. 1985). The effects at high concentrations are quite unpredictable. However covalent binding of DCCD to carboxyl residues (COO^-) of proteins is likely to occur. These residues form the main buffering constituent of the lumen (Walz et al. 1974). Since our calculations in fig. 3.3 do not contain any buffering effect, i.e. $\beta = 1$, this might explain the apparent similarity between calculation and experiment under these conditions.

3.3.3. The Buffering Capacity of the Lumen

In order to describe the buffering capacity in the lumen, it is necessary to derive a proper algorithm for β in eq. 3.2. From literature data (Helldt et al. 1973, Walz et al. 1974, Junge et al. 1979) it is possible to deduce such parameters as the concentration of certain buffer groups in the lumen B_i and their dissociation constants K_i . These parameters are related to a buffer reaction as follows:



$$K_i = [A_i^-] \cdot [H^+] / [HA_i]$$

$$B_i = [HA_i] + [A_i^-]$$

When the above equations are combined an expression can be derived for the total concentration of protonated buffer groups as a function of free proton concentration.

$$[HA_i] = \frac{B_i \cdot [H^+]}{K_i + [H^+]} = \frac{B_i \cdot c_{H^+}^{in}}{K_i + c_{H^+}^{in}} \quad (3.12)$$

If the change in both bound and free proton concentrations can be considered to be infinitesimal, both sides in eq. 3.12 can be differentiated with respect to the free proton concentration:

$$d[HA_i] = \frac{B_i \cdot K_i}{(K_i + c_{H^+}^{in})^2} dc_{H^+}^{in} \quad (3.13)$$

The sum of bound and free proton concentration changes (dh^+) is related to the net proton flux $\sum J_{H^+}$ and the incremental time period Δt as follows:

$$dh^+ = \frac{A}{V} \sum J_{H^+} \cdot \Delta t = d[HA_i] + dc_{H^+}^{in} \quad (3.14)$$

When more than one buffer type is present eq. 3.14 can easily be expanded (to incorporate all buffers present)

$$dh^+ = \sum_i d[HA_i] + dc_H^{i+} \quad (3.15)$$

By combining eqs. 3.13 and 3.15 the expression for β in eq. 3.2 results

$$\beta = \left[1 + \sum_i \frac{B_i \cdot K_i}{(K_i + c_H^{i+})^2} \right]^{-1} \quad (3.16)$$

This expression for β is not the proper buffer capacity as defined in (Junge 1979), but it can be transformed into it. However eq. 3.16 is useful once we know the values of B_i and K_i in the lumen of the thylakoid. When we try to extract the concentrations B_i from literature data we must keep in mind that different authors have determined the lumenal buffer capacity under different conditions, i.e. in vivo (Heldt et al. 1973), in isotonic suspension (Walz et al. 1974), or in hypotonic suspension (Junge et al. 1979). Since almost all proton buffers are either protein residues or lipid headgroups, a change in surface to volume ratio (A/V) will result in an equivalent change in B_i . The maximum surface to volume ratio reported on up till now is $A/V = 5.3 \cdot 10^6 \text{ cm}^{-1}$, which is equivalent to $3.3 \mu\text{l} \cdot \text{mg}^{-1} \text{ Chl}$ (Heldt et al. 1973). We estimate the concentrations B_i for this value of A/V and then multiply by the ratio of A/V actually used and this maximum value. In the calculations presented in this chapter this results in a ratio of 3.3/5. In Table 3.1 the concentrations B_i and dissociation constants K_i of the different buffer types in the lumen are given. The sum of the concentrations is assumed to be $\sum B_i = 0.3\text{M}$, which is based on the value of 1 mole buffer per mole chlorophyll found in (Walz et al. 1974) and $3.3 \mu\text{l} \cdot \text{mg}^{-1} \text{ Chl}$. In the pK range from 8 to 6.5 the buffering is constant (Junge et al. 1979). Below pH 6.5 there is a steep rise in buffering capacity peaking at pH 5.5 (Heldt et al. 1973, Walz et al. 1974). Beneath pH 4.5 the buffering capacity rises again very steeply (Walz et al. 1974), probably due to the fact that most phospholipids and sulpholipids are oriented to the lumenal side of the membrane (Sundby and Larson 1985). The values in table 3.1 must be considered as a crude approximation of reality. However the values give rise to a satisfactory fit to the experimental curve presented in (Walz et al. 1974).

Calculations of the time-course of the potential changes incorporating the buffers of table 3.1 are shown in fig. 3.4. The effect of the buffering on the potential changes is clear when

Table 3.1. Buffer concentrations B_i and their concomitant dissociation constants pK_i in the lumen estimated from literature data (Heldt et al. 1973, Walz et al. 1974, Junge et al. 1979) and based on a volume to chlorophyll ratio of $3.3 \mu\text{l} \cdot \text{mg}^{-1} \text{ Chl}$ and $\sum_i B_i = 300 \text{ mM}$.

B_i	10	10	10	10	15	40	40	45	50	70 mM
pK_i	8.0	7.5	7.0	6.5	6.0	5.5	5.0	4.5	4.0	3.5

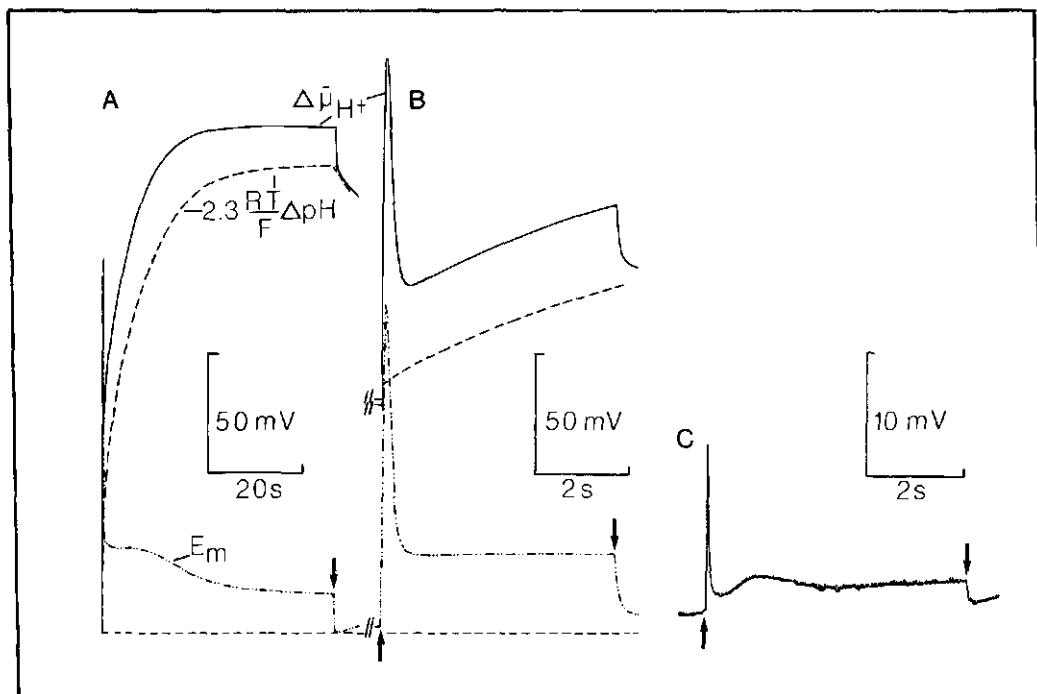


Figure 3.4. A: calculated time-course of the potentials in a fully buffered thylakoid (see table 3.1). The upward arrows indicate the start and the downward arrows the end of actinic illumination (illumination period = 50 s). After the light is turned off the calculation is continued simulating 4 minutes dark adaptation. B: calculated time-course of the potentials after 4 minutes dark adaptation. This potential time-course should be compared with the results of the microelectrode experiments. C: measured time-course of E_m in *P. metallica*. The complexity of this time-course is not reflected in the calculated profile shown in B. Note the difference in time scale between A and B.

fig. 3.4 is compared with fig. 3.3. The rise in chemical proton potential is slower and more in accordance with the associated light scattering changes found in Coughlan and Schreiber (1984a, 1984b). It takes about 50 s of saturating actinic illumination before steady-state is attained (fig. 3.4). The electric membrane potential (E_m) in the steady-state is higher due to the fact that the non-protonic ion fluxes have created a Nernst potential which is non-negligible. After 50 s of illumination (fig. 3.4a) the calculation is continued to simulate the process during 4 minutes dark adaptation. The reoxidation of the intermediary redox pool was assumed to be a pseudo first order process with a rate constant of 0.038 s^{-1} (Renger and Schultze 1985).

In fig. 3.4b a simulation of the potential changes in the light after the 4 minutes dark adaptation of fig. 3.4a is shown. These calculations were done to simulate the experimental procedure used in microelectrode measurements. Before a microelectrode recording, as shown in fig. 3.4c, can be performed

the chloroplast is preilluminated for at least a few minutes, due to the requirement of light for the visualization of the impalement (see paragraph 2.1.1.). Successive dark adaptation periods are usually about 4 minutes (Bulychev 1984b). When figures 3.4b and 3.4c are compared it is clear that the complexity of the experimental time course of E_m is not simulated by our model as yet. This is mainly due to the lack of active dissipation of $\Delta\bar{\mu}_{H^+}$ by a simulated proton conducting ATPase, as will be shown below.

3.3.4. The ATPase Dependent Proton Flux

In order to make our model a better reflection of reality it is necessary to incorporate the ATPase dependent proton flux density. A full algorithm for this flux density, containing both activation and chemical reaction rate, has been presented in (Gräber and Schlodder 1981). The validity of this algorithm was corroborated in (Gräber et al. 1984). The description of the ratio of activated to total ATPases (E_a/E_t), could be retained without modification in our calculations.

$$\frac{E_a}{E_t} = \frac{K_E^0 \exp\{-b\Delta\bar{\mu}_{H^+}/RT\}}{1 + K_E^0 \exp\{-b\Delta\bar{\mu}_{H^+}/RT\}} \quad (3.17)$$

The values $pK_E^0 = 5.9$ and $b = 1.7$ of (Gräber et al. 1984) have been used here. However the algorithm for the relative rate of ATP synthesis (v/v_{max}) could not be retained, because of the fact that the values of some parameters therein need to be estimated and moreover will change with pH in an unknown fashion. For our calculations we approach the relative rate of ATP-synthesis with a simple first order discontinuous function:

$$\frac{v}{v_{max}} = \begin{cases} 1 & \Rightarrow \Delta\bar{\mu}_{H^+} > \frac{\Delta G_{ATP}}{n} + \frac{RT}{a} \\ \frac{a}{RT} (\Delta\bar{\mu}_{H^+} - \frac{\Delta G_{ATP}}{n}) & \\ -\frac{1}{3} & \Rightarrow \Delta\bar{\mu}_{H^+} < \frac{\Delta G_{ATP}}{n} - \frac{RT}{3a} \end{cases} \quad (3.18)$$

In eq. 3.18 n equals the stoichiometry number (H^+/ATP) for which we used the well accepted value of three (Strotmann and Schumann 1983, Strotmann and Bickel-Sandkötter 1984). The value of the slope $a = 0.53$ was taken from (Junesch and Gräber 1984), i.e. ΔpH dependent ATP synthesis rate in pre-activated thylakoids. The value of $v_{max} = 380 \text{ mmol ATP} \cdot (\text{mol Chl})^{-1} \cdot \text{s}^{-1}$ (Gräber et al. 1984) converted to our coordinate system was $-2.2 \cdot 10^{-11} (\text{mol ATP}) \cdot \text{cm}^{-2} \cdot \text{s}^{-1}$. A combination of eqs. 3.17 and 3.18 leads to the ATPase dependent proton flux density:

$$J_{H^+}^{ATP} = n \frac{E_a}{E_t} \frac{v}{v_{max}} \quad (3.19)$$

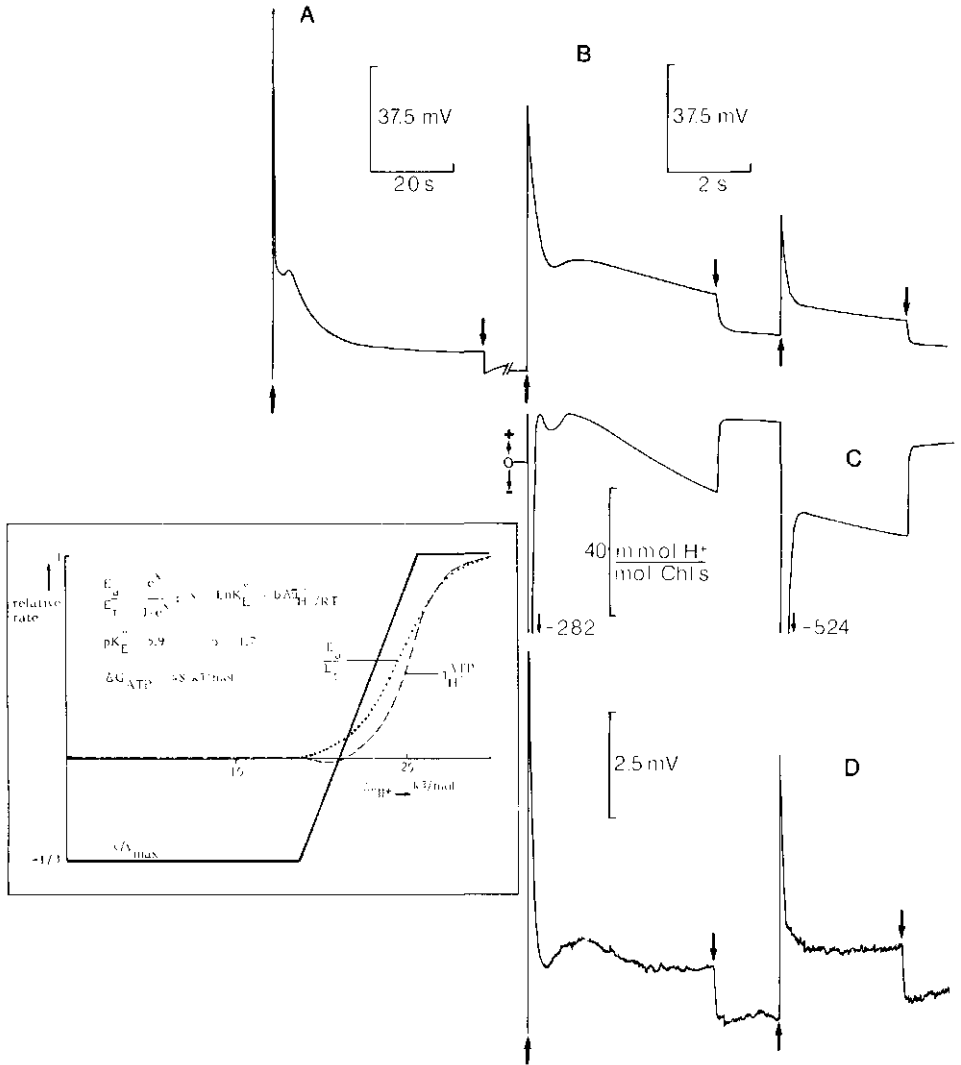


Figure 3.5. A: calculated E_m time-course equivalent to fig. 3.4a except that an active dissipation of $\Delta\bar{\mu}_{H^+}$ is now possible through a simulated ATPase. In the inset the proton flux density calculated for the ATPase, i.e. $J_{H^+}^{ATP}$, is shown. The mathematical formulation of $J_{H^+}^{ATP}$ is taken from Gräber et al. (1984) and $\Delta G_{ATP} = 46 \text{ kJ}\cdot\text{mol}^{-1}$. After a 50 s actinic illumination period the light is shut off and dark adaptation is simulated for a 4 min. period. **B:** two subsequent illumination periods simulated after 4 minutes dark adaptation. Upward arrows indicate the start and downward arrows the end of actinic illumination. The complex time-course of the two subsequent actinic illumination periods is a result of the steep slope in eq. 3.18. **C:** the calculated ATPase dependent proton flux from the same simulation as in B. Positive flux is equivalent to ATP hydrolysis and a negative flux is equivalent to ATP synthesis. The flux should be divided by the stoichiometry

Our model now allows a calculation of ΔG_{ATP} as a function of $J_{H^+}^{ATP}$ and changes in P, ADP and ATP concentrations. But for a proper simulation incorporating the changes in ΔG_{ATP} it is necessary to incorporate the functioning Calvin cycle and the adenylate kinases as well (Peters et al. 1986). Since it has been found that ΔG_{ATP} is not subject to large fluctuations, e.g. between 42 in the dark and 46 kJ·mol⁻¹ in the light (Giersch et al. 1980), in intact chloroplasts we have left it constant for the calculations shown in fig. 3.5, i.e. $\Delta G_{ATP} = 46$ kJ·mol⁻¹. When we compare the experiment (fig. 3.5d) with the calculations in fig. 3.5b the qualitative equivalence is evident. The amplitudes of E_m however differ by about a factor 10. The amplitude of the peak value of E_m differs strongly from impalement to impalement (our record to date is a maximum of 118 mV). In the experiment shown in fig. 3.5 the total resistance of the microelectrode rose by more than 10 M Ω after impalement, while a rise of 0.5 M Ω can be expected for a chloroplast of 30 μ m diameter and a membrane resistance of $R_m = 10^4 \Omega \cdot \text{cm}^2$ (Vredenberg 1976). This rise in impedance could indicate a clogging up of the electrode tip and might explain a certain attenuation of E_m .

The time course of E_m (fig. 3.5a, b, d) can now be explained by close inspection of the flux changes (fig. 3.5c). The transient initial peak of E_m after turning on the light is caused by the excessive imbalance in turnover rate of PSII and PSI common to obligate shade plants (Melis 1984). The second peak in E_m is mainly caused by a change from ATP hydrolysis to ATP synthesis (fig. 3.5c) when $\Delta \bar{\mu}_{H^+}$ surpasses $\Delta G_{ATP}/n$. This is corroborated by the fact that the second peak is absent when the chloroplast is preenergized or when DCCD is present, e.g. fig. 3.3 and (Bulychev et al. 1980).

3.4. Conclusions

The model presented in this chapter is a rough approximation of photosynthetic free-energy transduction in thylakoids. The description of the light-induced proton pump rates (eqs. 3.4, 3.5 and 3.8) meets the determined boundary conditions. The time-dependent change of the redox state of the intermediary PQ pool is too simple to describe the actual process. To improve this formulation it will be necessary to incorporate a set of differential equations describing charge separation and charge movement at the reducing side of PSII, as has been done before (Renger and Schulze 1985, Snel et al. 1987). Due to the fact that we compare saturating actinic illumination experiments with our simulations, eq. 3.8 gives a reasonable fit. Whenever the model will be used to simulate the fluxes at low light intensities, a more precise description of the

number $n (= 3)$ in order to obtain the actual rate of ATP synthesis or hydrolysis. D: measured E_m time-course of two subsequent illumination periods after 5 minutes dark adaptation in a *P. metallica* chloroplast. The complex kinetics of this time-course is clearly reflected in the calculated trace B. Note that the time axis is the same in B, C and D, but different in A.

light-induced proton fluxes with the intermediary redox reactions will be necessary.

The use of $\Delta\bar{\mu}_{H^+}$ instead of ΔpH (Huber and Rumberg 1981) in eq. 3.9 is not experimentally sustained. When $\Delta\bar{\mu}_{H^+}/RT$ was substituted by $-2.3\Delta pH$ the initial electric membrane potential E_m reached an 'unphysiological' transient level after the light was turned on. A transformation of E_m into ΔpH is assumed to occur at the PQH₂ oxidation site, i.e. $F E_m/RT$ inhibits PQH₂ oxidation in the same manner as $-2.3\Delta pH$. A similar mechanism has been suggested to occur within the ATPase (Gräber and Schlodder 1981).

The presence of different buffer groups in the model is a point of consideration. Although table 3.1 is derived from the available experimental data, these data are insufficient for our purpose. The buffering capacity has a profound influence on the time-resolved E_m (e.g. compare figs. 3.3 and 3.4). After the initial peak in the first 100 ms of illumination, E_m becomes a continuous descending function in the light, i.e. $dE_m/dt \leq 0$. This decay rate will be slower in the presence of luminal buffers. However, this will never result in a transient rise. As shown in figs. 3.4 and 3.5 a second transient rise in E_m during illumination occurs. To explain this rise an (extra) active influx of positive charges is required. A possible explanation is the influx caused by the hydrolysis of ATP (fig. 3.5c). The relative magnitude of the second rise in E_m during illumination will, amongst other things, be strongly dependent on ΔG_{ATP} (see eqs. 3.17-3.19). Microelectrode recordings of the liverwort *Anthoceros* sp. reveal a much higher secondary potential rise (Bulychev 1984a, Bulychev 1984b). This can be explained with our model either by assuming a higher ΔG_{ATP} in the stroma of these *Anthoceros* chloroplasts, or by a shift in the activation ratio curve (eq. 3.17) to lower values of $\Delta\bar{\mu}_{H^+}$ as has recently been shown to be the case (Gräber et al. 1987, Junesch and Gräber 1987). The latter explanation appears to be the most likely and when incorporated in our model should bring our rather high values of ΔG_{ATP} , used to simulate the responses shown in fig. 3.5, down to more realistic values.

In this chapter we have presented the basic version of our model. The model can also accommodate the effects of a Q-cycle, a Donnan potential, membrane modifying reagents and phosphorylation of the light harvesting complex. Some of these effects will be explored in the next chapter. However, the model needs further verification with regard to other readily measurable phenomena, such as proton uptake, oxygen evolution and electron transport. Recent measurements of $\Delta\bar{\mu}_{H^+}$ in *P. metallica* with an antimony pH sensitive microelectrode compare very well with our mathematical results (Remis et al. 1986a, Remis et al. 1986b).

4. Applications of the Model

4.1. Introduction

In this chapter we will show some possible applications of the model, which was presented in the previous chapter. We will enhance the validity of the model by introducing the Donnan potential, which is known to be present in thylakoids (Siggel 1981c). We will simulate the effect of certain ionophores and other uncouplers and compare them to experimental results (Vredenberg and Bulychov 1976). In the end we will give a tentative application of calculating the variable fluorescence curve incorporating both Q-dependent and energy dependent quenching (Krause and Weis 1984, Schreiber et al. 1986).

4.2. The Donnan Potential

From the work of U. Siggel (Siggel 1981a-c) we know that both the surface charge density and the Donnan potential are of a considerable magnitude in thylakoids. The surface charge density can be determined (Mansfield et al. 1982). The thylakoid Donnan potential is not determined directly. However as is shown by Werdan et al. (1975) its consequence is that $\Delta\text{pH} = 1$ in dark adapted thylakoids *in situ*. The Donnan potential is the consequence of the impermeability of the membrane to certain large or membrane bound electrolytes. This causes a difference in concentration of permeable electrolytes on both sides of the membrane. The resulting chemical potential is compensated by the Nernst potential, thus creating a true equilibrium with all $\Delta\mu_i = 0$. In order to calculate the Donnan potential it is necessary to envisage the process by which it is created. In fig. 4.1 we try to depict this process in an imaginary experiment. Consider a flat sheet of membrane floating in an infinite volume of an aqueous solution containing salts (fig. 4.1a). The surplus negative surface charge density of the membrane attracts mainly divalent cations in its Gouy-Chapmann diffuse charge layer. For simplicity we assume a solution containing 30 mM KCl and 10 mM Mg^{2+} . The surplus positive charge is assumed to be fully compensated by the presence of immobilized negative surface charges on a suspension of membrane sheets. The proton concentration is supposed to be pH 7.5. Imagine we possess a switch with which we can turn the flat membrane sheets into closed vesicles instantaneously. At a certain moment ($t = 0$) we activate this switch and create closed envelopes separating

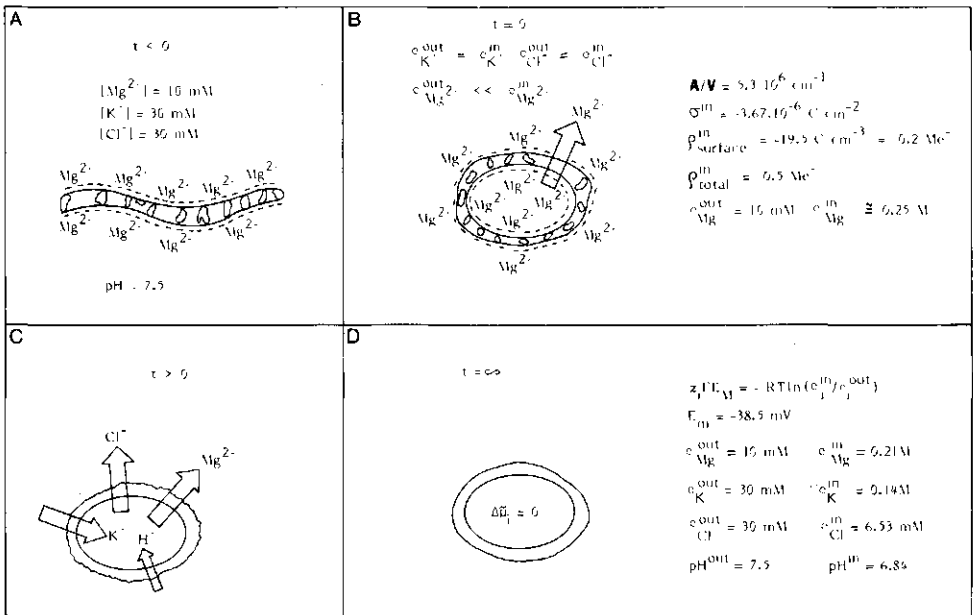


Figure 4.1. Imaginary experiment to calculate the Donnan potential in a thylakoid. **A:** A flat sheet of a proteo-lipid bilayer with a negative surface charge density is pictured in an ionic solution. The main ion in the Gouy-Chapmann diffuse charge layer is assumed to be magnesium. **B:** at a certain moment ($t = 0$) the bilayer is imagined to transform into a closed envelope separating inside (lumen) from outside (stroma). The surface to volume ratio (A/V) on the outside is virtually nil, i.e. $\leq 0.1 \text{ cm}^{-1}$. However on the inside it is very large, i.e. for thylakoids $\geq 10^6 \text{ cm}^{-1}$. As a consequence a large concentration difference in magnesium ions results. With a tendency to flow from the lumen to the stroma. **C:** after closure of the membrane ($t > 0$) different ionic fluxes across the membrane will occur. The magnitude and time dependence of these fluxes can be calculated. **D:** after a relatively long period ($t = \infty$) equilibrium is reached. If the starting parameters are chosen as shown in **B** then the final equilibrium situation will be as shown here.

inside (lumen) from outside (stroma). Mg^{2+} will still be the main ion near the lipid bilayer (fig. 4.1b). However the surface to volume ratio (A/V) for the external (stromal) side is considered to be 0 due to the infinite size of the suspension. The surface to volume ratio of the internal (luminal) side is very large, e.g. $A/V = 5.3 \cdot 10^6 \text{ cm}^{-1}$ (see chapter 3). This combined with the assumed surface charge density (σ^{in}) leads to a negative volume charge density $\rho_{\text{surface}}^{\text{in}} = -19.5 \text{ C} \cdot \text{cm}^{-3}$, which is equivalent to a concentration of 0.2 M negative charges exclusively due to the surface charge density. However the lumen is also filled with water soluble proteins with a negative charge (e.g. plastocyanin). This leads us to assume a total concentration of 0.5 M negative charges of non-permeable electrolytes in the lumen. The negative volume charge density $\rho_{\text{total}}^{\text{in}} = 0.5 \text{ Me}^-$ is compensated solely by Mg^{2+} ions at $t = 0$. This creates a concentration difference of Mg^{2+} concentration between the lumen and the stroma, i.e.

$c_{Mg^{2+}}^{out} = 10 \text{ mM}$ and $c_{Mg^{2+}}^{in} = 0.26 \text{ M}$. This would lead to a large efflux of Mg^{2+} , but requires compensating charge fluxes. To compensate for this Mg^{2+} efflux potassium ions and protons flow into the lumen and chloride ions will flow out (fig. 4.1c). When a new equilibrium is reached all concentration differences will be compensated by the Donnan potential, i.e. $\Delta\bar{\mu}_i = 0$ (fig. 4.1d). When calculated for our situation this leads to a Donnan potential of $E_m = -38.5 \text{ mV}$. This still falls short of the $\Delta pH = 1$ that was measured (Werdan et al. 1975). However it was shown that the chemiosmotic potential difference at equilibrium is not solely attributable to the Donnan potential. Overlap of Gouy-Chapmann layers due to the very high surface charge density also give rise to a potential gradient (Siggel 1981c). Although one would expect the extension of this layer to be minimal (e.g. a nanometer or less) due to the high salt concentrations on the inside. These concentrations are however calculated with the aid of the Goldman-Hodgkin-Katz equation, which does not include any provisions for activity changes. In these concentration ranges we expect the activity coefficients of both potassium and chloride to be near unity, while it is expected to be near 0.7 for magnesium (Bockris and Reddy 1977).

4.2.1. Calculating the Donnan Potential

The model described in the previous chapter is ideally suited to calculate the Donnan potential as described above. By leaving out the active fluxes in fig. 3.1, i.e. $J_{H^+}^{PSI}$, $J_{H^+}^{PSII}$ and $J_{H^+}^{ATP}$, and starting with the boundary conditions as shown in fig. 4.1b we can simulate the process of attaining Donnan equilibrium. The result of these calculations is shown in fig. 4.2. In fig. 4.2a we see the ionic flux densities in the first 100 s after closure of the membrane. It is clear that the efflux of both Mg^{2+} and Cl^- is compensated by the influx of K^+ . The influx of protons is negligible due to the high pH. Although the model contains no direct restrictions to enforce electroneutrality, calculations never reveal any violation of this. In fig. 4.2b the calculated potential changes in the first 100 min. after membrane closure are shown. The final Donnan potential, i.e. $E_m = -38.5 \text{ mV}$, is reached in a relatively short period of 1 or 2 minutes. Final equilibrium is not reached within these first 100 minutes. Due to the low proton concentration it takes several hours before full equilibrium is reached, i.e. $\Delta\bar{\mu}_i = 0$.

4.2.2. The effect of the Donnan potential

In order to study the effect of the Donnan potential we must compare light-induced potential changes in the presence and the absence of this potential. This is where the value of our model becomes clear since it is virtually impossible to perform the above experiment in reality. First we calculate the potential changes and flux densities as we have done in the previous chapter (see fig. 3.5). In chapter 3 we have used parameters to simulate the responses of an obligate shade plant like *P. metallica*. However, to be more in accord with the vast majority of photosynthetic free-energy transduction research, we will now

40 Photosynthetic Free Energy Transduction

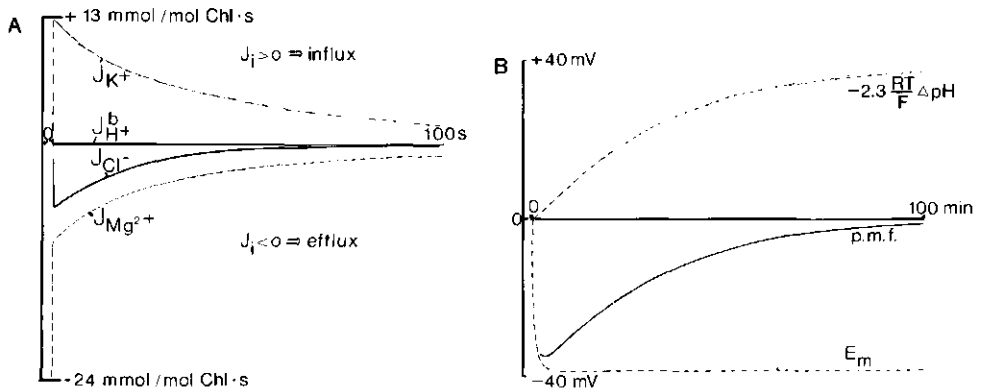
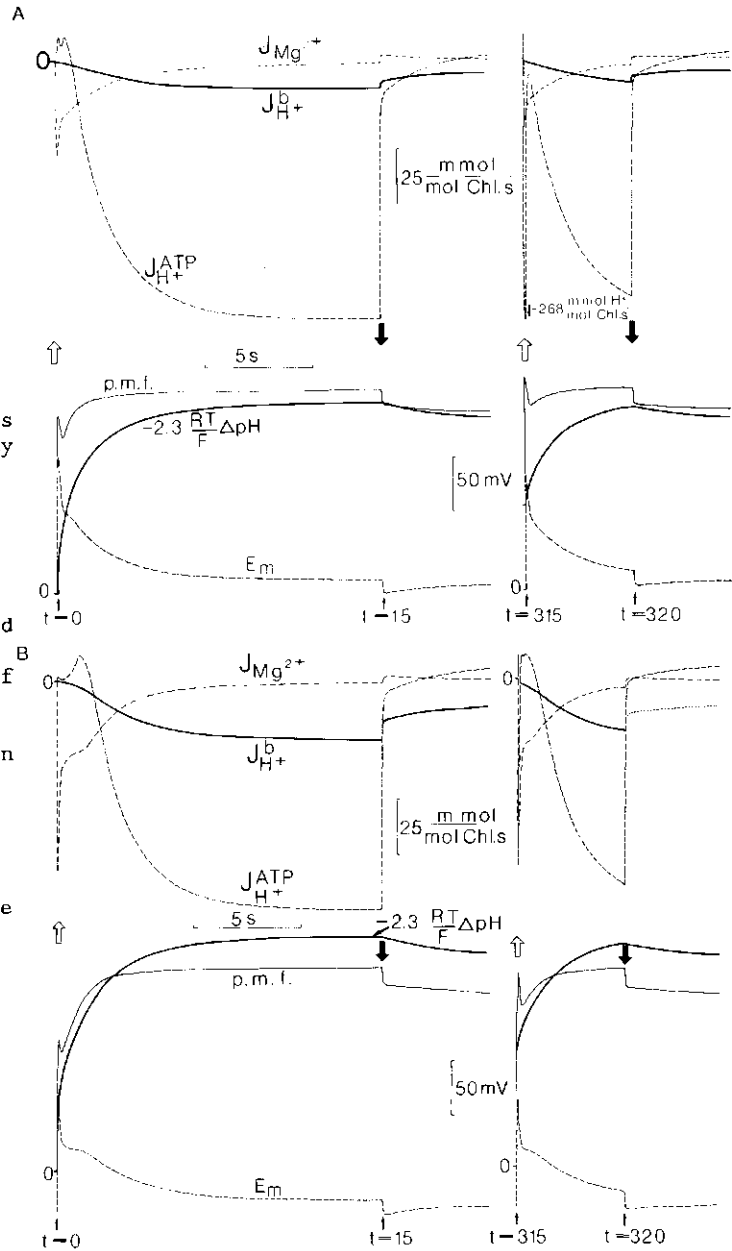


Figure 4.2. Calculated time-courses of the passive ionic fluxes A and the electrochemical potentials B from the imaginary experiment shown in fig. 4.1. **A:** ionic fluxes during the first 100 s after membrane closure. The large efflux of magnesium ions is mainly compensated by a large influx of potassium ions. Also an efflux of chloride ions is seen, but the magnitude of this efflux decays fast due to the depletion of chloride ions in the lumen. The proton influx is extremely small, due to the high pH chosen at $t \leq 0$. **B:** the time-course of the electrochemical proton potential and its components in the first 100 minutes after membrane closure. The electric potential E_m is seen to reach its final level relatively fast. The equilibration of the proton concentration in the lumen is very slow. An equilibration period of more than an hour needs to be simulated before "true" equilibrium is reached, i.e. p.m.f. = 0.0 ± 0.1 mV.

use parameters to simulate chloroplasts of a sun plant like spinach. The results of these calculations are shown in fig. 4.3. In order to simulate the chloroplasts of sun type plants the following values were used: $c_{chl} = 400$ Chl/cyt f = $1.43 \cdot 10^{-13}$ mol P_{700} cm^{-2} , based on 1 P_{700} /cyt f (Björkman 1981) and on 1.75 $m^2 \cdot mg^{-1}$ Chl (Barber 1980), $k_1 = 240$ s^{-1} (Dietz et al. 1984), $k_2 = 400$ s^{-1} and $n = 36/P_{700}$ (Björkman 1981). The free-energy of ATP was taken at a constant level, i.e. $\Delta G_{ATP} = 48$ $kJ \cdot mol^{-1}$. These parameters were used to perform essentially the same calculations as in fig. 3.5. In fig. 4.3a the potential changes and the changes in flux densities of three important fluxes are shown. Simulation of a 15 s illumination period appeared to be sufficient for the system to attain steady state, which is mainly due to the higher turn over rate of PSI (Coughlan and Schreiber 1984a and b). From $t = 15$ s to $t = 315$ s a dark adaptation period of 5 min. is simulated. Then a 5 min. illumination period followed by darkness is simulated. The pronounced fluctuations in E_m seen in fig. 3.5a and 3.5b are absent here, due to the change in the parameters involved in energy transduction. However the extreme fluctuations in $J_{H^+}^{ATP}$, which were evident in fig. 3.5c, can also be seen in fig. 4.3a.

In fig. 4.3b the same calculations are performed, but now in the presence of the Donnan potential. This is immediately clear when we look at the starting value of E_m at $t = 0$, i.e. $E_m = -38.5$ mV. Due to the relatively high concentrations of

Figure 4.3. A: Calculated fluxes (top) and potentials (bottom) for a thylakoid from a sun adapted plant such as spinach. Open upward arrows and closed downward arrows indicate the respective beginning and end of a saturating actinic illumination period. The first 15 s illumination period is used to reach a steady state level of photosynthetic free energy transduction. After the light is turned off a dark adaptation period of 5 minutes is simulated and a consecutive illumination period of 5 s is shown ($315 < t < 320$ s). Compared to the calculations in chapter 3 we have changed the turnover rates of the two photosystems, i.e. $k_1 = 300 \text{ s}^{-1}$ and $k_2 = 500 \text{ s}^{-1}$, the free energy of phosphorylation $\Delta G_{\text{ATP}} = 48 \text{ kJ}\cdot\text{mol}^{-1}$ and the size of the intermediary redox pool, i.e. $n = 22/P_{700}$. **B:** Same as in A, however at $t = 0$ we start with a Donnan potential as calculated in fig. 4.1d. As a consequence the electric potential will be more negative inside, which tends to enlarge the passive ion fluxes and has a damping effect on the strong fluctuations of the proton flux through the ATPase ($J_{\text{H}^+}^{\text{ATP}}$). The difference in ATP synthesis rates in the steady state ($t = 15$ s) is marginal.



cations on the luminal side, e.g. see fig. 4.1d, their passive flux densities are larger compared to the flux densities in

fig. 4.3a. This leads to a slight diminution of the steady state ATPase dependent proton flux density. However the extreme fluctuations in $J_{H^+}^{ATP}$ are damped to a certain extent. This last effect should be larger in reality due to the fact that our calculated Donnan potential is only a part of the total electric potential in the dark adapted state (Siggel 1981c). The measured value of $\Delta pH = 1$ in dark adapted intact chloroplasts (Werdan et al. 1975) indicates that in our calculation a third of the dark equilibrium E_m is still unaccounted for. Experiments with spinach thylakoids, albeit frozen and thawed, give a qualitative result in accord with these calculations (Siggel 1981d).

4.3. The Effects of Uncouplers

One of the most potent techniques of verifying the chemiosmotic hypothesis was the use of selective uncouplers of electron transport from photophosphorylation (Witt 1979). The more popular ones used in photosynthesis research are valinomycin, nigericin, ammonia, gramicidin and CCCP or FCCP. Each of these substances represents a different class of uncouplers, but they all have in common that they uncouple by dissipating part or the total of the generated $\Delta \mu_{H^+}$ in contrast to uncouplers like DCCD or tentoxin which are ATPase inhibitors. When applying ionophoric uncouplers in photosynthesis research one makes certain assumptions concerning specificity and effect. In our model it is possible to formalize the assumptions and then equate the effect.

4.3.1. (F) CCCP

CCCP and FCCP are known to be potent protonophoric uncouplers (Peters et al. 1984c), which selectively enhance the membrane's proton permeability. Since no values are known for the membrane permeability with CCCP present we assumed P_H to change from $2 \cdot 10^{-5}$ to $2 \cdot 10^{-2} \text{ cm} \cdot \text{s}^{-1}$. As was explained in (Vredenberg 1976) it is necessary to enhance the proton permeability by more than 2 orders of magnitude before the flux density starts competing with the other ionic flux densities. In fig. 4.4 the results of calculations with this enlarged proton permeability are shown and should be compared with fig. 4.3b. As expected with such a large P_H the passive proton flux density dominates all other fluxes. The ATPase dependent flux density remains virtually nil as compared to the flux shown in fig. 4.3b, which asserts the fact that CCCP and FCCP are potent uncouplers. However this does not imply that the proton gradient across the thylakoid membrane is abolished altogether. The electric potential E_m in the steady state, compared to the Donnan equilibrium potential in the dark adapted state, is almost zero. This results in a ΔpH in the steady state equivalent to about 50 mV. The large undershoot in E_m when the light is turned off reflects the large passive proton flux (Vredenberg 1976, Bulychev et al. 1980) and is the first calculation revealing the actual relation on theoretical grounds between the size of the undershoot after the light is switched off and the passive proton flux density. Other model calculations (Heinz 1982) show a similar response of E_m to illumination.

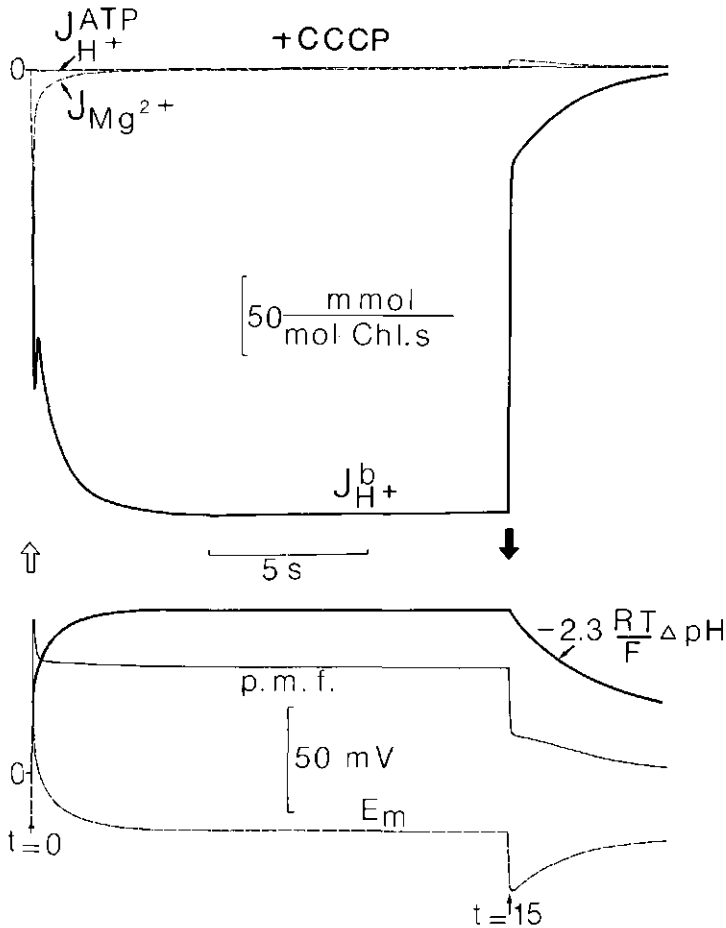


Figure 4.4. Calculated fluxes (top) and potentials (bottom) for a thylakoid as in fig. 4.3b. The presence of a protonophoric uncoupler CCCP or FCCP is simulated by changing the membrane proton permeability at $t = 0$ from $P_R = 2 \cdot 10^{-5}$ to $2 \cdot 10^{-2} \text{ cm} \cdot \text{s}^{-1}$. As a consequence the ATPase remains inactive and the passive proton flux is the main dissipative flux. However the p.m.f. in the steady state is not zero. Due to the large buffering power in the lumen a proton gradient equivalent to $\approx 100 \text{ mV}$ is reached. The relatively large undershoot in E_m when the actinic light is turned off, is indicative for the size of the passive proton flux in steady state at $t = 15 \text{ s}$.

4.3.2. Ammonia

Ammonia is known to uncouple electron transport ever since Hill measured oxygen evolution from isolated chloroplasts (Heber and Santarius 1970). Its mechanism is assumed to stem from the high membrane permeability of the electroneutral NH_3 , and the relative membrane impermeability of NH_4^+ . Thus lowering the pH in the lumen will induce a flux of NH_3 from the stroma to the lumen and thereby annihilate ΔpH . This type of uncoupling is comparable

44 Photosynthetic Free Energy Transduction

to an infinite buffer capacity of the lumen. We have tried to simulate the presence of ammonia by assuming a buffer concentration $\sum B_i = 30$ M. Although this high concentration is quite unrealistic one must keep in mind that it is the manner in which we simulate reality that forces us to use this concentration. If we could simulate the actual NH_3 flux density as a result of pH changes we would not need this high concentration. However in essence the effect would be similar. In fig. 4.5 we see the result of such a calculation. Due to the high buffering the passive proton flux remains negligible. The pH difference is seen to rise very slowly in the light. In the presence of ammonia however one would expect a rather fast rise in ΔpH in the first 0.5 s after the onset of illumination until the influx of NH_3 has reached a sufficient level. The electric potential is seen to rise slowly after the first transient peak. Again in reality one would expect this rise to speed up if the NH_3 flux density is able to compensate the proton influx after a certain illumination period. This has actually been determined in

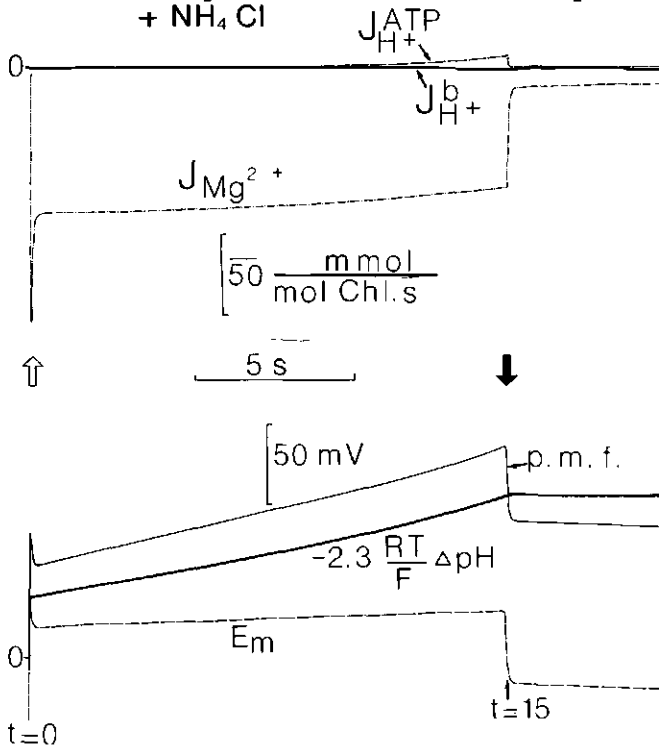


Figure 4.5. Calculated fluxes (top) and potentials (bottom) for a thylakoid as in fig. 4.3b. The presence of ammonium chloride (NH_4Cl) is simulated by assuming a two orders of magnitude higher buffer concentration. As a consequence the electric potential E_m reaches a relatively high steady state level, with a slight tendency to rise. Experiments by Remish et al. (1986a,b) also reveal a high steady state E_m , but a much stronger tendency to rise after passing the initial transient peak in E_m . This could explain why higher rates of ATP synthesis were found in the presence, as opposed to the absence, of low concentrations of NH_4Cl .

the presence of ammonia with an antimony pH sensitive microelectrode (Remis et al. 1986a,b).

4.3.3. Nigericin

This uncoupling antibiotic dissipates the proton gradient selectively by facilitating electroneutral proton-potassium exchange across the membrane (Pressman 1968). In order to simulate the antiport mechanism we developed the following formulation. When eq. 3.11 is taken to the extreme, i.e. $E_m = 0$ V, then an equation for electroneutral flux density results.

$$J_i = P_i \cdot (c_i^{out} - c_i^{in}) \quad (4.1)$$

Where P_i denotes the permeability coefficient of the antiport molecule for the ion species i . Since two cations are involved the general formulation for an electroneutral antiport flux density is:

$$J_{12} = P_1 \cdot (c_1^{out} - c_1^{in}) + P_2 \cdot (c_2^{out} - c_2^{in}) \quad (4.2)$$

In this equation the flux density of one ion species in relation to the concentration of both ion species is described. In order for eq. 4.2 to be a proper antiport flux density description it should satisfy the boundary condition:

$$J_{12} = 0 \text{ whenever } c_1^{out}/c_1^{in} = c_2^{out}/c_2^{in} \quad (4.3)$$

Combining eqs. 4.2 and 4.3 leads to a general description for an antiport induced flux density.

$$J_i^{anti} = P_i^{anti} \left\{ (c_1^{out} - c_1^{in}) - (c_1^{out}/c_2^{out}) \cdot (c_2^{out} - c_2^{in}) \right\} \quad (4.4)$$

For the case of nigericin eq. 4.4 can be converted to:

$$J_{H^+}^{nig} = P^{nig} \left\{ (c_{H^+}^{out} - c_{H^+}^{in}) - (c_{H^+}^{out}/c_{K^+}^{out}) \cdot (c_{K^+}^{out} - c_{K^+}^{in}) \right\} \quad (4.5)$$

When using eq. 4.5 for the proton flux density through nigericin the flux density for potassium through nigericin is then restricted to the following:

$$J_{H^+}^{nig} + J_{K^+}^{nig} = 0 \quad (4.6)$$

Combining eqs. 4.5 and 4.6 with eqs. 3.1-3.3 enables us to simulate the presence of nigericin in the thylakoid membrane by adding the nigericin flux to the respective passive fluxes, i.e. $J_{H^+}^p$ and $J_{K^+}^p$.

The value of P^{nig} has never been determined to our knowledge. We have assumed it to be $5 \cdot 10^{-3} \text{ cm} \cdot \text{s}^{-1}$ in order to assure a flux density of the same order of magnitude as the other flux densities. Since we have a rather high potassium concentration in the lumen, a nigericin-induced potassium flux of the same order of magnitude as the passive potassium flux implies a very large proton flux considering the pH values in the lumen and stroma.

46 Photosynthetic Free Energy Transduction
+ Nigericin

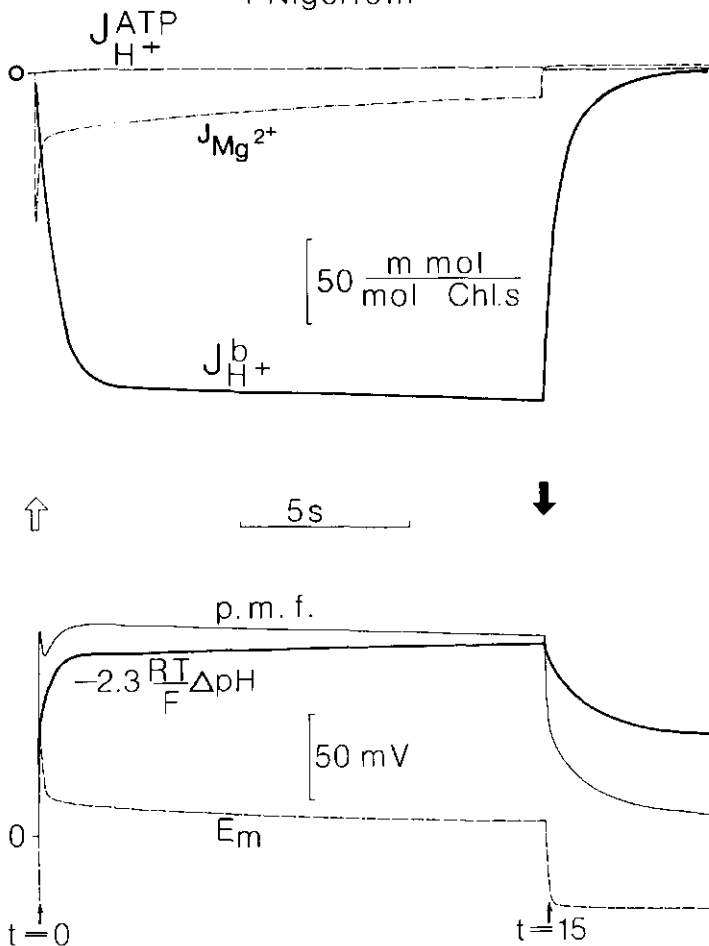


Figure 4.6. Calculated fluxes (top) and potentials (bottom) for a thylakoid as in fig. 4.3b. The presence of nigericin is simulated with the use of eqs. 4.5 and 4.6. The equations are applied at $t = 0$ with an assumed permeability coefficient $p_{nig} = 5 \cdot 10^{-3} \text{ cm} \cdot \text{s}^{-1}$. Evidently ATPase proton flux is virtually zero, whereby uncoupling is ensured. ATP synthesis at the onset of illumination, as it was measured elsewhere (Ort et al. 1976), is not seen here probably due to the fact that an oxidized ATPase was used to simulate this result. A considerable value is calculated for E_m in the steady state and a very small ΔpH . Combined with valinomycin a complete abolishment of $\Delta \psi$ should ensue.

In fig. 4.6 we see the result of simulated presence of nigericin on the potential and flux density changes. As can be expected both the passive proton flux, incorporating the nigericin mediated proton flux, and the magnesium ion flux are larger than in fig. 4.3b. Uncoupling is quite effective as no ATPase dependent proton flux can be seen. Although experiments have shown ATP synthesis to occur at the onset of illumination in the presence of nigericin (Ort et al. 1976). This can imply a much lower value

for P^{n15} in reality or a deviation from the basic chemiosmotic assumption of equilibrium in the lumen at the onset of illumination. We will digress on this last possibility in chapter 6. The electric potential E_m is seen to be rather high after 15 s of illumination, but it is slowly diminishing while ΔpH is slowly rising. This can be expected since the K^+ concentration in the lumen will rise to a level where the passive efflux will compensate the nigericin mediated influx.

4.3.4. A23187

This electroneutral antiport molecule is known to facilitate the exchange of one magnesium ion for two protons (Reed and Lardy 1972). Microelectrode experiments with this substance present have been performed (Vredenberg and Bulychev 1976). A similar derivation as performed in the previous paragraph can be used for this antiport mechanism:

$$J_{H^+}^{A23} = P^{A23} \{ (c_{H^+}^{out} - c_{H^+}^{in}) - (c_{Mg^{2+}}^{out}/c_{Mg^{2+}}^{in}) \cdot (c_{Mg^{2+}}^{out} - c_{Mg^{2+}}^{in}) \} \quad (4.7)$$

This formula can describe the A23187 mediated proton flux density if used with the following restriction:

$$2 \cdot J_{H^+}^{A23} + J_{Mg^{2+}}^{A23} = 0 \quad (4.8)$$

Thus by adding $J_{H^+}^{A23}$ to the passive proton flux density and by subtracting $0.5 \cdot J_{Mg^{2+}}^{A23}$ from the passive magnesium flux density we can simulate the presence of A23187 in the thylakoid membrane. In fig. 4.7 we can see the result of this calculation together with some previous results taken from (Vredenberg and Bulychev 1976). The uptake of magnesium in the light is corroborated by the measurement of Mg-activity in a suspension of broken spinach chloroplasts in the absence and in the presence ($10 \mu M$) of A23187. The very characteristic slow rise in E_m after the first transient peak is also apparent in our calculation. Although the experimental rise in E_m is faster indicating that the value $P^{A23} = 5 \cdot 10^{-3} \text{ cm} \cdot \text{s}^{-1}$ used in the calculation is probably too low.

4.3.5. Valinomycin

The antibiotic valinomycin is assumed to alter the membrane permeability specifically for potassium ions (Pressman 1965). The membrane permeability is enhanced from $P_K = 3.6 \cdot 10^{-8} \text{ cm} \cdot \text{s}^{-1}$ to $P_K = 4.5 \cdot 10^{-7} \text{ cm} \cdot \text{s}^{-1}$ (values taken from Vredenberg 1976). Assuming that valinomycin is 100% specific one can incorporate the new P_K value in our set of variables and recalculate the potential and flux density changes shown in fig. 4.3b. The result is shown in fig. 4.8 and it is immediately clear that the electric potential change is small but not zero. This has been experimentally verified (Vredenberg and Bulychev 1976), but it is astonishing when one remembers the very high potassium concentration in the lumen caused by the Donnan potential. When we compare the simulated E_m response to the measured one, in the presence of valinomycin, the high potential reached immediately

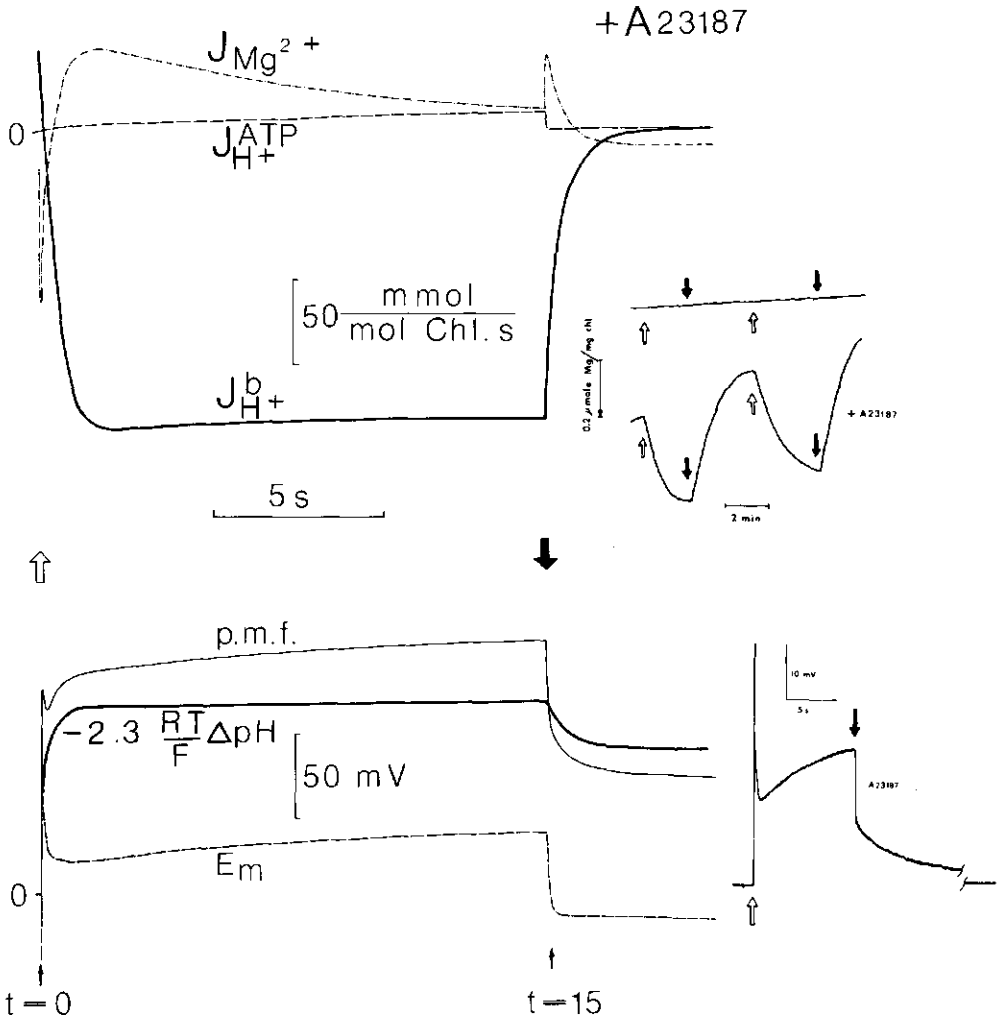


Figure 4.7. Calculated fluxes (top) and potentials (bottom) for a thylakoid as in fig. 4.3b. The presence of A23187 is simulated with the use of eqs. 4.7 and 4.8. This is applied at $t = 0$ with an assumed permeability coefficient $p^{A23} \approx 5 \cdot 10^{-3} \text{ cm} \cdot \text{s}^{-1}$. The uptake of magnesium ions in the light is corroborated by the measurement of Mg^{2+} -activity in a suspension of broken spinach chloroplasts in the presence ($10 \mu\text{M}$) and in the absence of A23187 (top inset). A downward moving trace means a decrease in Mg^{2+} -activity in the reaction medium. The slow rise in electric potential E_m after the first transient peak is substantiated by a microelectrode experiment (bottom inset from Vredenberg and Bulychev 1976). Thus the presence of A23187 should lead to a slow rise in ATP hydrolysis during actinic illumination.

after turning the light on, is much lower in the simulation. A possible explanation for this difference is the presence of valinomycin before the actinic light is turned on in the actual experiment. In the simulation presented in fig. 4.8 the actinic

light is turned on at the same instant that the change in P_x is introduced, i.e. $t = 0$. Thus two effects are combined in the simulation, a: actinic light induced electron transport and b: passive ionic fluxes instilling a new Donnan equilibrium. These last fluxes are most pronounced in the first few seconds, as can be seen in fig. 4.2, and they could be responsible for partially counteracting the build up of the light-induced electric potential E_m .

A transient second rise in E_m due to a prolonged period of ATP hydrolysis was also confirmed by experiment as can be seen from the inset of fig. 4.8 (Vredenberg and Bulychev 1976). This prolonged period of hydrolysis at the onset of illumination confirms the assumption of an increased lag time for ATP synthesis when valinomycin is present (Baker et al. 1981, Graan and Ort 1982). This prolonged period before the ATPases present switch from net hydrolysis to net synthesis does not imply a prolonged period before the maximum rate of ATP synthesis is attained. When comparing $J_{ATP}^{\dagger P}$ in figs. 4.3b and 4.8 it is clear that the maximum rate of ATP synthesis is attained at the end of the 15 s illumination period in the absence of valinomycin and within 5 s in the presence of the antibiotic. The level in steady state ATP synthesis is practically equal in both cases. These results are confirmed by other experiments (Horner and Moudrianakis 1983).

4.4. Fluorescence

Since the model presented in chapter 3 is able to calculate both the redox state of the acceptor side of PSII and ΔpH it is supposed to be able to calculate the variable fluorescence yield (Krause and Weis 1984). Although a proper simulation of the variable fluorescence yield would need a large amount of data on the redox state of the separate components of the electron transport chain, it should be possible to approximate the measurements. Since we can only simulate saturating light conditions it is possible to make some simplifying assumptions. First we regard all PSII as isolated units. Second we regard PSII to consist of a homogeneous population, e.g. there are no differences such as PSII $^{\alpha}$ and PSII $^{\beta}$ (Melis and Homann 1976, Melis and Duysens 1979, Anderson and Melis 1983). Third we assume the absence of any spill over of energy between PSII and PSI (Butler and Kitajima 1975, Strasser and Butler 1980). And fourth we assume that photochemical quenching (q_0) and energy dependent quenching (q_E) are fully independent from each other and are the only quenching factors involved in variable fluorescence (Krause et al. 1982).

4.4.1. Photochemical Quenching (q_0)

Since 1963 (Duysens and Sweerts 1963) it is well known that the redox state of the primary quinone acceptor of PSII, i.e. Q_A , is an important factor in determining the level of variable fluorescence (Fv). When Q_A is fully oxidized, as in dark adapted

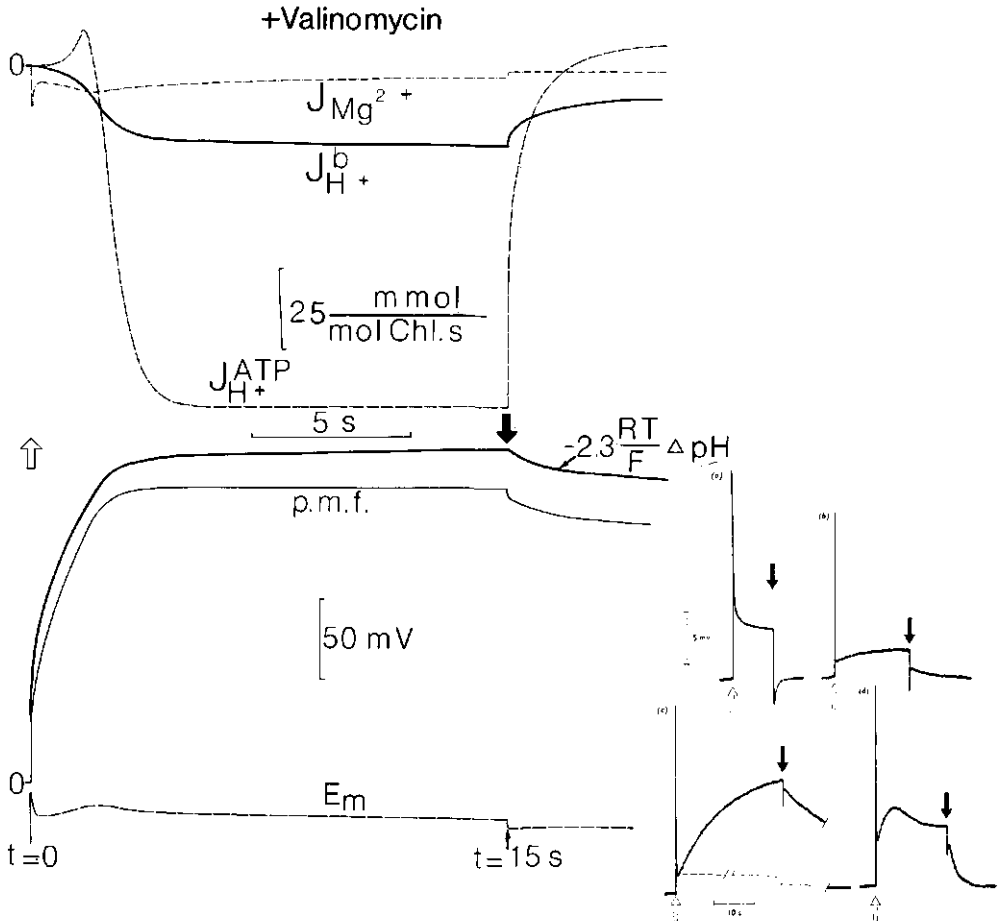


Figure 4.8. Calculated fluxes (top) and potentials (bottom) for a thylakoid as in fig. 4.3b. The presence of the antibiotic valinomycin is simulated by changing the permeability coefficient P_K from $3.6 \cdot 10^{-8}$ to $4.5 \cdot 10^{-7} \text{ cm} \cdot \text{s}^{-1}$ at $t = 0$. As a consequence potential changes caused by the light-induced proton pumping and those caused by a change in Donnan potential interfere with each other. This may cause the difference in amplitude of the initial transient peak value of E_m between the experiment (inset from Vredenberg and Bulychev 1976) and the calculated result. The ATP synthesis rate in the steady state is almost identical to fig. 4.3b, but there is a longer lag time before ATP synthesis starts. Results of previous microelectrode measurements in the absence and presence of valinomycin and at different potassium concentrations are shown in the inset. A secondary rise in the electric potential E_m after the first transient peak, as is evident at low potassium concentrations, can be reproduced in the calculations.

chloroplasts, the concomitant fluorescence intensity is minimal (F_0) and when Q_A is fully reduced the resulting fluorescence is maximal (F_m) assuming no significant ΔpH has been built-up (Krause and Weis 1984). If we suppose that Q_A is the relative concentration of oxidized and Q_A^- reduced primary quinone acceptor

then the level of variable fluorescence controlled by the primary PSII acceptor can be described as follows:

$$Fv = (Fm - Fo) \frac{Q_A^-}{Q_A + Q_A^-} + Fo \quad (4.9)$$

This implies that the degree of quenching by the primary acceptor, usually called photochemical quenching, can be described by

$$q_Q = \frac{Q_A^-}{Q_A + Q_A^-} \quad (4.10)$$

Since our model keeps track of the redox state of the intermediary redox pool between PSII and PSI, which must reflect the redox state of the primary quinone electron acceptor of PSII, eq. 4.10 can be rewritten to our convenience.

$$q_Q = \frac{J_{H^+}^{PSII}}{J_{H^+}^{PSII} + J_{max}^{PSII}} \quad (4.11)$$

In eq. 4.11 $J_{H^+}^{PSII}$ is considered to be the turn-over rate of PSII at $t=0$, i.e. in fully dark adapted chloroplasts.

4.4.2. Energy Dependent Quenching (q_E)

Apart from photochemical quenching other factors quenching fluorescence have been determined in abundance (Krause and Weis 1984). We neglect them all but for the *energy* dependent or non-photochemical quenching q_E , which is considered to account for most of the total quenching together with q_Q . This type of quenching has been shown to be linearly related to the proton concentration of the thylakoid lumen (Briantais et al. 1980, Krause et al. 1982). It was suggested that q_E is caused by increased thermal deactivation of excited chlorophyll molecules (Briantais et al. 1979). This would imply that the yield of both fluorescence and photochemistry are lowered by q_E . Assuming that

a: Fo is not affected by q_E

b: $Fo + Fv(0)$ is the maximum fluorescence intensity obtainable from the dark adapted chloroplasts, i.e. at the internal H^+ concentration $c_{H^+}^{in}(0)$

c: $Fo + Fv(t)$ is the maximum fluorescence intensity obtainable after t s of illumination, i.e. at the internal H^+ concentration $c_{H^+}^{in}(t)$

d: from fig. 4 in Briantais et al. (1980) it follows that there is a linear relationship between the quotient of the maximum fluorescence levels and their concomitant internal H^+ concentrations

the following equations can be derived:

$$\frac{Fo + Fv(0)}{Fo + Fv(t)} - 1 = k_f \cdot (c_{H^+}^{in}(t) - c_{H^+}^{in}(0)) \quad (4.12)$$

52 Photosynthetic Free Energy Transduction

Eq. 4.12 can be rearranged as follows:

$$Fv(t) = \frac{Fv(0) - k_f \cdot (c_{H^+}^{lumen}(t) - c_{H^+}^{lumen}(0)) \cdot F_0}{1 + k_f \cdot (c_{H^+}^{lumen}(t) - c_{H^+}^{lumen}(0))} \quad (4.13)$$

When we combine eq. 4.13 with the definition for q_E , i.e. $q_E = 1 - Fv(t)/Fv(0)$, a useful mathematical formulation for the energy dependent quenching emerges

$$q_E = \frac{k_f \cdot (c_{H^+}^{lumen} - c_{H^+}^{lumen}(0)) \cdot (1 + F_0/Fv(0))}{1 + k_f \cdot (c_{H^+}^{lumen} - c_{H^+}^{lumen}(0))} \quad (4.14)$$

with k_f : quenching constant (determined by the slope of curve 1 of fig. 4 in Briantais et al. 1980) with values taken between $2 \cdot 10^6$ and $2 \cdot 10^7$ $\text{cm}^3 \cdot \text{mol}^{-1}$.
 $Fv(0)$: variable fluorescence yield in the dark adapted state, usually about 0.75.
 F_0 : minimal constant fluorescence, usually about 0.25.
 $c_{H^+}^{lumen}(0)$: luminal proton concentration in the dark, which can range from pH 6.9 to pH 7.6.

In contrast to q_0 this energy dependent quenching is 0 in the dark adapted state and increases when a ΔpH is formed.

When both quenching processes are assumed to be independent an equation for the variable Chl a fluorescence yield can be constructed.

$$Fv = (F_m - F_0) \cdot (1 - q_0) \cdot (1 - q_E) + F_0 \quad (4.15)$$

In eq. 4.15 $J_{H^+}^{PSII}$ and $c_{H^+}^{lumen}$ are the independent variables simulated in the model. This enables us to calculate Chl a fluorescence induction curves from simulated data. A further assumption is that q_E responds instantaneously to changes in the luminal proton concentration.

Fig. 4.9 shows the normalized variable fluorescence curve, i.e. $(Fv - F_0)/(F_m - F_0)$, simulated in the presence (as in fig. 4.6) or in the absence of nigericin (as in fig. 4.3). In the presence of nigericin Fv rises to a maximum within 250 ms. Due to incomplete reduction of the PQ pool, caused by reoxidation of PQH_2 by oxygen, F_m is not reached. In the absence of nigericin the fluorescence yield starts to decline in comparison to the response in the presence of nigericin after 50 ms due to energy dependent quenching caused by the acidification of the lumen. However the difference becomes significant after 1 s of illumination.

The use of eq. 4.11 for calculation of q_0 is limited since no fluorescence can be calculated in the dark ($J_{H^+}^{PSII} = 0$) and the characteristic OIP transient (Schreiber 1983) is missing in fig. 4.9b. Therefore a more detailed description of charge separation and secondary electron flow in PSII is required for simulation of Chl a fluorescence induction. Inevitably this will increase the number of algorithms and hence computation time.

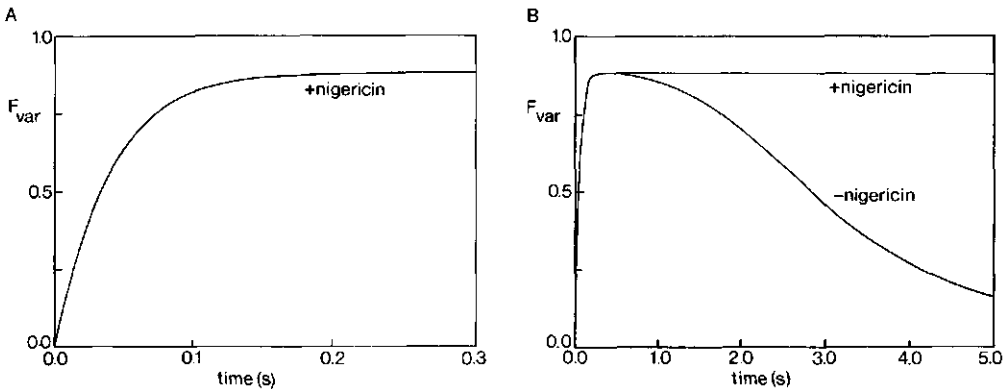


Figure 4.9. Simulation of chlorophyll fluorescence induction curves in the presence (parameters as in fig. 4.6) and in the absence (parameters as in fig. 4.3b) of nigericin. A: the induction curve in the first 0.3 s of saturating actinic illumination. The build-up of a ΔpH is small and little difference can be detected between the presence or absence of nigericin. The curve is determined by applying eq. 4.11. Due to incomplete reduction of the PQ-pool, caused by reoxidation of PQH_2 by oxygen, F_m is not reached. B: fluorescence induction curves on a longer time scale. The difference between the presence and absence of nigericin becomes evident as a ΔpH is build-up in the absence of the uncoupler. Eq. 4.12 is used with $k_f = 10000 M^{-1}$.

4.5. Conclusions

In this chapter we have shown that it is possible to use the simulation model developed in chapter 3 to verify the supposed action of membrane modifying agents related to membrane potential changes as measured by microelectrodes. And it enables us to do imaginary "experiments", which are in reality impossible to perform. To our knowledge this is the first time a theoretical model is capable of relating the size of the electric potential undershoot when the actinic light is switched off after a prolonged illumination period and the size of the proton flux density as in fig. 4.4.

In paragraph 4.4. we have merely touched on the possibility to take the model a step further and simulate experimentally measurable responses with other techniques than the microelectrode. The model could prove to be of invaluable import if a proper algorithm for electron transport were incorporated. Such an algorithm would have to describe not only electron transport within PSII (Renger and Schulze 1985) but also in detail other parts of the electron transport chain. The first attempts in this direction have revealed a vast lack of knowledge in this area. However the model opens for us a vista of possibilities comparing fluorescence, luminescence, photo-acoustic and other types of experimental responses with simulated data and thus enlarging our knowledge of the photosynthetic processes.

5. Measuring Changes in the Transmembrane Electric Potential

5.1. Introduction

In this chapter we will show the results obtained by measuring light-induced electric potential changes. The measurements are done with the open-ended glass capillary microelectrode and with the electrochromic absorbance change near 515 nm (P_{515}). The two techniques can only be compared on the level of flash-induced potential changes, since actinic illumination of a longer duration (e.g. > 1 s) introduces large scattering artifacts in the spectrophotometric response at 515 nm drowning the electrochromic absorbance change (Schapendonk 1980, Coughlan and Schreiber 1984a,b). When the P_{515} response to a long term actinic illumination (e.g. several seconds) was corrected for scattering artifacts a qualitative comparison could be made with the microelectrode response (Schapendonk 1980). However when flash-induced responses were compared directly a marked difference in the kinetics of the profile appeared (Schapendonk et al. 1979). This difference was denoted as reaction II by one group of scientists (Schapendonk et al. 1979, Vredenberg 1981, Schreiber and Rienitts 1982, Peters 1986) and as phase b by another group (Joliot and Delosme 1974, Bouges-Bocquet 1977, Horváth et al. 1978, Velthuys 1980, Crowther and Hind 1981, Jones et al. 1984). In recent years experiments have given us a better understanding of the causes influencing the presence of reaction II or phase b in the flash-induced P_{515} signal (Schuurmans et al. 1981, Schreiber and Rienitts 1982, Peters et al. 1983, 1984a, 1984b, 1984c, 1985, 1986). This has enabled us to compare flash-induced P_{515} responses with microelectrode responses under essentially identical conditions (Van Kooten et al. 1984), whereupon at least part of the differences appeared to be non-existent.

5.2. Microelectrode Measurements

Microelectrode experiments *in situ* in giant chloroplasts of *Peperomia metallica* were performed as described in chapter 2. A comprehensive article describing the basic physical principals involved has been published (Vredenberg 1976).

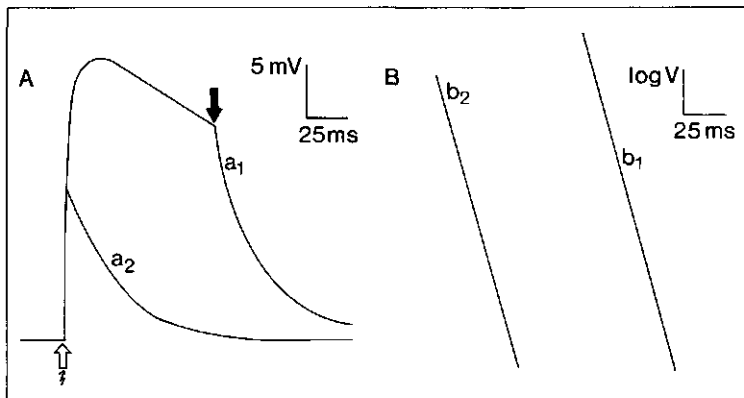


Figure 5.1. A: electric response of a *Peperomia metallica* chloroplast to a 100 ms saturating light pulse, measured *in vivo* with a microelectrode. The open and closed arrows mark the start and end, respectively of the light pulse. The decay of the membrane potential E_m in the dark is marked a_1 . The zig-zag arrow indicates a single turnover saturating light flash. The flash-induced response is measured in the same chloroplast. The decay in the dark of the flash-induced response is marked a_2 . B: semi-logarithmic plots of the potential decay after the 100 ms light pulse, marked b_1 , and after the single turnover flash, marked b_2 . In both responses the decay is clearly mono-phasic. Such responses are termed the "classical response" by us.

5.2.1. The "classical" Signal

In fig. 3.5 we have seen a microelectrode response to a relatively long actinic illumination. In fig. 5.1 we see the response to a single-turnover saturating actinic flash and to a saturating actinic illumination period of 100 ms measured in the same chloroplast. We expect that this illumination period does not significantly change ΔpH across the thylakoid membrane in comparison to the flash-induced change, as has also been calculated by others (Junge et al. 1979). The decay of the potential after the light has been turned off appears to be single exponential in both cases as can be seen in the semi-log plots. This is what one would expect if the chloroplast adhered to the assumptions made in chapter 3. One does not expect a significant change in Nernst potential during the illumination period and thus the membrane can be seen as a capacitor (C_m) charged during the illumination and dissipating its potential via a current of ionic charges through a resistor. The resistances are different for the ions present, but they can be seen to be in parallel (all are perpendicular to the membrane) and can be substituted by one resistor (R_m). Thus one would expect an exponential decay function like: $\exp(-t/R_m \cdot C_m)$ (see also Vredenberg 1976). If we simulate a short term illumination using the more sophisticated model described in chapter 3, then we see a deviation of single exponential decay mainly in the tail of the signal where the response is less than ten percent of the response when the light was turned off (see fig. 6.1). This deviation from an exponential decay is not caused by a change of R_m , which is expected to stay constant during such short illumination periods (Schapendonk

1980), but by rather large changes in the chloride concentration in the lumen. The signals shown in fig. 5.1 are what we call classical as they have been measured on many occasions before (Bulychev et al. 1976, Bulychev and Vredenberg 1976, Schapendonk et al. 1979 etc.).

5.2.2. The "new" Signal

The plants used for the measurements in the previous paragraph were cultured under $1.2 \text{ W}\cdot\text{m}^{-2}$ and on soil of relatively low nutritional potential. When the plants were grown under $1.5 \text{ W}\cdot\text{m}^{-2}$ and on the soil described in chapter 2 the growth rate increased markedly. The leaves contained less anthocyan and the number of chloroplasts per cell was usually found to be less, i.e. 2 instead of 4, while they were larger in diameter (40 to $60 \mu\text{m}$). When measuring light-induced responses with the microelectrode in these chloroplasts one could measure the same type of response as in the previous chapter, but on many occasions a "new" type of response was measured. In fig. 5.2 a typical "new" response to a flash and an actinic illumination of 100 ms duration is shown. When we compare these responses with

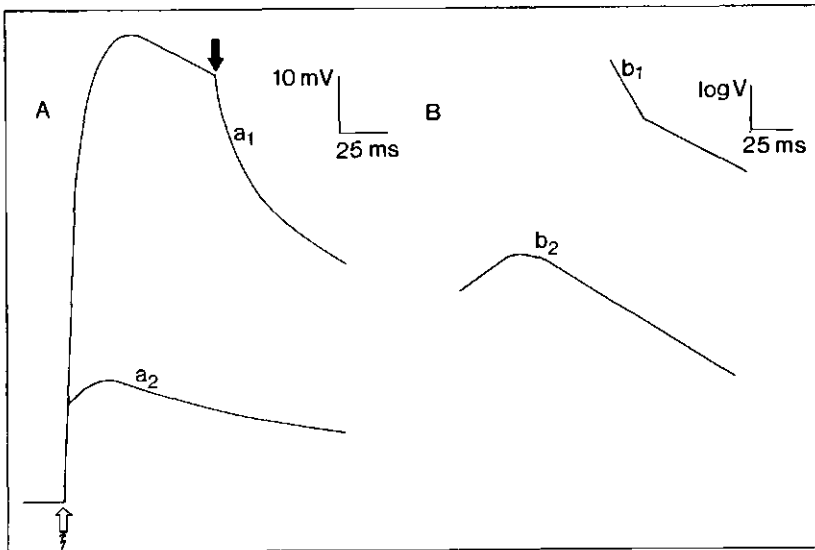


Figure 5.2. A: electric response of a *Peperomia metallica* chloroplast to a 100 ms saturating light pulse, measured *in vivo* with a microelectrode. B: semi-logarithmic plots of the potential decay in A. Meaning of symbols as in fig. 5.1. The decay after the 100 ms light pulse is bi-phasic. The decay rate of the slow component in b_1 is apparently equal to the decay rate in the flash-induced response. However the decay marked b_2 also contains a relatively slow rise, which is typical for responses measured with the P_{515} technique. Note that the amplitude of the flash-induced response in A is relatively smaller in relation to the peak value attained during the 100 ms light pulse as compared to the amplitude found in fig. 5.1a. Such responses are defined as the "new response" by us.

the ones in fig. 5.1 some striking differences are evident. First in fig. 5.2 the decay of both responses in the dark is clearly bi-phasic as can be seen in the semi-log plots. The fast decay ($\approx 12 \text{ s}^{-1}$) after the 100 ms illumination period is comparable to the decay rates found in fig. 5.1. The slower decay rate ($\approx 4 \text{ s}^{-1}$) is equal for the flash-induced and the 100 ms actinic illumination induced response. This decay rate is comparable to the rate of phase c defined as the decay rate of reaction II by Schapendonk (Schapendonk et al. 1979, Schapendonk 1980), while the faster decay rate can be compared to phase c' of reaction I. The relatively slow rise, known as phase b, is also present in the flash-induced response of fig. 5.2.

When we compare the maximum potential during the 100 ms illumination period in relation to the amplitude of the flash-induced response it is much higher in fig. 5.2 than in fig. 5.1. This ratio is generally 2 in a "classical" type of response (fig. 5.1), while it varies between 3 and 5 in the so-called "new" response (fig. 5.2). Also the time it takes to reach the maximum potential during actinic illumination differs between the two types of responses. As can be seen in fig. 5.1 this type of response usually reaches its maximum within 10 ms. For responses like the one in fig. 5.2 this appeared to be quit variable and the time ranged between 30 and 100 ms.

The flash-induced slow rising component in the dark (phase b) is not exclusive for single turnover flashes as can be seen in fig. 5.3. Here a 10 ms actinic pulse is compared to a single turnover flash response. It is clear that phase b is also present in this response after the 10 ms saturating actinic

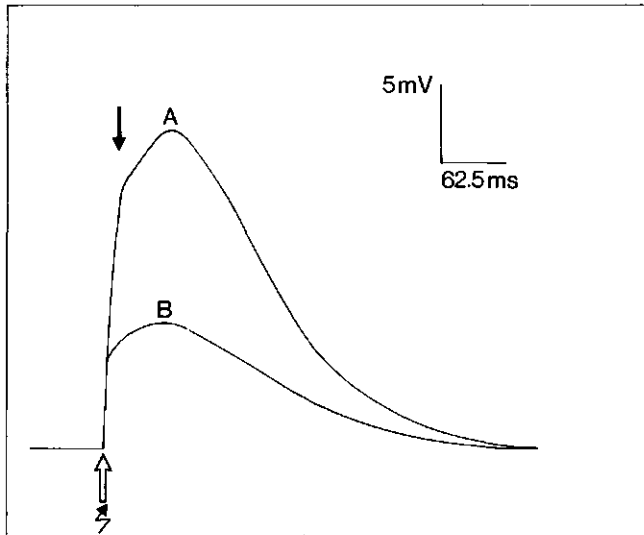


Figure 5.3. Electric response of a *Peperomia metallica* chloroplast to a 10 ms saturating light pulse (A) and a single turnover saturating light flash (B), measured in vivo with a microelectrode. Further explanations of the symbols and conditions in fig. 5.1. The relatively slow rising component in the single turnover flash-induced response is also present after the 10 ms light pulse.

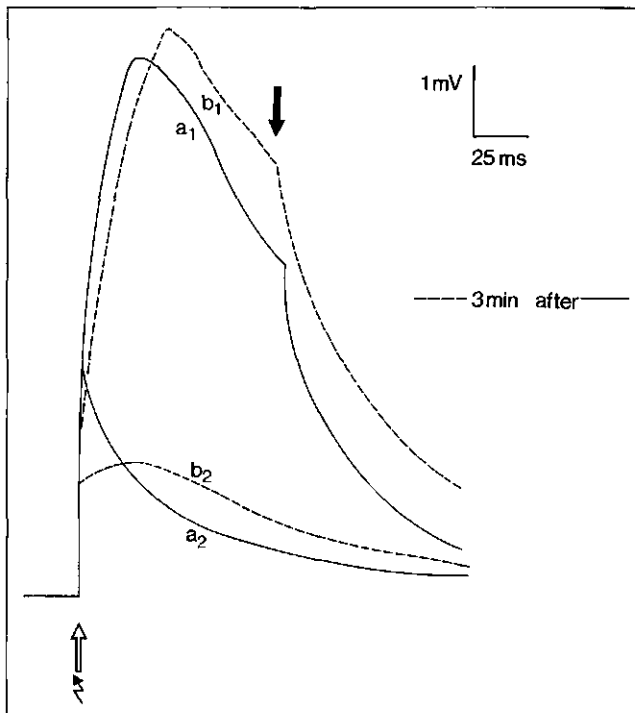


Figure 5.4. electric responses of a *Peperomia metallica* chloroplast, measured *in vivo* with a microelectrode. For the meaning of symbols and signs see fig. 5.1. The solid lines indicate a "classical" response to the 100 ms light pulse (a_1) and to the actinic flash (a_2), measured within 1 minute after impalement. The dashed lines indicate "new" responses to a 100 ms light pulse (b_1) and to an actinic flash (b_2) measured in the same chloroplast after a 3 minute dark adaptation period. This transition from a "classical" response to a "new" response in such a short period of time is only found in microelectrode experiments.

illumination period. This observation casts doubt on the equivalence between these responses and those observed with the P_{515} technique. With the latter method it is possible to abolish phase b with a few preceding flashes (Van Kooten et al. 1983).

The difference between the "classical" and the "new" type of response does not adhere to different types of chloroplasts. In fig. 5.4 we see both types of responses occurring in the same chloroplast. The "classical" signals are recorded within 1 minute after impalement, while the "new" signals were recorded after a 3 minute dark adaptation period. All the differences between the two types of signals that were discussed before can be seen again in these responses.

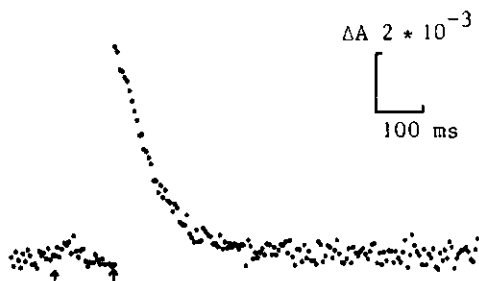


Figure 5.5. Flash-induced absorbance change at 518 nm of a spinach leaf, which has been subjected to a single turnover saturating flash 125 ms before the response that is shown here. The leaf has been dark adapted and kept at 3°C. The arrows mark the time the flashes are fired. The response to the first flash cannot be seen, because it was removed by data manipulation (see figs. 5.7 and 5.8). The first flash is assumed to have saturated any saturable component in the response. The decay of the response after the flash is monophasic with a rate of 12 s^{-1} . This response is a result of subtracting a single flash response from a double flash response, see fig. 5.7. A P_{515} response as shown here is denoted **reaction I** by us and is thought to be equivalent to the "classical" flash-induced response measured with the microelectrode.

5.3. P_{515} Measurements

The electrochromic absorbance change at 515 nm, first reported on by Duysens (1954), has been used to gauge the trans thylakoid electric potential changes (Junge and Witt 1968, Emrich et al. 1969, Witt and Zickler 1973). This has led to an overestimation of the electric potential generated by a single turnover flash (Zickler et al. 1976). Carefully prepared salt-induced absorbance changes at 515 nm permitted an estimate of the single turnover saturating flash-induced potential change in the range between 15 and 35 mV (Schapendonk and Vredenberg 1977). The kinetics of the flash-induced P_{515} response resembled those of the microelectrode when we speak of the "classical" response. A fast rise ($< 5 \text{ ns}$) and a single exponential decay with a decay rate varying between 20 and 10 s^{-1} (fig. 5.5). This was fully in agreement with the chemiosmotic theory as proposed by Mitchell (Mitchell 1961, 1966, 1976), which considered a biological free-energy transducing organelle to consist of two homogeneous aqueous phases separated by a closed inert membrane containing vectorial oriented hydrogen transport complexes.

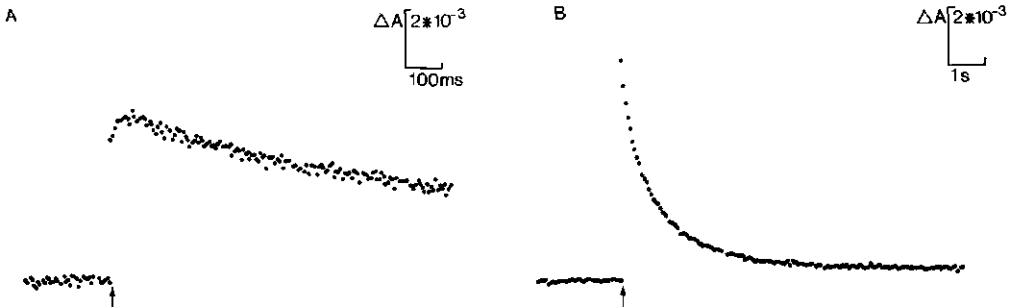


Figure 5.6. Flash-induced absorbance changes at 518 nm in a suspension of isolated intact spinach chloroplasts. The arrows mark the moment a single turnover saturating flash is fired. The chloroplasts are kept at 3°C in a reaction medium described in paragraph 2.2.2. These are averaged responses measured with a sampling frequency of 0.05 Hz. A: a response measured at a time scale of 1 s (200 A/D conversions, i.e. 5 ms between two points). This complex response is similar to the "new" flash-induced response measured with the microelectrode. B: a response measured at a time scale of 12 s (i.e. 60 ms between two points). The decay of the response contains a very slow component with a rate of $\approx 0.5 \text{ s}^{-1}$. This component is called phase d by us and is absent in responses measured with a microelectrode. It has been shown that phase d is non-electrochromic in origin (Vredenberg et al. 1984).

5.3.1. Kinetics of the Flash-Induced Response

However many publications reported on another type of response measured by P_{515} , upon a single turnover saturating flash (Joliot and Delosme 1974, Bouges-Bocquet 1977, Slovacek and Hind 1978, Velthuys 1978, Horváth et al. 1979). This response appeared

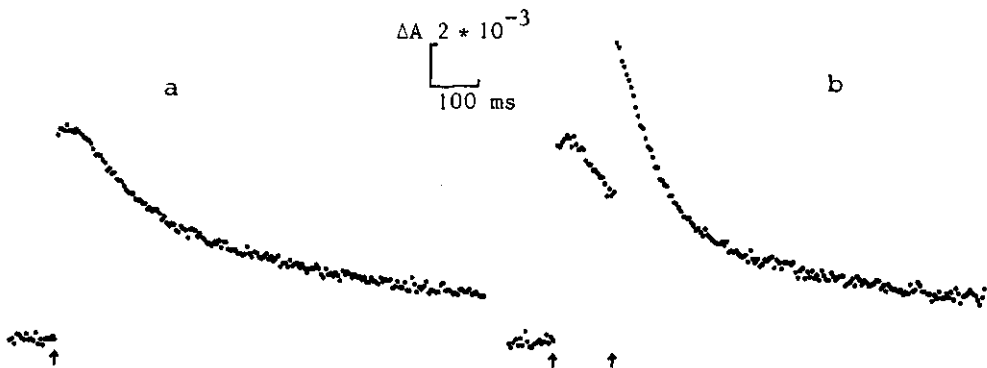


Figure 5.7. Absorbance changes at 518 nm in a dark adapted spinach leaf, induced by single (a) or double (b) flashes. Recorded and displayed on 1 s time scale. Average of 50 single or double flashes, fired at a rate of 0.1 Hz. The arrows mark the moment the flashes were fired. The leaf was kept at a constant temperature of 3°C. The time between two flashes in (b) was 125 ms. Apparently a slow rising component observed in the first is absent in the second flash.

to be much more complex as can be seen in fig. 5.6. The response was deconvoluted into a non-electrochromic part called phase d (Schapendonk et al. 1979) or reaction III (Vredenberg et al. 1984) and an electrochromic signal comprising of the phases a, b, c' and c (Schapendonk et al. 1979) or reaction I and II (Schapendonk and Vredenberg 1979, Vredenberg 1981). This last deconvolution was based on the fact that part of the P_{315} response could be saturated by a few single flashes closely spaced in time as can be seen in fig. 5.7.

5.3.1.1. Reaction I

Fig. 5.7a reveals the same type of response in a dark adapted spinach leaf as can be elicited from isolated chloroplasts (fig. 5.6a). However when a second flash is given 125 ms after the first (fig. 5.7b) part of the response seems to be saturated. These two signals were taken from the same leaf piece and are averaged by recording a single and a double flash response alternatingly with 10 s darkness between each recording. By subtracting fig. 5.7a from fig. 5.7b the response to the second flash, denoted as reaction I, is revealed in fig. 5.5. This response contained phases a (fast rise) and c' (single exponential decay) as defined in (Schapendonk et al. 1979) it was called reaction I to distinguish it from the rest of the response (phases b, c and d) because it resembled the "classical" response as measured with the microelectrode up till that time. Therefore it was believed that reaction I reflected the transmembrane electric field changes that can be measured from bulk phase (stroma) to bulk phase (lumen) (Schapendonk and Vredenberg 1979, Schapendonk 1980, Vredenberg 1981).

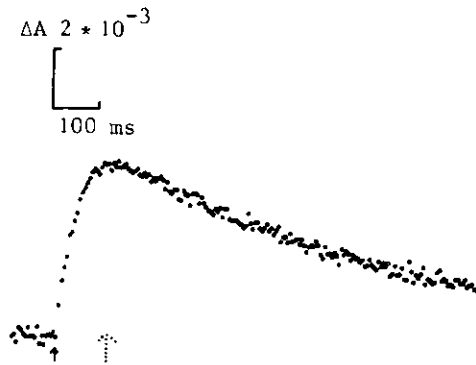


Figure 5.8. The satiable part of the absorbance change at 518 nm in dark adapted spinach leaves. This response is obtained by subtracting reaction I in fig. 5.5. from the complex single flash-induced response in fig. 5.7a. The resulting signal is defined as reaction II. It consists of a rising phase with a rate varying between 50 and 100 s^{-1} , and a biphasic decay. The slowest decaying phase, phase d, has a rate of about 0.5 s^{-1} and is non electrochromic in origin. The faster decaying phase, phase c, has a rate varying between 2.5 and 1.5 s^{-1} and is caused by an electrochromic absorbance shift. The solid arrow marks the moment the first flash is fired. The dashed arrow marks the moment the second flash is fired in fig. 5.7b. Since reaction II is fully saturated by the first flash no response is elicited by the second flash.

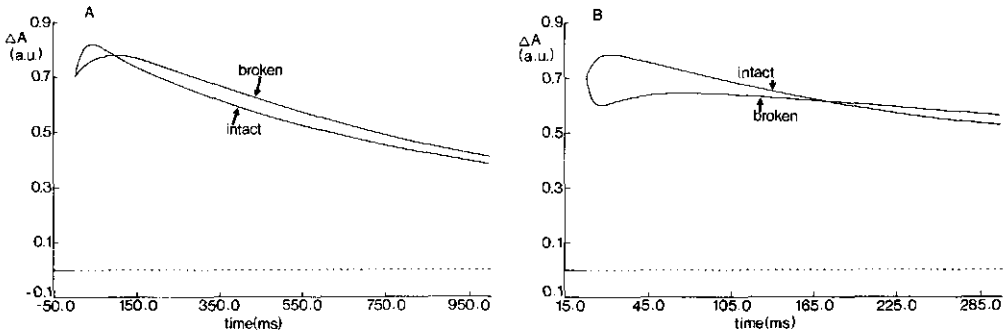


Figure 5.9. Flash-induced absorbance changes at 518 nm of isolated intact and broken spinach chloroplasts. Measurements were performed at 3°C and the response were scaled to the same amplitude for the first measurement after the flash. The drawn lines are not the actual measurements but the result of a multi-exponential fit (see paragraph 2.2.3.5.). **A:** measurement at a 1 s time scale of a suspension of intact chloroplasts and a suspension of broken chloroplasts from the same isolation batch. **B:** measurement from the same samples as in A but at a shorter time scale. The slow rising phase in the intact sample is slowed down in the broken sample, revealing the presence of reaction I.

5.3.1.2. Reaction II

By subtracting reaction I (fig. 5.5) from the total response (fig. 5.7a) the satiable part of the P_{515} response remained (fig. 5.8) and it was denoted as reaction II in order to separate it from the non-satiable part. In fig. 5.9 only small differences between broken and intact chloroplasts can be seen. After analysis it appears that reaction II has become slower in the broken chloroplasts. The fact that the secondary slow rise in the P_{515} response is of electrochromic origin can be seen in fig. 5.10 where the response at two times after the flash from isolated intact chloroplasts are shown. Clearly the later spectrum is equivalent to the first except that its amplitude is higher and the changes in the cytochrome part of the spectrum have disappeared. 5 ms after the flash we see a dip at 554 nm indicating oxidized cytochrome *f*, and a hump near 563 nm indicating reduced cytochrome b_{563} (Slovacek and Hind 1977, 1978, Slovacek et al. 1979, Shahak et al. 1980, 1981). These have disappeared after 36 ms. This is rather fast but one must keep in mind that 12.5 mM of NH_4Cl was present as an uncoupler, which is known to speed up electron transport (Heber and Santarius 1970).

5.3.2. The Q-cycle

We will deal with possible explanations of reaction II extensively in the next chapter, however we must mention here the possible involvement of a Q-cycle (Bouges-Bocquet 1977, Crowther and Hind 1980, Velthuys 1980, Crowther and Hind 1981, Jones et al. 1984, Jones and Whitmarsh 1985) in order to explain our interest for the redox kinetics of cytochrome b_{563} .

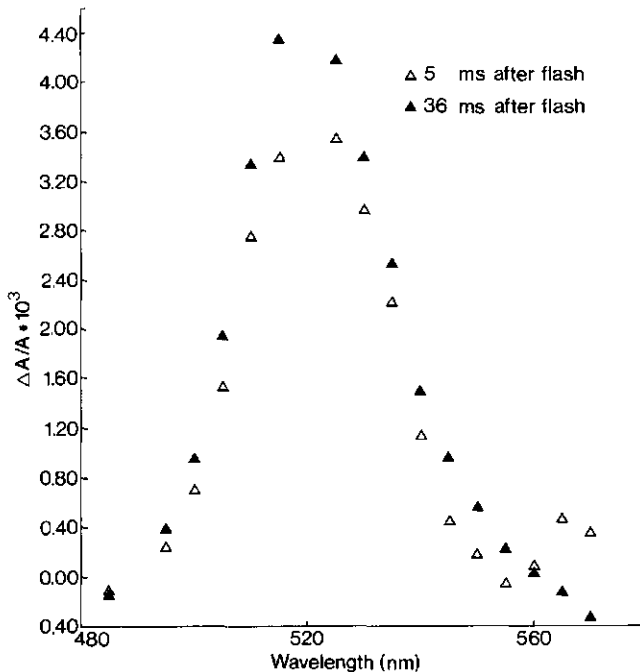


Figure 5.10. Difference spectra of the flash-induced absorbance change of isolated intact spinach chloroplasts in the presence of 3.3 mM NH_4Cl . The difference spectra are measured at two time intervals after the flash. In the spectrum taken at 5 ms after the flash the presence of oxidized cyt *f* at 554 nm and of reduced cyt *b*₆ at 563 nm is evident. The spectrum measured 36 ms after the flash reveals a higher amplitude at 515 nm due to the presence of reaction II. However while reaction II is present, all redox reactions in the cyt *b*/*f* complex have subsided. The high rate of these redox reactions is explained by the presence of NH_4Cl .

The Q-cycle was first proposed as a possible means to transport an extra proton across the membrane (Mitchell 1976). Plastoquinone is thought to donate an electron to cyt *f* via the Rieske Iron-Sulphur protein and in a concerted reaction an electron to cyt *b*₆ (Cramer and Crofts 1982, Trebst 1985). The first electron will continue to travel towards the acceptor of PSI, the second electron is believed to be transported across the membrane through cyt *b*₆ and reduce a plastoquinone anion on the stromal side of the membrane (Vermaas and Govindjee 1981, Cramer et al. 1985, Jones and Whitmarsh 1987a,b). Thus a Q-cycle would be electrogenic in origin if it were to contribute to the build-up of $\Delta\bar{\mu}_{\text{H}^+}$, else it would be a futile cycle (Olsen et al. 1980). It has been believed that the slow rising phase (phase b) in the flash-induced P_{515} response reflects the occurrence of a Q-cycle (Bouges-Bocquet 1977, Crowther and Hind 1980, Velthuys 1980, Crowther and Hind 1981).

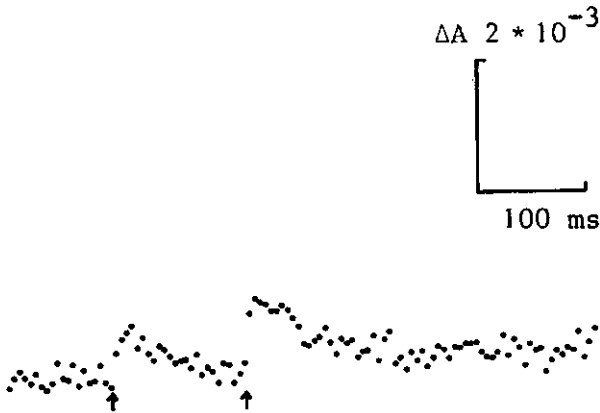


Figure 5.11. Absorbance changes at 563 nm in a dark adapted spinach leaf, induced by double flashes 125 ms apart and displayed on a 0.5 s time scale. Average of 100 double flashes, fired at a rate of 0.1 Hz. The arrows mark the moments the flashes were fired. The measurement was performed on the same leaf and directly after the measurement in fig. 5.7b. This signal is corrected for the absorbance changes caused by the P_{515} at this wavelength. The correction was executed by subtracting 9% of the response in fig. 5.7b. from the response measured at 563 nm.

5.3.2.1. Cytochrome b_{563}

In order to verify the assumed relation between the Q-cycle and the slow rising phase (phase b) in the flash-induced P_{515} response we monitored the spectrophotometric changes in the same leaf piece used in fig. 5.7 under the exact same conditions but at 563 nm. In order to correct for the electrochromic change still present at this wavelength (see fig. 5.10) we subtracted 9% (Slovacek et al. 1979) of the signal at 518 nm (fig. 5.7b). The result is shown in fig. 5.11 where it is assumed that the response results solely from changes in the redox state of the cyt b_6 population in the leaf piece.

In view of the absence of a slow rising component after the second flash in fig. 5.7b and taking the close relation between cyt b_6 and a Q-cycle or even a b-cycle (Wikström et al. 1981) into consideration one would expect a lower redox turnover of cyt b_6 after the second flash in fig. 5.11. This is clearly not the case and therefore we conclude that reaction II, as we measure it, is not caused by a secondary electrogenic step involving cyt b_6 as proposed for the Q-cycle or the b-cycle. Other arguments supporting this conclusion will be treated in the next chapter.

5.4. Comparing the Microelectrode to the P_{515} Measurements

The flash-induced potential change measured with the spectrophotometric method (P_{515}) has been compared to the change measured with the microelectrode (Schapendonk 1980, Vredenberg 1981). In the comparison the responses of isolated spinach

chloroplasts (P_{515}) were matched with responses of *Peperomia metallica* chloroplasts in situ. From the literature it is well known that there are large differences in thylakoid composition between obligate shade plants and sun plants (Björkman 1981, Dietz et al. 1984, Melis 1984). The measuring technique also induces large differences in that the microelectrode is invasive while P_{515} is non-invasive in principle. But, as was also described in chapter 3, dark adaptation is longer and better controlled in P_{515} experiments than in the electrophysiological setup. Also the temperature of the P_{515} set-up is well defined (usually cooled below 15°C), while the temperature of the microelectrode assembly is rather undefined (usually between 20 and 25°C). If, however, we adhere to the simple description of free energy transduction in the thylakoid given in paragraph 5.2.1., then a rough comparison can still be made. The amplitudes of the signals could be quite different but the kinetics should be roughly similar excluding the influence of temperature differences. As reaction II had been measured with the P_{515} technique whereas "classical" responses (i.e. only reaction I) had been measured with the microelectrode, not even a rough similarity could be claimed. Differences in the signals were mainly attributed to the fact that the microelectrode can only measure macroscopic field changes (i.e. field changes between lumen and stroma), while an intrinsic pigment like P_{515} should be susceptible to microscopic local changes in electric field (Schapendonk 1980, Vredenberg 1981, Westerhoff et al. 1983).

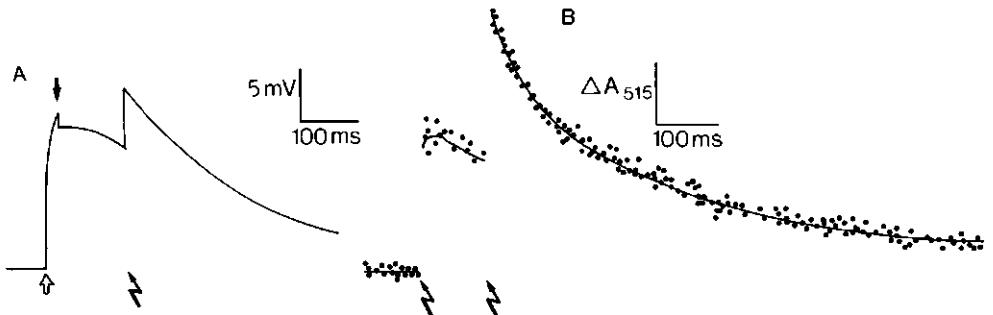


Figure 5.12. A: electric response of a *Peperomia metallica* chloroplast to a 10 ms light pulse followed by a single turnover saturating flash, measured with the microelectrode. The open arrow indicates the start of the illumination, the shaded arrow indicates the end. The zig-zag arrow marks the moment the flash is fired. A slow rising component present after the first light pulse, seems to be absent after the saturating flash. B: flash-induced absorbance changes at 515 nm measured in a dark adapted *P. metallica* leaf. The zig-zag arrows mark the moments the flashes were fired. Average of 32 double flashes, fired at a rate of 0.05 Hz. Reaction II appears to be present in the response to the first flash, however it is completely absent in the response to the second flash. Both measurements were performed at 20°C .

After measuring the "new" type of response with the microelectrode, as described in paragraph 5.2.2, the necessity became evident that a proper comparison should be made. Therefore we compared a double flash experiment in a dark adapted leaf of *Peperomia metallica*. In the microelectrode experiment we had to

use a 10 ms light pulse as our first flash, since a double flash setup was hard to achieve (fig. 5.12a). This was compared with a P_{515} experiment on a similar leaf of *P. metallica* (fig. 5.12b) at 20°C. Although this is not the same leaf we can still notice the great similarity between the two types of measurements. The main difference between the two signals is not visible in fig. 5.12. The microelectrode response decays to its original pre-flash level within 2 s, while the P_{515} response needs more than 10 s to decay completely. This difference is called phase d (Schapendonk et al. 1979) or reaction III (Vredenberg et al. 1984) and has been shown to be non-electrochromic in origin. The amplitude of the response upon the second flash is larger in the P_{515} experiment than in the microelectrode experiment. This must be attributed to the difference of the first flash in both experiments, i.e. for technical reasons a 10 ms light pulse was given in the microelectrode experiment while a single turnover saturating actinic flash was used for the P_{515} response. Although a 10 ms flash has been shown to retain a "new" type of response, its amplitude is much higher than a single turnover flash-induced response (see fig. 5.3). However, the presence of what we call reaction II after the first flash and its absence after the second flash in both measurements is conspicuous.

5.5. Conclusions

When we look at the electric potential changes in this chapter we are confronted with a variety of responses. The rather simple response (i.e. reaction I or the so-called "classical" response) fits in well with the model proposed in the chapters 3 and 4. The more complex reaction II or "new" response cannot be explained by that model. From fig. 5.12 one would conclude that reaction II can be measured as a change in electric field from bulk stroma to bulk lumen. But one must keep in mind that the apparent similarity between fig. 5.12a and 5.12b may be nothing more than apparent. In order to understand the possible difference between reaction II and the "new" response we have to explain the origin of the secondary slow rise in the flash-induced electric potential. This will be dealt with in the next chapter.

6. The Secondary Slow Rise in the Flash-Induced Electric Potential Change

6.1. Introduction

In the previous chapter we have shown several light-induced electric potential changes which cannot be explained directly with the aid of the model presented in chapters 3 and 4. This model assumes two homogeneous compartments (i.e. stroma and lumen) separated by an inert semi-permeable membrane in which reaction centers are able to perform a transmembrane charge separation at the picosecond scale, e.g. less than 175 ps in chloroplasts (Trissl and Kunze 1985). The resulting electric field change will propagate through both compartments with the speed of light. If both compartments are assumed to be highly conductive, consider the high salt concentrations mentioned in paragraph 4.2.1, and when the membrane is the sole electric resistant homogeneous dielectric, then the field change induced by the charge separation will occur only across the membrane (Farkas et al. 1984). Any voltage dependent probe whether it measures with its reference in the stroma and its probe in the lumen as is the case with the microelectrode, or intrinsic within the membrane as P_{S15} does, should measure this charge separation within the rise-time of the measuring technique. Subsequently, if the membrane is considered to be an ohmic resistance (Schapendonk 1980), the electric field should decay in an exponential manner. Deviations from this single exponential decay resulting from the presence of different ions, can be calculated with the aid of our model. In fig. 6.1 we see the result from such a calculation based on the same parameters used in paragraph 4.2.2. It should be evident from the paragraphs 5.2.1. and 5.3.1.1. that the decay is expected to be single exponential. However this is based on the assumption that the ion concentrations do not change either in the stroma or the lumen. The concentrations in the stroma are kept constant within the model calculations. In paragraph 4.2.1. it is shown that both the Mg^{2+} and the K^+ concentration in the lumen are very high and are thus not expected to change significantly. In paragraph 3.3.3. it is shown that although the proton concentration in the lumen is relatively low this concentration is not bound to change significantly due to the high buffer capacity. The luminal concentration of Cl^- however can be expected to change since it is very small by virtue of the Donnan equilibrium. It is clear that the deviation from a single exponential decay would not be detectable considering the signal to noise ratio of the experiments. This type of response was

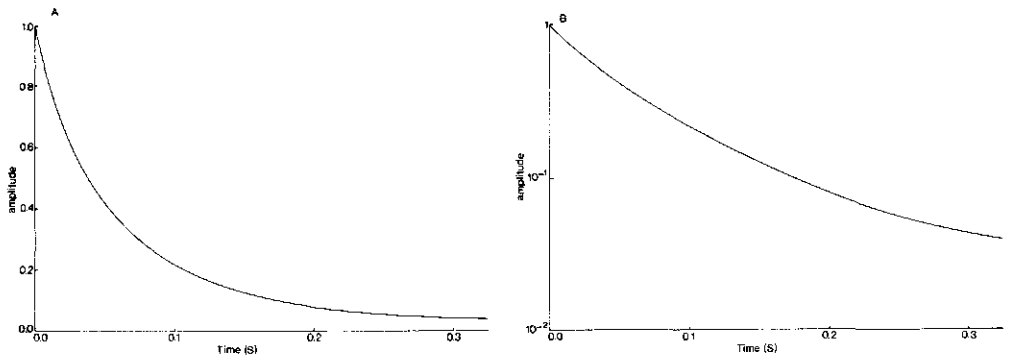


Figure 6.1. A: calculated passive decay of a sudden (i.e. flash-induced) change in membrane potential. The parameters for the type of thylakoid simulated are identical to those used in fig. 4.3b. A Donnan potential is present and consequently a high concentration of Mg^{2+} and K^+ and a low concentration of Cl^- is present in the lumen. The proton concentration is also higher in the lumen than in the stroma, but the passive proton flux is calculated to be too small to contribute to the decay of E_m . B: the semi-logarithmic plot of the result in A. Although the response shown in A appears to be a mono-phasic exponential curve, this curve in B reveals how inaccurate the concept of the single exponential decay is. The reason for the deviation from a single exponential decay must be found in the changes in concentration of Cl^- during the decay. Considering that 90% of the decay occurs in the first 200 ms after the flash and that the signal to noise ratio of microelectrode and P_{515} measurements precludes an accuracy beyond 10%, it is clear that the deviation from a single exponential decay will not be detected during the measurements.

called reaction I in relation to the P_{515} measurements or "classical" with regard to the microelectrode measurements.

6.1.1. The Q^- or b-cycle

The model cannot explain a biphasic rise of the transmembrane potential without fundamental change unless a secondary charge separation occurs after the flash-induced charge separation and it is spread-out in time. A candidate for such a charge separation would be a Q^- -cycle (Bouges-Bocquet 1977, Crowther and Hind 1980, Velthuys 1980, Jones et al. 1984, Jones and Whitmarsh 1985, 1987a, 1987b) or a b-cycle (Olsen et al. 1980, Wikström et al. 1981). In paragraph 6.2.2. we will discuss why we do not suppose that a Q^- - or b-cycle is the cause of the secondary slow rise in the flash-induced electric potential change.

6.1.2. "Localized" Chemiosmosis

Consequently we will look at other possible explanations of the biphasic rise in potential, while not adhering to our previous model. Here mainly structural effects are considered, which do not only explain the biphasic rise but also the slower decay of reaction II in comparison to reaction I, as will be explained in paragraph 6.2.3. However these explanations are not in accord with the basic assumptions of the chemiosmotic theory as proposed

by Mitchell (Mitchell 1961, 1966, Mitchell and Moyle 1983) and tend to be associated by another view of biological free-energy transduction originally proposed by Williams (Williams 1961, 1975, 1985). This view of membrane-linked free-energy transduction has been called "localized" chemiosmosis by some (Baker et al. 1981, Theg and Homann 1982, Theg and Junge 1983, Dilley and Schreiber 1984, Westerhoff et al. 1984, Nagle and Dilley 1986, Beard and Dilley 1986, 1987) or micro-chemiosmosis by others (Haraux and de Kouchkovsky 1983, de Kouchkovsky et al. 1984, Sigalat et al. 1985). The gist of these models comes down to the fact that they do not consider the lumen to be a homogeneous highly conductive phase. After translocation the protons are considered to remain either within the membrane (Baker et al. 1981, Kell and Morris 1981, Theg and Junge 1983, Dilley and Schreiber 1984, Peters 1986) or at the interface between membrane and solute (Kell 1979, Haraux and de Kouchkovsky 1983, de Kouchkovsky et al. 1984, Sigalat et al. 1985) or constrained within small coupling units (Westerhoff 1983, Westerhoff et al. 1984, Westerhoff 1985, Westerhoff and Chen 1985). The grand idea unifying these adherents of "localized" membrane-linked free-energy transduction is that the efficiency of the energy transduction must be regulated to meet the needs dictated by the external circumstances (Van Kooten 1984).

6.2. The Q-cycle

As we explained in paragraph 5.3.2 and 6.1.1 the relative slow rising component (phase b) in the flash-induced P_{515} response was thought to be caused by a secondary trans-membrane charge separation spread out over a 20 to 100 ms time period after the charge separations in the reaction centers have taken place. The candidate for this charge separation was a Q- or b-cycle. In either case this would involve cyt b_6 in the redox chain. We know of only one publication where another unknown molecule was proposed to mediate this charge separation instead of cyt b_6 (Bouges-Bocquet 1981). A report by Slovacek et al. (1979) revealed the possibility to remove phase b from the P_{515} response by adding antimycin A, known to be an inhibitor of cyt b_{562} reoxidation in mitochondria (Rieske 1971). Velthuys (1980) and Crowther and Hind (1981) revealed the possibility to remove phase b by adding DBMIB, which is known to inhibit reduction of cyt b_{563} in chloroplasts (Trebst 1985). These were strong indications that a secondary charge separation involving cyt b_6 was the cause of phase b, despite the fact that the thermodynamics of a Q-cycle is still a matter of debate (Hendler et al. 1985). Up till this date we are not aware of a publication bringing forth any non-controversial evidence for the actual occurrence of a Q-cycle in chloroplasts. Recent data of Matthews and Hope (1987) have even further enhanced the prevailing misunderstanding on this matter.

6.2.1. Cytochrome b_{563}

When we compare figs. 5.11 and 5.7 it is clear that there is no less redox turnover of cyt b_{563} after the second flash as there is after the first flash, while the phase b is absent at

518 nm after the second flash. This would imply no clear cut correlation between a secondary charge separation involving reduction and oxidation of cyt b_6 and phase b.

The experiments with antimycin A (Slovacek et al. 1979) were repeated in Szeged (Garab and Farineau 1983), but could not be reproduced in the absence of NH_4Cl . Under standard conditions, with carefully isolated thylakoids, an intrinsic phase b was present. Concentrations up to $50 \mu\text{M}$ antimycin A were unable to abolish this phase b.

6.2.2. The Decay Rates

Fig. 5.5 shows the P_{515} response when phase b has been saturated by a preceding flash. This response, called reaction I by us, has been shown to be elicited by pre-energizing the membranes either by light-induced electron transport or by ATP hydrolysis (Schapendonk et al. 1979, Schuurmans et al. 1981, Vredenberg and Schapendonk 1981, Schreiber and Rienitts 1982, Peters et al. 1983). When we compare reaction I with the dark adapted P_{515} response fig. 5.7a we see that not only phase b has disappeared but also most of the response after 100 ms. By subtracting the non-satiabile P_{515} response (fig. 5.5) from the total response (fig. 5.7a) one retains the satiable P_{515} response shown in fig. 5.8. This response is called reaction II by us. The rise time of reaction II is not the only difference from reaction I. Also the decay rate is much slower, i.e. $\approx 12 \text{ s}^{-1}$ for reaction I and between 4 and 1 s^{-1} for reaction II apart from an even slower decay rate (0.1 s^{-1} reaction III or phase d) which is not electrochromic in origin (Vredenberg et al. 1984). It is this difference in decay rate which precludes a secondary charge separation to be the cause of phase b.

6.2.3. The Theory

If the main assumptions of the "delocalized" chemiosmotic theory are true, i.e. two homogeneous conducting phases are separated by an inert semi-permeable membrane, then we can describe the flash-induced electric potential as follows: the two photosystems (50% PSI and 50% PSII in sun type plants) generate an instantaneous electric potential of 15 to 35 mV (Schapendonk and Vredenberg 1977) due to the semi permeable character of the membrane this potential will decay with a rate of $\approx 12 \text{ s}^{-1}$.

$$E_m(t) = E_m(0) \cdot \exp\{-12 \cdot t\} \quad (6.1)$$

After the flash cyt b_6 can be reduced and a Q- or b-cycle can take place. If we assume that for every PSI there is one Q-cycle and the rate of this reaction is 50 s^{-1} the resulting potential change would rise as follows:

$$E_{m_Q}(t) = 0.5 \cdot E_m(0) \cdot (1 - \exp\{-50 \cdot t\}) \quad (6.2)$$

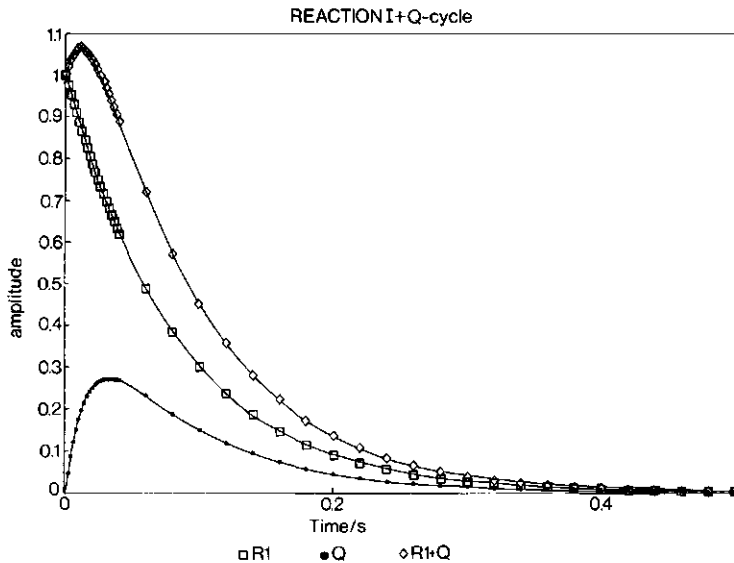


Figure 6.2. Calculated exponential curves taken from eqs. 6.1, 6.2 and 6.3. Reaction I (here denoted as R1) is described as a single exponential decay with a decay rate of 12 s^{-1} . The potential changes induced by a Q-cycle (reaction I/Q according to Ooms et al. 1987) is assumed to rise with a rate of 50 s^{-1} ; The decay rate is equal to that of reaction I. The sum of both curves is calculated by eq. 6.3. This type of response can be elicited by adding a PQ reducing agent to chloroplasts, which reveal only reaction I in their flash-induced P_{515} response before the addition, e.g. DQH_2 as by Jones et al. (1984).

Since we assume that these charge separations will transport protons from the stroma to the lumen, we must recognise that $Em(t)$ must decay with the same rate as eq. 6.1. These assumptions enable us to describe the rise and fall of the flash-induced electric potential when a Q- or b-cycle is present.

$$Em(t) = Em(0) \cdot \exp(-12 \cdot t) \cdot (1.5 - 0.5 \cdot \exp(-50 \cdot t)) \quad (6.3)$$

In fig. 6.2 the calculated curves of eqs. 6.1, 6.2 (but with a single exponential decay) and 6.3 are shown. The top curve in fig. 6.2 does not equate to the P_{515} response as we measure it, e.g. see fig. 5.7a. This implies that the phenomena leading to the apparent rise in potential (phase b) must have a strict dielectric separation from the phenomenon which generates the fast rise (phase a). Only then it is possible to associate the slow rise (eq. 6.2) with the appropriate slow decay.

$$Em_{R_2}(t) = Em_{R_2}(0) \cdot \exp(-2.5 \cdot t) \cdot (1 - \exp(-50 \cdot t)) \quad (6.4)$$

As we will show when we try to explain the origin of eq. 6.4 we have no possibility of predicting the actual value of $Em_{R_2}(0)$. In fig. 6.3 we have taken the value $Em_{R_2}(0) = 0.8 \cdot Em(0)$. This is

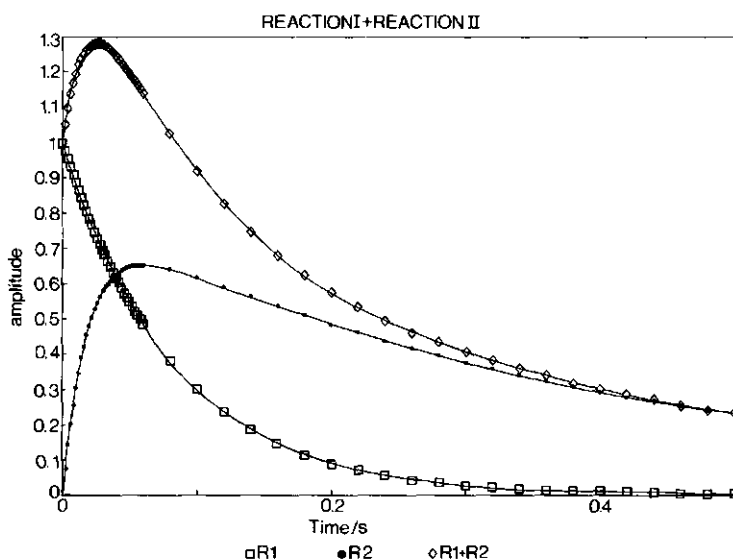


Figure 6.3. Calculated exponential curves taken from eqs. 6.1 and 6.4. Reaction I (here denoted as R1) is equal to the curve in fig. 6.2. Reaction II (here denoted as R2) is described by eq. 6.4 where the same rate for the rising exponential is assumed as for the Q-cycle induced potential change in fig. 6.2. However the decay rate is much slower than reaction I, i.e. 2.5 s^{-1} , due to a difference in potential dissipation assumed for the two reactions. The resulting sum of the two curves, i.e. R1 + R2, obviously is a better reflection of the P_{515} responses revealed in the previous chapter, than the curve shown in fig. 6.2.

clearly more in accord with the actual measurements than fig. 6.2.

When we agree on the basis of the evidence presented here, that the P_{515} response must be described by two phenomena separated by a non-permeable dielectric medium, then we must exclude a secondary charge separation as the sole cause of reaction II or phase b. Also other explanations pertaining to a two step charge separation (Zimanyi and Garab 1982) can be repudiated on the same grounds.

6.2.4. The Addition of Reductant

Most of the reports claiming the involvement of a Q-cycle in the P_{515} response mention the addition of powerful reductants to the thylakoid suspension. At first dithionite was mainly used (Joliot and Delosme 1974, Bouges-Bocquet 1977, Slovacek and Hind 1978) later on reduced duroquinone (DQH_2) was added (Selak and Whitmarsh 1982, Jones et al. 1984, Jones and Whitmarsh 1985, 1987a, 1987b, Hope and Matthews 1987). Our experiments are not performed in the presence of these reductant (Peters et al. 1983, 1984a, 1984b, 1984c, 1985, 1986, Peters 1986). Instead we rely on culturing our plants and isolating the chloroplasts carefully in order to retain an intrinsic phase b or reaction II in our flash

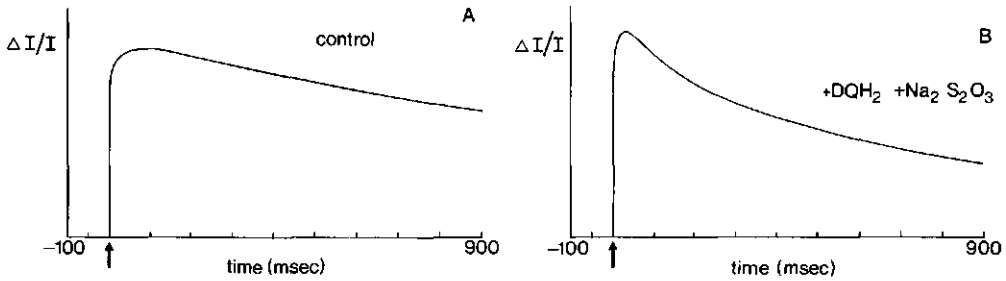


Figure 6.4. Flash-induced absorbance changes at 518 nm in a suspension of broken spinach chloroplasts. The measurements were performed at 3°C and recorded on a 1 s time scale. The arrows mark the moment the flashes are fired, i.e. $t = 0$. **A:** control measurement (for the conditions see paragraph 2.2.2.). **B:** same as in A, but with 0.83 mM DQH₂ and 1 mM Na₂S₂O₄, added 5 minutes before the measurement. The response can only be caused by a charge separation in PSI and possibly by a Q- or b-cycle. The addition of reductant induces an extra rise and decay in the response. The part added to the response in B as compared to A, reveals an evidently faster decay rate than the overall decay rate in A. These rates are much faster than the rates pertaining to reaction II.

induced P₅₁₅ response. In fig. 6.4a we see a flash-induced response from isolated broken chloroplasts under our standard conditions, e.g. see paragraph 2.2.2, and when dithionite together with DQH₂ are added to the suspension (fig. 6.4b). The difference between the two responses, i.e. in the presence or in the absence of reductant, is rather similar to eq. 6.2 including a decay rate equivalent to reaction I. This observation makes us wary of the possibility that, when speaking of a secondary slow rise in the flash-induced P₅₁₅ response, different phenomena can cause this slow rise depending on the measuring conditions. If a phase b is induced in chloroplasts with the same decay rate as the rate measured in pre-energized chloroplasts then this could be caused by a Q-cycle type of charge separation. If on the other hand phase b is correlated to a slower decay rate (i.e. phase c in Schapendonk et al. 1979), we speak of reaction II and assume a structural cause for this phenomenon (Ooms et al. 1987). Vredenberg et al. (1987) have proposed a new nomenclature for the two distinguishable slow phases and refer to it as R1/Q when it is caused by a Q-cycle or as RII when it is caused by intrinsic membrane structures in the dark adapted state.

6.3. A Model for Reaction II

When we examine the evidence of the previous paragraph it becomes almost inevitable to propose two separate events involved in the flash-induced electric potential change. One event will then explain reaction I, while the other event must explain reaction II. After the charge separation the majority of the charges will equilibrate with the water phases on both sides of the thylakoid membrane. Since the conductivity of these phases is very high this will immediately be sensed by the P₅₁₅ carotenoid as a field over a flat capacitor C_m which is dissipated through a

76 Photosynthetic Free Energy Transduction

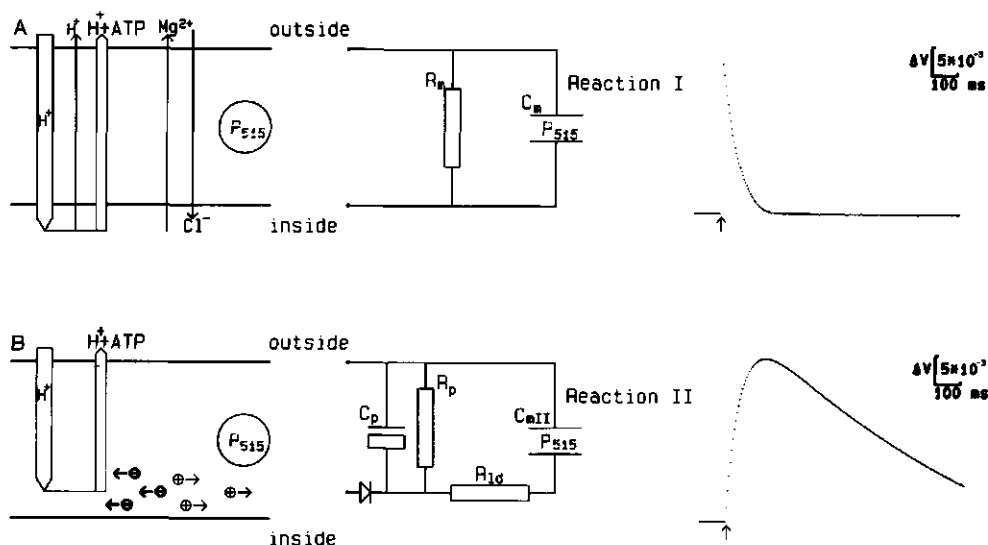


Figure 6.5. A: (right) Schematic view of transverse charge transport across the thylakoid membrane. The photosystems actively transport positive charges from the outside to the inside. The resulting electric potential is dissipated by passive charge movement across the membrane and by a proton flux through the ATPase. A carotenoid situated within the membrane will respond linearly to any change in electric field by an absorbance change at 515 nm. (middle) Electrical network equivalent of the charge fluxes depicted on the right. R_m is viewed as the total resistance of the membrane to charge flow. The field sensed by the P_{515} carotenoid is depicted as the field in the membrane capacitor C_m . (left) Response of the potential measured over the capacitor C_m . The network was build and charged with a square positive current pulse of 10 mA, pulse width 100 μ s. The arrow indicates the moment the pulse was fed to the network. $R_m = 60 \text{ k}\Omega$ and $C_m = 1 \text{ }\mu\text{F}$. This response is described by eq. 6.5.

B: (right) Schematic drawing of the transverse and lateral charge transport in the thylakoid membrane, assuming the impossibility for part of the transported protons (depicted by the diode) to equilibrate with the lumen. Such protons are stabilized within the membrane and are thought to take part in the activation of the ATPase. The stabilized charges within the membrane will induce a movement of large membrane intrinsic proteins. This movement will spread the localized field inhomogeneity along the plane of the membrane. The carotenoids will sense a rise in the electric potential depending on the average distance to the stabilized protons and the mobility of membrane intrinsic proteins. The decay of the potential will be governed by the rate at which the stabilized protons are allowed to leave the membrane. (middle) Electrical network equivalent of the charge fluxes depicted on the right. The protons are stabilized in a limited capacitance C_p and can leave the membrane via a resistor R_p . The spreading of the localized field is pictured as a current passing through a resistor of lateral diffusion R_{1d} . The carotenoid senses the field in a membrane capacitance C_{mII} , which is not necessarily the same as in A. (left) Response of the potential measured over the capacitor C_{mII} . The network was build and charged through the diode with the same square positive current pulse as in A. The arrow indicates the moment the pulse was fed to the network. $R_p = 1 \text{ M}\Omega$, $R_{1d} = 0.8 \text{ M}\Omega$, $C_p = 1 \text{ }\mu\text{F}$ and $C_{mII} = 0.47 \text{ }\mu\text{F}$. This response is described by eq. 6.6.

resistor R_m in parallel (see fig. 6.5a). This would explain reaction I adequately as the instantaneous loading of the capacitor C_m by a charge Q , i.e.

$$V(t) = (Q/C_m) \exp[-t/(R_m \cdot C_m)] \quad (6.5)$$

However if not all charges equilibrate with the aqueous phases and some are stabilized within the membrane (Baker et al. 1981, Theg and Homann 1982, Dilley et al. 1982, Westerhoff et al. 1983, Theg and Junge 1983, Dilley and Schreiber 1984, Beard and Dilley 1986, 1987) then the electric field change they induce can be considered additive to reaction I. In fig. 6.5b we have depicted this by drawing a diode through which an electrolytic capacitor C_p can be charged. Since these charges are stabilized within a non-natural environment the resistance of charge dissipation R_p is of a different nature than the resistance for charges which have equilibrated with the bulk aqueous phases. Hence the possibility of a different decay rate of this field. From Zimanyi and Garab (1982) we know that the field induced by C_p will be sensed as homogeneous throughout the membrane except in the vicinity of the charges (<1 nm). In thylakoids there is a high ratio of proteins to lipids (Barber 1983), which are all polarized molecules and some even have charges within the hydrophobic part of the membrane (Nelson 1981). We assume that a protein within the vicinity of the membrane stabilized charge (C_p) will readjust the position of its dipole in order to align it as much as possible with the local inhomogeneous field lines. As a consequence the inhomogeneous field will broaden and another protein, previously not sensing the field inhomogeneity, will now also sense it and move accordingly. In this manner the strong localized field inhomogeneity caused by a charge stabilized within the membrane is spread with the consecutive movements of proteins in that membrane. This spreading of the field can be seen as a current flowing through a resistor of lateral diffusion R_{1d} . A field sensitive pigment like P_{515} will sense this as a rising potential with its rise time depending on its position relative to the stabilized charge (R_{1d}) and within the membrane $C_{m_{II}}$. The dissipation of this field will be dominated by C_p and R_p . The electric diagrams shown in fig. 6.5 were built and fed with a short ($\approx 20 \mu s$) current pulse, the responses measured over the capacitors C_m and $C_{m_{II}}$ are shown on the right. The schematic diagram in fig. 6.5b can aid us in determining a differential equation for the potential changes over the capacitor $C_{m_{II}}$.

$$d^2V/dt^2 + ((1/R_p C_p) + (1/R_{1d} C_{m_{II}}) + (1/R_{1d} C_p)) dV/dt + (1/R_p C_p R_{1d} C_{m_{II}}) V = 0.$$

The solution of this equation based on the instantaneous loading of the capacitor C_p by a charge Q' is as follows:

$$V(t) = A (\exp[-k_1 \cdot t] - \exp[-k_2 \cdot t]) \quad (6.6)$$

with

$$\begin{aligned} A &= Q' \cdot R_p / B \\ k_1 &= ((C_{m_{II}} + C_p) \cdot R_p + C_{m_{II}} \cdot R_{1d} - B) / (2 \cdot C_p \cdot R_p \cdot C_{m_{II}} \cdot R_{1d}) \\ k_2 &= ((C_{m_{II}} + C_p) \cdot R_p + C_{m_{II}} \cdot R_{1d} + B) / (2 \cdot C_p \cdot R_p \cdot C_{m_{II}} \cdot R_{1d}) \\ B &= \sqrt{((C_{m_{II}}^2 + 2C_p \cdot C_{m_{II}} + C_p^2) \cdot R_p^2 + 2(C_{m_{II}}^2 - C_p \cdot C_{m_{II}}) \cdot R_{1d} \cdot R_p + C_{m_{II}}^2 \cdot R_{1d}^2)} \end{aligned}$$

This model can explain the satiability of reaction II by a few charge separations (Vredenberg and Schapendonk 1981, Schreiber and Del Valle-Tascon 1982, Van Kooten et al. 1983, Peters et al. 1983, 1984a-c, 1985, 1986) and by ATP hydrolysis (Schuurmans et al. 1981, Schreiber and Rienitts 1982, Morita et al. 1982, Peters et al. 1983). The electron transport chain can charge a limited capacitor C_p through the diode depicted in fig. 6.5b, while reversed electron flow caused by ATP hydrolysis can do the same. When C_p is fully charged further charge separations are incapable of inducing a potential change in C_p , thus all charges are forced to equilibrate with the aqueous phases and no reaction II will occur. If we refer to the model proposed by Dilley et al. (1982) then the charges on the capacitor C_p must be protons and part of our R_p can be seen to be the ATPase. The model would also explain why a transmembrane field measurement like the microelectrode would not see a reaction II type response, while an intrinsic probe like P_{515} would see it. However in paragraph 5.2.2. microelectrode measurements were shown, which appeared to contain a reaction II type of response (see also Van Kooten et al. 1984). This prompted us to look for other possible explanations for reaction II.

6.4. Resistance to Lateral Diffusion

When we first proposed the model presented in the previous paragraph (Westerhoff et al. 1983) we had a strict separation in mind between protons equilibrating with the lumen, causing a reaction I type of response, and protons stabilized in intramembrane domains (Murphy 1982), causing a reaction II type of response. In this view it is still possible to regard the lumen as a homogeneous conductive phase. As has been suggested, this is highly unlikely to be the case in thylakoids or, for that matter, in the matrix space of mitochondria (Williams 1985). As the microelectrode definitely measures potential changes from lumen to stroma and can record reaction II type responses (see paragraph 5.2.2) we must look at other possibilities to explain reaction II.

Experiments by Hong and Junge (1983) revealed that when chloroplasts retained some of their original structure after preparation, the movement of protons in the lumen was highly restricted. These diffusion barriers were clearly identified on the appressed side of the thylakoid stacks (Polle and Junge 1984, 1986) and are allegedly caused by high concentrations of immobilized buffer groups attached to intrinsic membrane proteins. As was discussed in paragraph 3.3.3 it is clear that high concentrations of immobilized buffer groups must be present in the lumen. We will first calculate whether these immobilized buffer groups severely inhibit proton movement in the lumen before discussing its possible involvement in reaction II.

6.4.1. Diffusion in a plane

In order to calculate the effect of buffer groups in the lumen on the diffusion of protons it is necessary to describe the thylakoid system in simple terms. Due to the proximity of the membranes in the lumen, which is less than 8 nm (Deamer et al.

1967, Williams 1985) and to the relatively large diameter of the thylakoid disks, which is more than 300 nm (Junge 1977, Witt 1979), we assume the lumen to be a planar region where diffusion can take place in two dimensions only, e.g. x and y . When we imagine the reaction centre to be a point in the origin of the plane where under the influence of light a constant flux of protons is injected, then the boundary conditions for Fick's second law of diffusion can easily be expressed (Crank 1975).

6.4.1.1. Boundary Conditions

- 1) The concentration profile has perfect rotational symmetry around the origin in the plane and can be described as $c(r,t)$ with $r = \sqrt{(x^2 + y^2)}$, and the coefficient of diffusion (D in $\text{cm}^2 \cdot \text{s}^{-1}$) is constant throughout the plane.
- 2) At $t = 0$ we assume the concentration to be zero throughout the plane.
- 3) When $t \geq 0$ a constant flux j (in $\text{mol} \cdot \text{s}^{-1}$) of protons is injected in the origin of the plane.
- 4) At infinity the concentration must always be zero $c(\infty, t) = 0$.

6.4.1.2. Fick's Second Law

With this set of conditions it is possible to solve Fick's second law of diffusion:

$$\frac{\partial c}{\partial t} = D \cdot \nabla^2 c \quad (6.7)$$

Since we have rotational symmetry we can convert eq. 6.7 to cylindrical coordinates and perform a Laplace transformation to rid ourselves temporarily of the time variable.

$$pe = \frac{D}{r} \frac{d}{dr} \left(r \cdot \frac{de}{dr} \right) \quad (6.8)$$

With a few substitutions eq. 6.8 can be transformed into a well known differential equation:

$$q^2 = p/D \Rightarrow \frac{d^2 e}{dr^2} + \frac{1}{r} \frac{de}{dr} - q^2 e = 0 \quad (6.9)$$

$$x = qr \Rightarrow x^2 \frac{d^2 e}{dx^2} + x \frac{de}{dx} - x^2 e = 0 \quad (6.10)$$

This differential equation (eq. 6.10) has the zero order modified Bessel functions $I_0(x)$ and $K_0(x)$ as a solution (Abramowitz and Stegun 1972). Since $I_0(x) \rightarrow \infty$ and $K_0(x) \rightarrow 0$ as $x \rightarrow \infty$, we have to use $K_0(x)$ as a solution to stay in accord with the fourth assumption made in paragraph 6.4.1.1.

$$e = K_0 \left(\frac{r}{D} \cdot \sqrt{p} \right) \quad (6.11)$$

We perform an inverse Laplace transformation on eq. 6.11 and a general solution for the concentration function in time emerges.

$$c = \frac{A}{t} \exp\left(-\frac{r^2}{4Dt}\right) \quad (6.12)$$

The concentration in eq. 6.12 is expressed in quantity per unit of surface area, i.e. $\text{mol}\cdot\text{cm}^{-2}$ and A is an unknown constant. To solve eq. 6.12 for the proper value of A we first assume that a unit of solute j is diffusing in the plane after a unit of time before solving the time dependent part.

$$j = \int_0^{2\pi} d\theta \int_0^{\infty} c r dr = \frac{2A\pi}{t} \int_0^{\infty} r dr \exp\left(\frac{-r^2}{4Dt}\right) \quad (6.13)$$

Now the time dependent solution can be solved:

$$c(r,t) = \frac{1}{4\pi D} \int_0^t j \exp\left(\frac{-r^2}{4D(t-t')}\right) \cdot \frac{dt'}{(t-t')} \quad (6.14)$$

With a few substitutions eq. 6.14 can be recognized as the exponential integral function E_1 . Thus the analytical solution to our problem can be written as:

$$c(r,t) = \frac{j}{4\pi D} E_1\left(\frac{r^2}{4Dt}\right) \quad (6.15)$$

Eq. 6.15 is the actual solution to the diffusion bounded by the four assumptions made. Now it is possible to calculate the effect of buffer groups on this dynamic concentration profile.

6.4.1.3. Mobile Buffers

The reaction with the buffers proceeds rapidly enough, in comparison to the diffusion process, to assume local equilibrium between protons in solution and the buffered protons. In the simplest case the concentration of buffered protons (S) is directly proportional to the concentration of free protons (c), i.e.

$$S = R \cdot c \quad (6.16)$$

Now there are two extreme possibilities, in one case the buffer is as mobile as the free protons. These mobile buffers cannot influence the diffusion process in any way. Therefore their only effect will be the homogeneous diminution of the concentration of free protons by a factor R.

$$c(r,t) = \frac{j}{4\pi DR} E_1\left(\frac{r^2}{4Dt}\right) \quad (6.17)$$

6.4.1.4. Immobile Buffers

The other extreme is when the buffers are immobile. The diffusion coefficient for free protons in water is estimated to be $10^{-4} \text{ cm}^2\cdot\text{s}^{-1}$ (Franks 1972) and that of intrinsic membrane proteins between 10^{-9} and $10^{-12} \text{ cm}^2\cdot\text{s}^{-1}$ (Sowers and Hackenbrock

1981, Barber 1982, 1983b). The buffered protons are then not free to diffuse and this must be taken into account in the second law of Fick.

$$\frac{\partial c}{\partial t} = D \cdot \frac{\partial^2 c}{\partial x^2} - \frac{\partial S}{\partial t} \quad (6.18)$$

When we substitute eq. 6.16 into eq. 6.18 it appears that the diffusion coefficient is altered:

$$\frac{\partial c}{\partial t} = \frac{D}{1+R} \cdot \frac{\partial^2 c}{\partial x^2} \quad (6.19)$$

When we insert this apparent coefficient of diffusion, i.e. $D/(R+1)$ in eq. 6.17 the effect of the immobilized buffers becomes clear:

$$c(r, t) = \frac{j(R+1)}{4\pi DR} \cdot E_1 \cdot \left(\frac{r^2 (R+1)}{4Dt} \right) \quad (6.20)$$

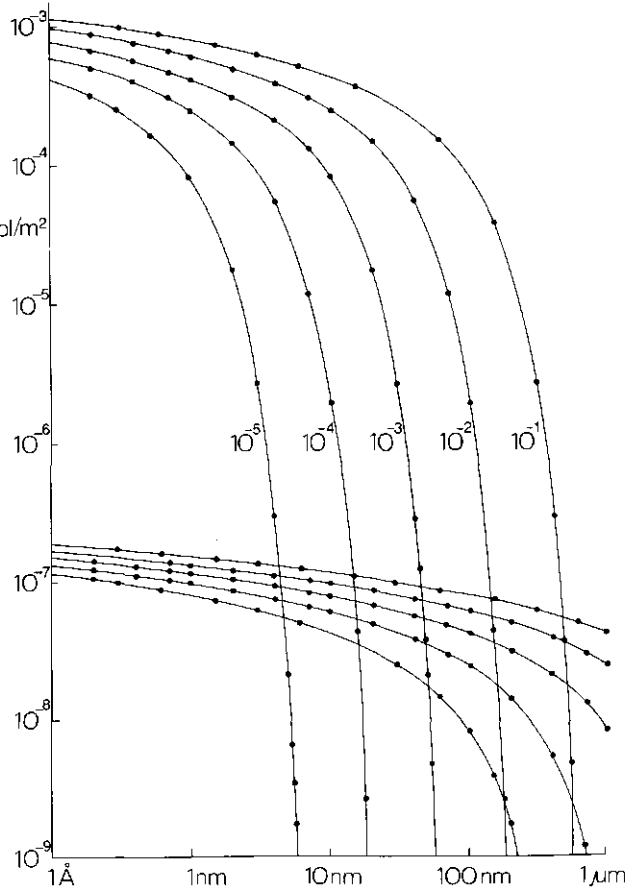
The luminal buffering capacity was discussed in paragraph 3.3.3. This capacity is so large that a value of $R = 10^4$ can be considered as conservative. As a consequence the ratio $(R+1)/R$ in eq. 6.20 approaches 1. In fig. 6.6 we compare the calculated results of eqs. 6.17 and 6.20 at five different moments in time after the onset of the proton pump. When we assume an average distance between the reaction centers of 17 nm (Barber 1980) it is clear that with the mobile buffers in solution the pH will not deviate much from pH 7 and will be more or less homogeneous in the plane within 10^{-5} s. In the case of the immobilized buffers the pH can reach a local value of 3 and it will take longer than 10^{-3} s before the local profiles will overlap to create a homogeneous pH. Although we have simplified the situation to a great extent, the results are still similar to a numerical solution of Fick's second law incorporating a concentration dependent term (eq. 3.18) in the diffusion coefficient (Ott and Rys 1973).

6.4.2. Retarded Diffusion and the Electric Potential

As we have discussed in paragraph 6.3 it is necessary to assume a strict dielectric separation between the two phenomena leading to reaction I and reaction II. Retarded diffusion of protons in the lumen would thus *not* be sufficient to explain reaction II as measured by P_{515} . However structural effects do tend to play an important part in the generation of reaction II (Schapendonk 1980, Hong and Junge 1983, Dilley and Schreiber 1984, Peters 1986). These effects also tend to determine whether $\Delta\mu_{H^+}$ functions within a "localized" or a "delocalized" coupling scheme (Beard and Dilley 1986, 1987). It is therefore possible that retarded diffusion does not explain reaction II but it can explain the so-called "new" responses measured with the microelectrode as in paragraph 5.2.2. As is evident in fig. 5.4 a "classical" response can turn into a "new" one when the

Figure 6.6. Calculated proton concentration profiles in a plane as a function of distance to the source flux and at different time intervals after the onset of the flux. The source is considered to be a constant point flux of $10^{-12} \text{ mol} \cdot \text{s}^{-1}$. The diffusion coefficient for protons is assumed to be $10^{-5} \text{ cm}^2 \cdot \text{s}^{-1}$. Two different sets of concentration profiles are calculated:

- 1) profiles calculated with eq. 6.20, based on the assumption of the presence of immobilized buffer groups. The amplitude of these concentration profiles at 1 \AA from the source flux is in the order of magnitude of $10^{-3} \text{ mol} \cdot \text{m}^{-2}$.
- 2) profiles calculated with eq. 6.17, based on the assumption that the buffers present are as mobile as the free protons. The amplitude of these concentration profiles at 1 \AA from the source flux is in the order of magnitude of $10^{-7} \text{ mol} \cdot \text{m}^{-2}$. It is assumed that the rate of the buffering reaction is much faster than the speed of diffusion of the protons, allowing thermodynamic equilibrium in the vicinity of the buffer. The buffering groups are assumed to possess an infinite buffering capacity, see eq. 6.16, with $R = 10^6$. The inset values give the time in seconds of the specific concentration profile after the onset of the source flux. This is done for the profiles calculated on the basis of immobilized buffers only. A similar set of time values is used for the profiles calculated on the assumption of mobile buffers.



6.4.2.1. Destruction Upon Impalement

When a microelectrode penetrates a thylakoid granum stack it is very likely that this structure is severely disrupted. However, as is evident from paragraph 5.2, we do measure the light induced potential changes. Therefore we must assume that the thylakoid membrane promptly seals around the electrode creating a rather large luminal bleb-like space. This sealing can be expected to occur in a short period of time due to the high fluidity of the thylakoid membrane (Barber 1983). Such a bleb-like space may or

may not be in direct contact with the rest of the thylakoid lumen. If after the impalement a single closed bleb has formed around the electrode tip this space must by virtue of its dimensions respond in a "classical" sense to light-induced potential changes. If however the connection to the rest of the unperturbed thylakoid lumen is restored the response can change drastically. Now we have a situation as described by Kara-Ivanov (1983). The lumen can be considered as deep invaginations and the flash-induced potential must travel a distance in the order of micrometers where diffusion of protons, but probably also of other cations chelated by proteins, is retarded to the rate of protein diffusion ($D \approx 10^{-9} \text{ cm}^2 \cdot \text{s}^{-1}$). With this type of movement and using Einstein's equation (Einstein 1908) we can calculate that it takes 2.5 s to diffuse a distance of $1 \mu\text{m}$!

The "new" response can then be explained in a similar manner as we have used in paragraph 6.3. There is now a less strict localization. Charge separations in the thylakoid membrane at a distance from the electrode stay localized at first. Retarded diffusion slows the spreading of this potential on the ms time scale. This can explain the slow rise measured by the microelectrode in the same manner as in fig. 6.5b, i.e. R_{1d} . Since *Peperomia metallica* thylakoids consist almost exclusively of granum stacks the equilibration of the local field on the stromal, but appressed, side of the membrane will also be retarded. This can explain a slowing down of the passive dissipation through equilibration in the appressed space, i.e. R_p . This barrier was already found to cause an equilibration rate of 60 ms in spinach thylakoids (Polle and Junge 1984, 1986) were the extent of the appressed areas is far less than in *Peperomia metallica*.

6.5. Conclusions

Although it has been shown that the flash-induced response measured with P_{515} and the one measured with the microelectrode can be compared, e.g. see fig. 5.12, when we analyze the probable cause of these signals possible differences emerge. For reaction II as measured with P_{515} we propose a strict dielectric separation of membrane stabilized protons from "free" protons in the lumen as depicted by the diode in fig. 6.5b. For the "new" response measured with the microelectrode we propose a temporary separation by retarded diffusion of protons and other ions. This structural effect is thought to be caused in part by the penetration itself of the microelectrode. A question remains to be answered, i.e. "Why are the two responses in fig. 5.12 so alike when their origins are different?". According to our explanation presented in this chapter the equivalence in decay rate between reaction II and the "new" response should bear no causal relationship.

7. General Discussion

7.1. Introduction

From the material presented in this thesis it is evident that we have to scrutinize our concept of chemiosmotic coupling in order to understand the results. Chapters 3 and 4 are fully in accord with the chemiosmotic hypothesis as proposed by Mitchell (1961, 1966). More precisely it assumes that membrane-linked biological free energy transduction takes place in a system consisting of two compartments separated by a membrane capable of vectorial transport. The compartments are viewed as homogeneous high conductance aqueous phases. The concept based on this assumption is sometimes characterized as "delocalized" chemiosmosis (Westerhoff et al. 1984). In chapter 5 results are presented which cannot be explained without augmenting this concept of chemiosmosis. Models explaining these results are presented in chapter 6. The introduction of a Q-cycle (Mitchell 1976) or a b-cycle (Wikström et al. 1981) would not change the concept of "delocalized" chemiosmosis, but it was shown in paragraph 6.2 that it cannot be the cause of the relatively slow rising and decaying components in the flash-induced electric potential changes. The possible explanations presented in paragraphs 6.3 and 6.4 have in common that protons involved in chemiosmotic coupling can have differences in electrochemical potential amounting to much more than their thermal energy, which implies a serious deviation from the so-called "delocalized" protonic coupling (Mitchell 1981). This leads to set of various coupling hypotheses commonly denominated by the term "localized" protonic coupling (Westerhoff et al. 1984, Sigalat et al. 1985).

The "delocalized" chemiosmotic hypothesis has been successfully verified on many occasions (Boyer et al. 1977). Still it is the urge to understand the precise mechanism by which primary and secondary proton pumps are coupled together, which tend to augment the "delocalized" theory with "localized" aspects (e.g. Kell et al. 1981, Dilley et al. 1982, Theg and Junge 1983, Hareaux and de Kouchkovsky 1983, Westerhoff et al. 1984, Westerhoff and Chen 1985, Sigalat et al. 1985, Nagle and Dilley 1986, Beard and Dilley 1986, 1987, Theg and Dilley 1987). Apart from the need to explain certain anomalies between experiment and theory (as in chapter 6), it is the possibility to change the efficiency of energy transduction which makes the concept of "localized" coupling appealing (Van Kooten 1984). When the substrate (i.e. light for chloroplasts) level is low and the phosphorylation potential high, e.g. $46 \text{ kJ}\cdot\text{mol}^{-1}$ (Giersch et al.

1980), then an activated ATPase can lead to severe losses of useful energy due to ATP hydrolysis (Gräber et al. 1984, 1987). Under those conditions a shift from "delocalized" protonic coupling to a "localized" coupling unit (Westerhoff 1985) would enable ATP synthesis to occur, while the apparent free energy contained within the proton gradient does not exceed the phosphate potential divided by the proton-per-ATP stoichiometry of the ATPase (Westerhoff and Chen 1985). Indications for reversible shifts between "localized" and "delocalized" coupling in osmotically shocked thylakoids have been found (Sigalat et al. 1985, Beard and Dilley 1986, 1987).

7.2. The Electric Potential and the Nature of Coupling

This thesis concerns itself with two different ways to determine the light-induced trans-membrane electric potential changes. When we try to relate these results to the manner of membrane linked free energy transduction involved, it is necessary to assess the influence of the measurement itself on the measured response.

7.2.1. Microelectrode Measurements

As is clear from fig. 3.5, it is possible to simulate the electric potential changes involved in photosynthetic free energy transduction, when we base our assumptions on the concept of "delocalized" chemiosmotic coupling (Mitchell 1961, 1966, Vredenberg 1976). It appears that the diodic nature (Jackson 1982, Jackson et al. 1987) of the membrane is described well by an algorithm proposed by Gräber et al. (1984, 1987). Also recent experiments performed with an antimony tipped pH sensitive microelectrode (Remis et al. 1986a, 1986b) reveal that light-induced changes in ΔpH are also described by the model presented in chapter 3. Even the influence of NH_4Cl on the ΔpH changes, measured by Remis et al. (1986b), can be qualitatively simulated by assuming an extreme buffer capacity in the lumen (see fig. 4.5). The equivalence between measurement and calculations in view of the application of membrane modifying reagents such as valinomycin (fig. 4.8) or A23187 (fig. 4.7), further enhances our confidence that microelectrode experiments can be fully explained with "delocalized" chemiosmotic coupling.

7.2.1.1. The "classical" Response

These responses (see fig. 5.1) were termed "classical" in paragraph 5.2.1. Since they can be simulated by a model based on the assumption of "delocalized" chemiosmosis, the response may as well have been called the "delocalized" response. There are two reasons why we do not expect to measure effects related to "localized" protonic coupling with a microelectrode. One being the microelectrode tip diameter in relation to the dimensions of the luminal space where it is supposed to measure the potential changes. The other is the need to pre-illuminate the chloroplasts in microelectrode experiments (e.g. see paragraph 2.1.1.2), which is known to suppress a reaction II type of response caused by

continued ATP hydrolysis in the dark (Peters et al. 1983). The first argument we call structural and the second catalytic.

7.2.1.1.1. The Structural Reason

The outer diameter of the microelectrode tip varies between 0.1 and 0.3 μm . The diameter of a grana disc in *Peperomia metallica* chloroplasts varies between 1 and 1.5 μm (Schapendonk 1980, personal observations data not shown). Electron micrographs reveal a dense grana structure in these chloroplasts without any detectable stroma lamellae (see Vredenberg 1976). This thylakoid ultra-structure is typical for obligate shade plants (Björkman 1981). Thus when a microelectrode penetrates a *P. metallica* chloroplast it is bound to strike a granal stack. Biological free energy transducing membranes tend to be quite appressed in general (Skulachev 1980, Malhotra and Sikerwar 1983). The average distance between the membranes in the lumen of the chloroplast is 8 nm in the dark and 4 nm under saturating light conditions (Barber 1980). In the appressed regions the membranes are believed to be spaced by 1.5 nm or less (Polle and Junge 1986b, Junge and Polle 1986). The thickness of the membrane itself varies between 5 and 10 nm. Taking these dimensions in consideration one would expect that if impalement does not disturb the thylakoid structure, one would stand a chance of 10% to land the tip in an appressed region, 40% in the lumen and 50% in the membrane itself! Our experience is that a practiced electrophysiologist can measure light-induced electrical responses 9 out of 10 times that a chloroplast is tentatively impaled. A positive response, indicating that the microelectrode tip is situated in the lumen, is then perceived at least in 19 out of 20 times (Vredenberg 1976). A negative response, indicating that a type of inside-out vesicle has formed itself like a patch around the tip, is only seen on very few occasions (Bulychev et al. 1976). These negative responses are usually characterized by a faster decay rate when the light is shut off, indicating a larger membrane permeability.

These observations lead us to the assumption that the thylakoid membrane is temporarily disturbed upon impalement. This combined with the fact that thylakoids are able to form bleb-like structures (i.e. balloons of 5 μm diameter) after hypotonic shock (Farkas et al. 1984), which are still capable of electron transport and photophosphorylation, provokes the following idea: upon impalement part of the granal stack being hit is destructed. In a very short time period, i.e. less than 1 s, since responses have been observed within that time after impalement, the membrane material rearranges itself to form a closed bleb-like volume around the electrode tip. In most cases this is a right-side-out vesicle giving a positive light-induced electric response, however in some cases this can also be an inside-out vesicle with a negative light-induced response. The integrity of the membrane after reformation can be considered to be complete with regard to the ionic permeability. On many occasions we have measured the same decay rate, after a flash-induced potential change, with the microelectrode as with the P_{515} technique following a pre-illumination period, see paragraph 2.1.1.2. and Bulychev et al. (1976). However the intrinsic structure enabling a reaction II type of response has been shown to be of a volatile nature, see paragraph 7.2.2.1. and Peters (1986), and is not expected to survive the destruction and subsequent reformation of the membrane.

Explanations of the anomalies found in the literature are usually based on localized protonic coupling, e.g. the local coupling unit as proposed by Westerhoff et al. (1984), Westerhoff and Chen (1985) and Westerhoff (1985). The size of such a coupling unit is very small in comparison to a probe size of 0.1 to 0.3 μm . Thus it cannot be expected that the microelectrode would measure the response of such a local coupling unit directly. Other explanations of the anomalies depend on the thylakoid structure (Hong and Junge 1983, Dilley and Schreiber 1984, Beard and Dilley 1986, Theg and Dilley 1987), which is not expected to be retained during impalement. However, it was determined that the presence of reaction II in flash-induced responses was dependent on the structural intactness of the thylakoid membrane after isolation (Schapendonk 1980, Vredenberg 1981, Peters 1986, and see fig. 5.9). This structural intactness seems to be a general necessity to measure any of the anomalies (Sigalat et al. 1985) and could explain some contradictions between results found by different people, e.g. well documented reversible "localized" to "delocalized" coupling (Beard and Dilley 1986, 1987) versus the very elegant work following the proton in the stroma, lumen and membrane (Junge et al. 1987). Since we do not expect a fully intact membrane structure upon impalement we do not anticipate to measure any effect pertaining to "localized" protonic coupling with the microelectrode.

7.2.1.1.2. The Catalytic Reason

As is clear from paragraph 2.1.1. it is necessary to illuminate the chloroplast before and during the impalement process. The intensity of this light is sufficiently energizing to ensure substantial activation of the H^+ -ATPases in the thylakoid membrane, e.g. see paragraph 3.3.4. In spinach leaves it was shown that a 10 s pre-illumination was sufficient to suppress reaction II and in intact chloroplasts isolated therefrom a 40 s illumination period was necessary for a full suppression (Peters et al. 1983). This suppression was linked to ATP hydrolysis in the dark (Schreiber and Rienits 1982, Peters et al. 1986). The same experiments were performed with leaves of *Peperomia metallica* (data not shown). It appeared that a 10 s pre-illumination was sufficient to suppress a reaction II, which could be measured after a dark adaptation of 1.5 hour. Although recuperation of reaction II started directly and could be detected by slowing the decay rate of the response, it took more than 15 minutes before a slow rise became detectable. More than an hour of dark adaptation was needed before a full recovery of reaction II had taken place. This is a much slower rate of reaction II recovery than was found for spinach, e.g. see fig. 4 of Peters et al. 1983 where a full recuperation takes place in 20 minutes.

If reaction II were detectable as a transmembrane electric phenomenon, then we would only expect to measure it after long periods of dark adaptation. Since microelectrode measurements are never done with dark adaptation periods longer than 5 minutes, usually shorter, we do not expect to measure a reaction II type of response of considerable magnitude with this technique.

7.2.1.2. The "new" Response

As is evident from figs. 5.2, 5.3 and 5.4 responses containing a reaction II type component, denoted as "new" (see

paragraph 5.2.2), were measured with the microelectrode. From the previous paragraphs it must be clear that we did not expect to measure a response like this. However the switch from a complete absence of a reaction II to a full presence within 3 minutes in one and the same chloroplast (see fig. 5.4) can be considered as an indication of the origin of the "new" response. In paragraph 6.4.2 we described the effect of immobilized buffers and chelating agents on the transversal dislocation of the electric potential. We now picture the course of events upon impalement as follows. The first sequence of events are described in paragraph 7.2.1.1.1., which explains why we measure a reaction I or "classical" response upon impalement. After 3 minutes of dark adaptation we do not expect a substantial deactivation of ATPases as was explained in paragraph 7.2.1.1.2. However it is possible that the vesicle of thylakoid membrane around the tip of the microelectrode re-integrates itself in the surrounding thylakoid fret-work. In doing this the free luminal space "seen" by the microelectrode tip becomes smaller. Part of the charge separations occurring at some "distance" from the tip will not be sensed immediately, which may account for the slow rising component in the "new" response.

The slower decay, which is not substantially slower in fig. 5.4, can be explained by retarded diffusion in the appressed membrane regions (Polle and Junge 1984, 1986a, 1986b). Considerable permeability changes due to the impalement occur from time to time. However pre-illuminated *Peperomia metallica* leaves reveal a decay rate of reaction I of 15 s^{-1} at 20°C (personal observation) as measured with the $P_{5,15}$ technique. The decay rate of the "classical" response in fig. 5.4 is of the same order and others have measured the same rates (Bulychev et al. 1980).

Therefore we assume that the so called "new" response is caused by the retarded diffusion of protons and other ions in a narrow confined space with a high concentration of immobilized buffer and chelating groups. This concept was first suggested by Hong and Junge (1983) and later stressed by Williams (1985). Although this concept has been used to explain a type of "localized" chemiosmosis (Kara-Ivanov 1982), it has been refuted by others as the cause for "localized" coupling, e.g. see paragraph H.4.4.2 in Westerhoff (1983). Our calculations in paragraph 6.4.1 reveal that a localized effect can occur on a short time scale or by short pulse induced changes such as flashes. However under steady state conditions, where no concentration profile changes occur any more, this could not explain a localization of $\Delta\mu_{\text{H}^+}$ in the lumen. Thus we do not believe that our microelectrode measurements necessitate a drastic change in the chemiosmotic theory (Mitchell 1961, 1966, 1981).

7.2.2. $P_{5,15}$ Measurements

The fact that $P_{5,15}$ is a pigment situated within the membrane precludes that it senses the same electric field changes as the microelectrode (Schapendonk et al. 1979, Vredenberg 1981). Original mono-phasic flash-induced responses were measured (Junge and Witt 1968, Junge 1977) with chloroplasts that were isolated

and stored in liquid nitrogen, until they were used in experiments. However when chloroplasts were isolated from carefully cultured spinach and used within hours after the isolation responses appeared to be much more complex (e.g. Schapendonk 1980, Theg et al. 1982, Hong and Junge 1983, Horner and Moudrianakis 1983, Dilley and Schreiber 1984). Moreover as we discussed in paragraph 6.2.4 we should distinguish between the P_{515} response measured in the presence and the absence of externally added reducing equivalents, i.e. dithionite or DQH_2 (Joliot and Delosme 1974, Bouges-Bocquet 1977, Slovacek and Hind 1978, Jones et al. 1984). Adding these substances even to maltreated chloroplasts induces a slow rising component, i.e. phase b as in fig. 6.2, but does not slow down the decay as in fig. 6.3. The slow rise in the P_{515} response observed in the presence of reductants is extensively explained elsewhere (Jones and Whitmarsh 1987a, 1987b). We will discuss here the P_{515} response of dark adapted leaves or freshly isolated chloroplasts therefrom without addition of reductants.

7.2.2.1. Reaction I and II

The first description of a difference in response between thylakoids which had been frozen and thawed before the experiment and freshly isolated chloroplasts was given by Hong and Junge (1983). They report a decay rate of the flash-induced P_{515} response of between 5 and 2 s⁻¹ for the freshly isolated thylakoids. This is a slower decay rate than our reaction I, but their response does not contain any slow rising component. This means that what we call reaction II might be present in their response, but only to a smaller extend. Chloroplasts which do reveal "localized" protonic coupling behaviour also have a slow rising and decaying component in their flash-induced P_{515} response upon examination (Dilley and Schreiber 1984, Schreiber personal communication). In the rigorous experiments proving bulk phase equilibration of protons before being utilized for ATP synthesis (Junge et al. 1987) one does not discern the presence of any reaction II in the P_{515} response from their chloroplasts (e.g. see figs. 1 and 2 of Junge et al. 1987). This is even true in the presence of tentoxin, an inhibitor of the ATPase (Arntzen 1972), which was shown to prevent saturation of reaction II by pre-illumination (Peters et al. 1983). We found a loss of part of reaction II in chloroplasts which had been suspended in a hypotonic medium at room temperature (see fig. 5.9). The experiments performed by Junge et al. (Polle and Junge 1986a,b,c, Junge et al. 1987) were done at room temperature, while experiments claiming "localized" protonic coupling effects (Dilley and Schreiber 1984, Beard and Dilley 1986, 1987, Theg and Dilley 1987) were all done at temperatures of 10°C or lower.

On many occasions reaction II in isolated chloroplasts without additives and in leaves was not, hardly or temporarily present. Since we could not explain this effect it was never published to our knowledge. Results indicating that two flashes separated by 1 s could induce long term ATP hydrolysis in fully dark adapted chloroplasts (Schreiber and Del Valle-Tascon 1982) together with the complementarity of ATP hydrolysis and the disappearance of reaction II (Schreiber and Rienits 1982, Peters et al. 1983) explained why reaction II was not present in some

averaged P_{515} responses. Differences in adenylate kinase equilibrium of ΔG_{ATP} in different cultivars of spinach explained why reaction II was measured in one cultivar and not in another (Peters et al. 1986). However other causes for the irreversible disappearance of reaction II have not been reported on. As we have stated before freezing and thawing the chloroplasts is guaranteed to destroy any reaction II in the P_{515} response. But also suspending chloroplasts at high salt concentrations, e.g. 100 mM KCl, or breaking chloroplasts at room temperature do cause an irreversible inhibition of reaction II (personal observations). This would link the occurrence of reaction II to the localized proton gradients as Beard and Dilley (1986, 1987), conclude from their experiments

7.3. Simulating the Electric Potential

As discussed in paragraph 7.2.1.2. the chemiosmotic theory is adequate to explain our microelectrode measurements. Also the close correlation between experiment and calculations in fig. 3.5 confirms this.

7.3.1. Redox State of the Simulated ATPase

The free energy of ATP, i.e. $\Delta G_{ATP} = 46 \text{ kJ}\cdot\text{mol}^{-1}$, necessary to simulate the microelectrode response in fig. 3.5 is rather high. Although the levels found in spinach *in vivo* varied between $42 \text{ kJ}\cdot\text{mol}^{-1}$ in the dark adapted state and $46 \text{ kJ}\cdot\text{mol}^{-1}$ under saturating illumination (Giersch et al. 1980), it is reasonable to expect a lower free energy in *Peperomia metallica* as it is cultured under extremely low light conditions (see paragraph 2.1.2.). However the algorithm we used to describe J_{ATP}^A was based on work by Gräber et al. (1984). Later publications by Gräber and co-workers (Gräber et al. 1987) reveal two possible states for the ATPase. An oxidized state in which the activation curve is as depicted in the inset of fig. 3.5 and a reduced state with an activation curve shifted to lower energies, i.e. the activation curve intersects the abscissa at $\approx 11 \text{ kJ}\cdot\text{mol}^{-1}$ in the reduced state and at $\approx 15 \text{ kJ}\cdot\text{mol}^{-1}$ in the oxidized state. In the dark adapted state the ATPase is oxidized. Electrons from PSI are expected to reduce the ATPase at the onset of illumination. With a proton to ATP stoichiometry of 3 this results in an activation energy shift for ΔG_{ATP} of about $12 \text{ kJ}\cdot\text{mol}^{-1}$. It was speculated in paragraph 3.4. that such a shift, if incorporated in our model, could simulate the microelectrode measurements with more realistic values for ΔG_{ATP} . Incorporating such a redox shift in the activation curve within our model would be a simple matter. It would however have a profound influence on the results depending on the moment of reduction or oxidation, because large changes in proton fluxes might occur. It must be explicitly stated however, that all calculations in this thesis were performed simulating a population of oxidized ATPases.

7.3.2. The Capabilities of the Model

Both figs. 3.3 and 3.5 give striking similarities between simulated and measured results. Also a comparison of calculations and experiments in the presence of membrane modifying reagents, i.e. figs. 4.7 and 4.8, reveals the capability of the model to simulate photosynthetic free energy transduction under defined conditions. In the presence of (F)CCCP a large undershoot is detected after the light is turned off, while ΔpH is relatively small. To our knowledge this is the first time a calculation relates this undershoot to the size of the proton flux. Although actual experiments (Bulychev et al. 1980) have revealed this fact and theory has predicted it (Vredenberg 1976, Heinz 1982). Actual experiments with an antimony microelectrode, which measures $\Delta \bar{\mu}_{H^+}$ directly (Remis et al. 1986a,b), reveal a light-induced $\Delta \bar{\mu}_{H^+}$ profile which is clearly in accord with our model calculations of chapter 3. Also the measured influence of NH_4Cl on these profiles is qualitatively simulated in fig. 4.5. But besides being capable of simulating actual experiments the model is also capable of imaginary experiments, which cannot be performed in reality. Such an experiment is testing the influence of the Donnan potential by comparing the results in its presence and in its absence, as is done in paragraph 4.2.2. In paragraph 4.4. we have shown that it is possible to augment this model with calculations pertaining to other more readily measurable parameters such as fluorescence. When this is tried it becomes immediately evident that the model is insufficient in its description of electron transport. The description of electron transport presented in paragraph 3.3.1. can only simulate an experiment performed under saturating actinic illumination, as is the case with microelectrode experiments (see paragraph 2.1.1.1.).

7.3.3. The Future of the Model

At present the model presented in chapter 3 is developed further to include a full description of the redox components in the electron transport chain (J. Snel private communications). Preliminary exercises have shown the possibility to simulate Chl a fluorescence induction curves at low light levels. We intend to use the model to study the Chl a fluorescence emission response to modulated actinic light. Such a combined use of a model with experimental data should enable us to overcome the problem of disentangling the cross-correlated phenomena.

The model has also been combined with another computational model intended to simulate CO_2 fixation in the stroma, based on the description by Laisk (1973). An augmented version of the model could, in future, serve as a basic input to other models describing Calvin cycle activity and substrate transport.

7.4. Conclusions

Based on the results and the arguments presented in this thesis we conclude that the presence of reaction II in the flash-induced P_{515} response of intact leaves or carefully isolated chloroplasts (without additives) is an indication for the stabilization of charges within localized domains separated from the bulk phase lumen by a dielectric medium with a very large resistance. These charges are thought to be protons and there is strong evidence that these protons play an important role in the onset of ATP synthesis (Dilley and Schreiber 1984, Theg and Dilley 1987). It has been shown that coupling units with only a few protons as the intermediate can seemingly violate the second law of thermodynamics (Westerhoff and Chen 1985). But whether these localized protons also play a role in steady state photophosphorylation remains to be investigated. As long as this has not been proven to be the case we believe that the concept of "delocalized" chemiosmosis is adequate to explain the anomalies found with chloroplasts. The absence of reaction II during continuous illumination therefore is no proof of a "localized" chemiosmotic concept, but it does not refute that concept either.

It is also clear that the presence of a reaction II type of response can have different origins. Adding reductants can add a signal as in fig. 6.2 which is believed to be caused by a Q-cycle. Although similar to reaction II we propose to call this response reaction I/Q (Vredenberg et al. 1987, Ooms et al. 1987). The "new" response measured with the microelectrode is explained as finding its origin in retarded diffusion of protons and other ions through the compressed luminal space, due to immobilized buffering and chelating groups (Hong and Junge 1983). Although this can lead to substantial differences in $\Delta\mu_{H^+}$ in the lumen when we have single flash or short pulse excitation, it cannot explain "localized" protonic coupling during steady-state photophosphorylation (Westerhoff 1983, Junge and Polle 1986). A response as identified in paragraph 6.3 in our interpretation is a direct reflection of reaction II. It can be measured in dark adapted intact leaves both at room temperature and at 0°C. However recent experiments have revealed that a combination of reaction I, reaction I/Q, reaction II and reaction III can be measured both in leaves and in intact chloroplasts (Ooms et al. 1987, Vredenberg et al. 1987).

Summary

This thesis is concerned with a particular part of the photosynthesis process. This part consists of the light-induced transmembrane electric potential gradient, the electrochemical pH gradient and the subsequent transformation of the energy contained in these gradients into chemical free energy of adenylates (ATP). This transformation of energy, originally in the form of an electromagnetic quantum, into a metabolic useful and stable chemical bond is called photosynthetic free energy transduction. After this process, which is sometimes inadequately referred to as the light reaction, the chemical energy is used, together with reduction equivalents from the electron transport chain, to bind protons and carbon molecules in order to form sugar molecules. In this last process, i.e. the Calvin cycle or the "dark reaction", free energy is not transduced, but shifted from one chemical bond to another. The reactions pertaining to the transduction of free energy are linked to the thylakoid membranes and are described in a general fashion in chapter 1.

Three different approaches were used to study the free energy transduction. First the electrophysiological approach, i.e. measurements of the transmembrane electric potential with a microelectrode inserted in a single chloroplast. Second the spectrophotometric approach, in which a light-induced absorbance change of an ensemble of chloroplasts was studied with the aid of a spectrophotometer (P_{515}). And third the modelling approach, from whence we have tried to encompass the host of experimental results in photosynthesis research in a rigorous mathematical formulation. The description of the methods used can be found in chapter 2.

The basic model of photosynthetic free energy transduction, as it was originally developed to explain our electrophysiological results, is presented in chapter 3. It is based on the chemiosmotic hypothesis of membrane linked free energy transduction. Potential traces simulating the light-induced electric potential changes across the thylakoid membrane of an obligate shade plant like *Peperomia metallica* L. tend to reproduce experimental recordings measured with a microelectrode impaled in a chloroplast of that plant. A crucial role in this model is played by the formalism for the proton flux through the ATPase. The formalism developed by Gräber et al. (1984, 1987) for an oxidized ATPase was adapted to be applied in our model.

Applications of the model and a comparison with earlier experiments are given in chapter 4. There it becomes evident that the model can be used for other techniques in photosynthesis research such as chlorophyll fluorescence induction curves. We compare simulations with microelectrode traces of the thylakoid membrane electric potential. Measurements by Remish et al. (1986a, b) of the combined pH gradient and the electric potential also confirm our model calculations.

In chapter 5 we present electrophysiological (microelectrode) and spectrophotometric (P_{515}) results, which appear to challenge the premises on which the model presented in the previous chapters is based, namely Mitchell's hypothesis of chemiosmotic free energy transduction (Mitchell 1961). These results pertain to a deviation from a single exponential decay expected after a flash-induced rise in the electric potential. When measured with the microelectrode this is called a "new" response by us as opposed to the "classical" response. When measured with the P_{515} technique it is called reaction II plus reaction I as opposed to reaction I alone. The P_{515} response and the "new" response measured with the microelectrode show a striking similarity.

In chapter 6 the phenomena underlying reaction II and the "new" response are explained. It appears that the Q-cycle, an explanation generally used for a particular component of reaction II (i.e. the relative slow rise), cannot be used to explain the P_{515} measurements in view of the experiments and on theoretical grounds. We develop a model for reaction II based on stabilization of protons within the membrane matrix. This implies a dielectric separation of charges. Some charges reach the lumen and others stay within the membrane. The protons remaining within the membrane appear to leave the membrane via the membrane bound proton ATP synthase complex. This is incompatible with a basic assumption of the chemiosmotic hypothesis, i.e. all charges are transferred from the stroma to the lumen and both stroma and lumen are highly conductive and homogeneous phases. It appears that our model of reaction II is more in accord with an alternative hypothesis for membrane linked free energy transduction and usually referred to by the name of "localized" chemiosmosis (Williams 1961, Westerhoff et al. 1984). Although the "new" response measured by the microelectrode is similar to the P_{515} response, it is explained by a different phenomenon. The structural effects of a microelectrode tip of $0.15 \mu\text{m}$ diameter penetrating a thylakoid membrane structure (granum) of $1.5 \mu\text{m}$ diameter is taken into consideration. This combined with the effect of a large concentration of "immobilized" buffer groups gives a completely different explanation for the "new" response.

In chapter 7 we deliberate whether the "new" response and reaction II can be considered as an indication that the basic assumption of the chemiosmotic theory is violated. For the "new" response this is clearly not the case, since it is a consequence of the measuring method and its explanation can only lead to temporary inhomogeneities in the lumen. While for a true violation of the chemiosmotic theory the concept of a heterogeneous lumen must be sustained even under steady-state actinic illumination. For reaction II the answer is not so simple since an obvious connection exists between the membrane stabilized protons and the ATPase. However reaction II saturates after a short illumination period and stays saturated while the ATPase stays active. Thus it is not clear whether these protons play an active role during steady-state photophosphorylation. As was also shown by others it is likely that these protons play a role in the activation of the ATPase.

Samenvatting

Fotosynthetische vrije energie omzetting is een benaming voor een proces waarbij de energie van het licht dat door een plant ingevangen wordt, wordt omgezet in chemische bindings energie. De eindprodukten van dit proces zijn de suikers en andere organische bouwstoffen waarmee het leven op aarde zich in stand houdt. Een neveneffect van dit proces is het vrijkomen van zuurstof. Deze omzetting van energie van de ene vorm (licht) in de andere vorm (bv. suiker) gebeurt in een aantal stappen. Eerst wordt het ingevangen licht "pakketje" omgezet in trillings energie van electronen. Dan ontstaat er een electricch veld over een membraan, waarna een concentratie verschil van waterstof ionen over dat membraan ontstaat. Het electricch veld en het concentratie verschil herbergen een energie die wij electrochemische potentiaal noemen. Deze electrochemische potentiaal wordt in staat geacht een chemische binding tot stand te brengen in een molekuul (ATP). Het ATP bevat een hoge en stabiele chemische bindings energie dat gebruikt kan worden om bijvoorbeeld koolstof te binden in een suiker molekuul. Een deel van dit hele proces wordt in dit proefschrift behandeld. En wel het deel vanaf het ontstaan van het electricch veld tot de formatie van ATP. In hoofdstuk 1 wordt dit deel van het fotosynthese proces uitgelegd.

Drie verschillende methoden zijn gebruikt om de verschijnselen die gepaard gaan met deze energie omzetting te bestuderen: ten eerste de electrofysiologische methode, waarbij een microelectrode in een chloroplast (bladgroenkorrel) wordt gestoken en aldus de licht geïnduceerde electricch potentiaal veranderingen over een thylakoid membraan meet. Ten tweede de spectrofotometrische methode, waarbij de absorptie verandering van een intrinsiek pigment P_{515} wordt gemeten. Deze door een lichtflits opgewekte absorptie verandering is lineair gerelateerd aan de electricch potentiaal en wordt gemeten aan een ensemble van chloroplasten. De derde methode heeft te maken met de sub-titel van dit proefschrift, namelijk het opstellen van wiskundige beschrijvingen van het energie omzettings proces en deze met behulp van de computer uit te rekenen. Op deze manier kunnen hypothesen getoetst worden en inzichten verkregen worden die anders niet te verkrijgen zijn. De materialen en methoden van deze drie technieken staan beschreven in hoofdstuk 2.

De sub-titel van dit proefschrift "Modelbeschrijven der elektrochemische verschijnselen." komt het meest tot uitdrukking in hoofdstuk 3. Hierin wordt een wiskundige beschrijving gegeven van het elektronen transport, passieve en actieve diffusie van ionen over het membraan en de vorming van ATP. Het model steunt geheel op de chemiosmotische hypothese van Peter Mitchell (1961). Met behulp van dit model worden de door licht geïnduceerde potentiaal veranderingen over een thylakoid (fotosynthetisch) membraan gesimuleerd. Het objekt van simulatie is het thylakoid membraan van de obligate schaduw plant *Peperomia metallica* L.,

welke ook gebruikt wordt voor de elektrofysiologische metingen. Het blijkt mogelijk te zijn om de gecompliceerde potentiaal veranderingen bij een belichting van enige seconden te berekenen met behulp van het model. Hierin speelt de wiskundige formulering van het omschakelbare en proton geleidende gedrag van de ATPase een cruciale rol. De wiskundige beschrijving van dit gedrag werd door Gräber et al. (1984, 1987) geformuleerd en is door ons in aangepaste vorm overgenomen. Hierbij is uitgegaan van een ATPase in geoxideerde toestand.

In hoofdstuk 4 worden de verdere toepassings mogelijkheden van het model uit hoofdstuk 3 uitgewerkt. Een berekening van de Donnan potentiaal leidt tot een vergelijking van het potentiaal gedrag van de thylakoid membraan in aan- en afwezigheid van deze potentiaal. De effecten van zogenaamde ontkoppelaars van de vrije energie transductie worden berekend en vergeleken met microelectrode experimenten uitgevoerd in de zeventiger jaren. Ook een vergelijking met zeer recente experimenten met een pH gevoelige microelectrode (Remish et al. 1986a, b) leidt tot een kwalitatief goed en kwantitatief hoopgevend resultaat. Aan het einde van hoofdstuk 4 wordt een nieuwe toepassings mogelijkheid van het model aangestipt. Chlorofyll fluorescentie karakteristieken kunnen met een uitgebreide versie van het model worden gesimuleerd. Dit type onderzoek krijgt hoge prioriteit in de komende jaren.

Nadat het model door zoveel experimenten ondersteund is komen wij in hoofdstuk 5 met experimenten die ogenschijnlijk niet stroken met één van de axioma's van de chemiosmotische theorie. Met de microelectrode gemeten signalen met een afwijkend gedrag worden door ons "nieuw" genoemd in tegenstelling tot de zogenaamde "klassieke" signalen die direkt door het model te simuleren zijn. Deze nieuwe signalen lijken veel op een komponent in het P_{515} signaal dat ook niet direkt vanuit de chemiosmotische theorie te verklaren valt. Deze komponent wordt door ons reactie II genoemd en door anderen fase b of de trage opzwaai. Een relatie tussen dit signaal en een specifiek eiwit (cytochroom b_{563}) dat verantwoordelijk wordt verondersteld te zijn voor een extra stap in het elektronen transport proces (Q-cyclus) bleek niet aanwezig te zijn.

In hoofdstuk 6 wordt een poging ondernomen om de afwijkende signalen, d.w.z. het "nieuwe" signaal voor de microelectrode en reactie II voor de P_{515} methode, uit hoofdstuk 5 te verklaren. Op basis van de experimentele gegevens en op grond van theoretische overwegingen wordt een door anderen gesuggereerde verklaring met behulp van de Q-cyclus van de hand gewezen. Voor reactie II wordt een eenvoudig model ontwikkeld waarin een deel van de getransporteerde lading in het membraan blijft. Deze ladingen geven aanleiding tot de reactie II respons en zij worden gedacht het membraan te verlaten via de ATPase. Dit model is in principe strijdig met de chemiosmotische theorie van Mitchell (1961, 1966) en komt meer overeen met een andere theorie over membraan gebonden vrije energie transductie, namelijk die welke bekend staat onder de naam "lokale" chemiosmose (Williams 1961, Westerhoff et al. 1984).

Hoewel het "nieuwe" signaal dat met de microelectrode gemeten wordt in veel opzichten lijkt op het P_{515} signaal, wordt de verklaring toch in een heel andere richting gezocht. Hierbij

wordt betrokken dat bij een microelectrode meting een glas naald van $0,15 \mu\text{m}$ diameter binnendringt in een thylakoid stapel (granum) van $1,5 \mu\text{m}$ diameter. Gekombineerd met de aanwezigheid van een grote concentratie geïmmobiliseerde buffer groepen levert dit een verklaring op voor het "nieuwe" signaal vanuit een vertraagde ion diffusie in de lumen (binnenkant van het thylakoid membraan).

In hoofdstuk 7 wordt nagegaan of de verklaringen die in hoofdstuk 6 geformuleerd zijn, in strijd zijn met de chemiosmotische theorie. Voor de verklaring van het "nieuwe" signaal gemeten met de microelectrode is dit zeker niet het geval. In de eerste plaats is dit signaal het gevolg van de meetmethode zelf. In de tweede plaats leidt de verklaring hooguit tot een tijdelijke inhomogeniteit van de electrochemische potentiaal in de lumen. Om in strijd te zijn met de chemiosmotische theorie moet de inhomogeniteit in de chemiosmotische potentiaal stand houden bij belichting gedurende enige tijd. Voor de verklaring van reactie II is het antwoord niet zo simpel. Doordat er een aangetoonde verbinding bestaat tussen de ATPase en reactie II lijkt het er op dat hier wel sprake kan zijn van strijdigheid met de chemiosmotische theorie. Echter reactie II is al na een zeer korte belichtings duur voltooid en verzadigd. De verzadiging blijft zolang de ATPase actief is. De protonen die bij reactie II betrokken zijn spelen zeker een rol in de aktivatie van de ATPase. Of zij echter ook een rol blijven spelen gedurende continue belichting, zal nog moeten blijken.

References

- Abramowitz M. and Stegun I.A. (1972) Handbook of Mathematical Functions, Dover Publications, Inc., New York
- Akerlund H.E. and Andersson B. (1983) *Biochim. Biophys. Acta* 725, 34-40
- Allen J.F., Bennet J., Steinback K.E. and Arntzen C.J. (1981) *Nature* 291, 25-29
- Allred D.R. and Staehelin L.A. (1985) *Plant Physiol.* 78, 199-202
- Allred D.R. and Staehelin L.A. (1986) *Biochim. Biophys. Acta* 849, 94-103
- Andersson B. and Anderson J.M. (1980) *Biochim. Biophys. Acta* 593, 427-440
- Anderson J.M. and Boardman N.K. (1973) *FEBS Lett.* 32, 157-160
- Anderson J.M. and Melis A. (1983) *Proc. Natl. Acad. Sci. USA* 80, 745-749
- Arntzen C.J. (1972) *Biochim. Biophys. Acta* 283, 539-542
- Baker G.M., Bhatnagar D. and Dilley R.A. (1981) *Biochem.* 20, 2307-2305
- Barber J. (1972) *Biochim. Biophys. Acta* 275, 105-116
- Barber J. (1976) in: *The Intact Chloroplast* (Barber J. ed.), Vol 1, pp. 89-134, Elsevier, North-Holland
- Barber J. (1980) *Biochim. Biophys. Acta* 594, 255-308
- Barber J. (1982) *Annu. Rev. Plant Physiol.* 33, 261-295
- Barber J. (1983) *Plant Cell Environ.* 6, 311-322
- Barber J. (1983b) *Photobiochem. Photobiophys.* 5, 181-190
- Beard W.A. and Dilley R.A. (1986) *FEBS Lett.* 210, 57-62
- Beard W.A. and Dilley R.A. (1987) in: *Progress in Photosynthesis Research* (Biggins J. ed.), Vol. III, pp.165-168, M. Nijhoff Pub., Dordrecht
- Bertrand D.C., Henauer R. and Bader C.R. (1983) *J. Neurosci. Meth.* 7, 171-183
- Björkman O. (1981) in: *Encyclopedia of Plant Physiology*, vol. 16A (Lanse O.L., Nobel P.S., Osmond C.B. and Ziesler H. eds.), pp. 57-107, Springer Verlag, Berlin
- Bockris J.O'M. and Reddy A.K.N. (1977) *Modern Electrochemistry*, Vol. 1, Plenum Publishing Co., New York
- Bouges-Bocquet B. (1977) *Biochim. Biophys. Acta* 462, 371-379
- Bouges-Bocquet B. (1981) *Biochim. Biophys. Acta* 635, 327-340
- Boyer, P.D., Chance B., Ernster L., Mitchell P., Racker E. and Slater E. (1977) *Annu. Rev. Biochem.* 46, 955-1026
- Brettel K., Setif P. and Mathis P. (1987) in: *Progress in Photosynthesis Research* (Biggins J. ed.), Vol.I, pp.233-236, M. Nijhoff Pub., Dordrecht
- Briantais J.M., Vernotte C., Picaud M. and Krause G.H. (1979) *Biochim. Biophys. Acta* 548, 128-138
- Briantais J.M., Vernotte C., Picaud M. and Krause G.H. (1980) *Biochim. Biophys. Acta* 591, 198-202
- Bruinsma J. (1961) *Biochim. Biophys. Acta* 52, 576-578
- Bulychev A.A., Andrianov V.K., Kurella G.A. and Litvin F.F. (1971) *Soviet Plant Physiol.* 18, 204-210

- Bulychev A.A., Andrianov V.K., Kurella G.A. and Litvin F.F. (1972) *Nature* 236, 175-177
- Bulychev A.A., Andrianov V.K., Kurella G.A. and Litvin F.F. (1976) *Biochim. Biophys. Acta* 420, 336-351
- Bulychev A.A. and Vredenberg W.J. (1976a) *Biochim. Biophys. Acta* 423, 548-556
- Bulychev A.A. and Vredenberg W.J. (1976b) *Biochim. Biophys. Acta* 449, 48-58
- Bulychev A.A., Andrianov V.K. and Kurella G.A. (1980) *Biochim. Biophys. Acta* 590, 300-308
- Bulychev A.A., Remis D. and Kurella G.A. (1983) *Plant Sci. Lett.* 29, 73-79
- Bulychev A.A. (1984a) in: *Membrane Transport in Plants* (Cram W.J. et al. eds.), pp.255-260, Wiley and Sons, New York
- Bulychev A.A. (1984b) *Biochim. Biophys. Acta* 766, 647-652
- Bulychev A.A., Niyazova M.M. and Turovetsky V.B. (1985) *Biochim. Biophys. Acta* 808, 186-191
- Bulychev A.A., Niyazova M.M. and Turovetsky V.B. (1986) *Biochim. Biophys. Acta* 850, 218-225
- Butler W.L. and Kitajima (1975) *Biochim. Biophys. Acta* 396, 72-85
- Cockburn W. and Walker D.A. (1968) *Plant Physiol.* 43, 1415-1418
- Coughlan S.J. and Schreiber U. (1984a) *Z. Naturforsch.* 39c, 1120-1127
- Coughlan S.J. and Schreiber U. (1984b) *Biochim. Biophys. Acta* 767, 606-617
- Crank J. (1975) *The Mathematics of Diffusion* 2nd ed., Clarendon Press, Oxford
- Cramer W.A. and Crofts A.R. (1982) in: *Photosynthesis* (Govindjee ed.), Vol I, pp. 387-467, Academic Press
- Cramer W.A., Widger W.R., Herrmann R.G. and Trebst A. (1985) *Tr. Biochem. Sci.* 10, 125-129
- Crowther D., Mills J.D. and Hind G. (1979) *FEBS Lett.* 98, 386-390
- Crowther D. and Hind G. (1980) *Arch. Biochem. Biophys.* 204, 568-577
- Crowther D. and Hind G. (1981) in: *Chemiosmotic Proton Circuits in Biological Membranes* (Skulachev V.P. and Hinkle P.C. eds.), pp. 245-257, Addison-Wesley Publishing Co., Reading, MA
- Dahse I., Bulychev A.A., Kurella G.A. and Liebermann B. (1985) *Physiol. Plant.* 65, 446-450
- Deamer D.W., Crofts A.R. and Packer L. (1967) *Biochim. Biophys. Acta* 131, 81-96
- Dietz K.J., Neimanis S. and Heber U. (1984) *Biochim. Biophys. Acta* 767, 444-450
- Dilley R.A., Prochaska L.J., Baker G.M., Tandy N.E. and Millner P.A. (1982) *Curr. Top. Membr. Transp.* 16, 345-369
- Dilley R.A. and Schreiber U. (1984) *J. Bioenerg. Biomembr.* 16, 173-193
- Dilley R.A. (1986) in: *Encyclopedia of Plant Physiology, Photosynthesis III* (Staehelin L.A. and Arntzen C.J. eds.) Vol 19, pp. 570-575, Springer-Verlag, Berlin
- Duysens L.N.M. (1954) *Science* 120, 353-354
- Duysens L.N.M. and Sweers H.E. (1963) in: *Studies on Microalgae and Photosynthetic Bacteria* (Ashida J. ed.), pp. 353-372, Special Issue of *Plant Cell Physiol.*, Univ. of Tokyo Press, Tokyo

- Einstein A. (1908) *Zeitschr. für Elektrochemie* 14, 235-239
- Emrich H.M., Junge W. and Witt H.T. (1969) *Z. Naturforsch.* 24b, 144-146
- Farkas D.L., Korenstein R. and Malkin S. (1984) *Biophys. J.* 45, 363-373
- Franks F. (1972) in: *Water - A Comprehensive Treatise*, Vol. 1 (Franks F. ed.), pp. 115-149, Plenum Press
- Garab Gy., Zimanyi L. and Faludi-Daniel A. (1980) in: *Book of Abstracts, UNESCO-ICRO BR-ITC, Szeged, Hungary*
- Garab Gy. and Farineau J. (1983) *Biochem. Biophys. Res. Comm.* 111, 619-623
- Garab Gy. and Hind G. (1987) in: *Progress in Photosynthesis Research* (Biggins J. ed.), Vol. II, pp. 542-544, M. Nijhoff Pub., Dordrecht
- Giersch C., Heber U., Kobayashi Y., Inoue Y., Shibata K. and Heldt H.W. (1980) *Biochim. Biophys. Acta* 590, 59-73
- Goldmann D.E. (1943) *J. Gen. Physiol.* 27, 37-60
- Graan T. and Ort D.R. (1982) *Biochim. Biophys. Acta* 682, 395-403
- Gräber P. and Witt H.T. (1976) *Biochim. Biophys. Acta* 423, 141-163
- Gräber P., Schlodder E. and Witt H.T. (1977) *Biochim. Biophys. Acta* 461, 426-440
- Gräber P. (1980) in: *Hydrogen Ion Transport in Epithelia* (Schultz et al. eds.), Vol. I, pp. 19-31, Elsevier Biomed. Press, North-Holland
- Gräber P. and Schlodder E. (1981) in: *Photosynthesis* (Akoyunoglou G. ed.) Vol II, pp. 867-879, Balaban Int, Philadelphia
- Gräber P., Rögner M., Buchwald H.-E., Samoray D. and Hauska G. (1982) *FEBS Lett.* 145, 35-40
- Gräber P. (1982) in: *Current Topics in Membranes and Transport*, Vol. 16, pp. 215-245, Academic Press, Inc.
- Gräber P. (1984) in: *Charge and Field Effects in Biosystems* (Allen M.J. and Usherwood P.N.R. eds.), pp. 227-242, Abacus Press
- Gräber P., Junesch U. and Schatz G.H. (1984) *Ber. Bunsenges. Phys. Chem.* 88, 599-608
- Gräber P., Junesch U. and Thulke G. (1987) in: *Progress in Photosynthesis Research* (Biggins J. ed.), Vol. III, pp. 177-184, M. Nijhoff Pub., Dordrecht
- Haehnel W. (1984) *Ann. Rev. Plant Phys.* 35, 659-693
- Haehnel W. (1987) in: *Progress in Photosynthesis Research* (Biggins J. ed.), Vol. II, pp. 513-520, M. Nijhoff Pub., Dordrecht
- Hauska G. (1986) in: *Encyclopedia of Plant Physiology, Photosynthesis III* (Staehelein L.A. and Arntzen C.J. eds.) vol. 19, pp. 496-507, Springer Verlag, Berlin
- Haraux F. and de Kouchkovsky Y. (1983) *Physiol. Vég.* 21, 563-576
- Heber U. and Santarius K.A. (1970) *Z. Naturforsch.* 25b, 718-728
- Heinz E. (1982) in: *Current Topics in Membranes and Transport*, Vol. 16, pp. 249-256, Academic Press, Inc.
- Heldt H.W., Werden K., Milovancev M. and Geller G. (1973) *Biochim. Biophys. Acta* 314, 224-241
- Hendler R.W., Bunow B. and Rieske J.S. (1985) *J. Bioenerg. Biomembr.* 17, 51-64
- Holzwarth A.R. (1987) in: *Progress in Photosynthesis Research* (Biggins J. ed.), Vol. I, pp. 53-60, M. Nijhoff Pub., Dordrecht
- Hong Y.Q. and Junge W. (1983) *Biochim. Biophys. Acta* 722, 197-208

104 Photosynthetic Free Energy Transduction

- Hope A.B. and Mathews D.B. (1987) *Austr. J. Plant Physiol.* 14, 29-46
- Horner R.D. and Moudrianakis E.N. (1983) *J. Biol. Chem.* 258, 11643-11647
- Horváth G., Droppa M., Mustárdy L. and Faludi-Daniel A. (1978) *Planta* 141, 239-244
- Horváth G., Niemi H.A., Droppa M. and Faludi-Daniel A. (1979) *Plant Physiol.* 63, 778-782
- Hosler J.P. and Yocum C.F. (1985) *Biochim. Biophys. Acta* 808, 21-31
- Huber H.L. and Rumberg B. (1981) in: *Photosynthesis I* (Akoyunoglou G. ed.), pp. 419-429, Balaban Int., Philadelphia
- Hurt E. and Hauska G. (1981) *Eur. J. Biochem.* 117, 591-599
- Hurt E. and Hauska G. (1982) *J. Bioenerg. Biomem.* 14, 405-424
- Interschick-Niebler E. and Lichtenthaler H.K. (1981) *Z. Naturforsch.* 36c, 276-283
- Jackson J.B. (1982) *FEBS Lett.* 139, 139-143
- Jackson J.B., Myatt J.F., Taylor M.A. and Cotton N.P.J. (1987) in: *Progress in Photosynthesis Research* (Biggins J. ed.), Vol. III, pp.127-132, M. Nijhoff Pub., Dordrecht
- Jagendorf A.T. and Uribe E. (1966) *Proc. Natl. Acad. Sci. USA* 55, 170-179
- Joliot P. and Delosme R. (1974) *Biochim. Biophys. Acta* 357, 267-284
- Joliot P. and Joliot A. (1985) *Biochim. Biophys. Acta* 806, 398-409
- Joliot P. and Joliot A. (1986) in: *Encyclopedia of Plant Physiology, Photosynthesis III* (Staehelein L.A. and Arntzen C.J. eds.) vol. 19, pp.528-538, Springer Verlag, Berlin
- Jones R.W., Selak M.A. and Whitmarsh J. (1984) *Biochem. Soc. Trans.* 12, 878-879
- Jones R.W. and Whitmarsh J. (1985) *Photobiochem. Photobiophys.* 9, 119-127
- Jones R.W. and Whitmarsh J. (1987a) in: *Progress in Photosynthesis Research* (Biggins J. ed.), Vol. II, pp.441-444, M. Nijhoff Pub., Dordrecht
- Jones R.W. and Whitmarsh J. (1987b) in: *Progress in Photosynthesis Research* (Biggins J. ed.), Vol. II, pp.445-452, M. Nijhoff Pub., Dordrecht
- Junesch U. and Gräber P. (1984) in: *Advances in Photosynthesis Research* (Sybesma C. ed.) Vol. II, pp. 431-436, Nijhoff & Junk Pub., The Hague
- Junesch U. and Gräber P. (1987) in: *Progress in Photosynthesis Research* (Biggins J. ed.), Vol. III, pp.173-176, M. Nijhoff Pub., Dordrecht
- Junge W. and Witt H.T. (1968) *Z. Naturforsch.* 23b, 244-254
- Junge W. (1977) *Ann. Rev. Plant Physiol.* 28, 503-536
- Junge W., Ausländer W., McGeer A. and Runge T. (1979) *Biochim. Biophys. Acta* 546, 121-141
- Junge W. and Jackson J.B. (1982) in: *Photosynthesis* (Govindjee, ed.), Vol. I, pp. 589-646, Academic Press
- Junge W., Hong Y.Q., Qian L.P. and Viale A. (1984a) *Proc. Natl. Acad. Sci. USA* 81, 3078-3082
- Junge W., Lill H., Qian L.P. and Hong Y.Q. (1984b) in: *H⁺-ATP Synthase* (Papa S. ed.), pp. 273-280, Adriatica Ed., Bari
- Junge W. and Polle A. (1986) *Biochim. Biophys. Acta* 848, 265-273

- Junge W., Schönknecht G. and Lill H. (1987) in: Progress in Photosynthesis Research (Biggins J. ed.), Vol. III, pp.133-140, M. Nijhoff Pub., Dordrecht
- Kara-Ivanov M. (1983) J. Bioenerg. Biomembr. 15, 111-119
- Kell D.B. (1979) Biochim. Biophys. Acta 549, 55-99
- Kell D.B. and Morris J.G. (1981) in: Vectorial Reactions in Electron and Ion Transport in Mitochondria and Bacteria (Palmieri F. et al. eds.), pp. 339-347, Elsevier, Amsterdam, New York
- Kell D.B., Clarke D.J. and Morris J.G. (1981) FEMS Microbiol. Lett. 11, 1-11
- Kouchkovsky Y. de, Haraux F. and Sigalat C. (1984) Bioelectrochem. Bioenerget. 13, 143-162
- Krause G.H., Briantais J-M and Vernotte C. (1982) Biochim. Biophys. Acta 679, 116-124
- Krause G.H. and Weis E. (1984) Photosynth. Res. 5, 137-157
- Laisk A. (1973) Biophysics 18, 679-684
- Lam E. and Malkin R. (1982) Proc. Natl. Acad. Sci. USA 79, 5494-5498
- Lill H., Engelbrecht S. and Junge W. (1987) in: Progress in Photosynthesis Research (Biggins J. ed.), Vol. III, pp.141-144, M. Nijhoff Pub., Dordrecht
- Lowe A.G. and Jones M.N. (1984) Trends Biochem. Sci. 9(1), 11-12
- Lundin A., Thore A. and Baltscheffsky M. (1977) FEBS Lett. 79, 73-76
- Malhotra S.K. and Sikerwar S.S. (1983) Trends Biochem. Sci. 8, 358-359
- Mansfield R.W., Nakatani H.Y., Barber J., Mauro S. and Lannoye R. (1982) FEBS Lett. 137, 133-136
- Mathis P. (1987) in: Progress in Photosynthesis Research (Biggins J. ed.), Vol. I, pp.151-160, M. Nijhoff Pub., Dordrecht
- McCauley S.W., Taylor S.E., Dennenberg R.J. and Melis A. (1984) Biochim. Biophys. Acta 765, 186-195
- McLaughlin S. (1977) in: Current Topics in Membranes and Transport Vol. 9, pp. 71-144, Academic Press Inc.
- Melis A. and Homann P.H. (1976) Photochem. Photobiol. 23, 343-350
- Melis A. and Duysens L.N.M. (1979) Photochem. Photobiol. 29, 373-382
- Melis A. (1984) J. Cell Biol. 24, 271-285
- Mills J.D. and Mitchell P. (1982) Biochim. Biophys. Acta 679, 75-83
- Mitchell P. (1961) Nature 191, 144-148
- Mitchell P. (1966) Biol. Rev. 41, 445-502
- Mitchell P. and Moyle J. (1968) Eur. J. Biochem. 7, 471-484
- Mitchell P. (1976) J. Theor. Biol. 62, 327-367
- Mitchell P. (1979) Science 206, 1148-1159
- Mitchell P. (1981) in: Of Oxygen, Fuels and Living Matter, Part 1 (Semenza G. ed.), pp. 1-160, John Wiley & Sons, New York
- Mitchell P. and Moyle J. (1983) FEBS Lett. 151, 167-178
- Morita S., Itoh S. and Nishimura M. (1982) Biochim. Biophys. Acta 679, 125-130
- Morrissey P.J., McCauley S.W. and Melis A. (1987) in: Progress in Photosynthesis Research (Biggins J. ed.), Vol. II, pp.305-308, M. Nijhoff Pub., Dordrecht
- Murphy D.J. (1982) FEBS Lett. 150, 19-26

106 Photosynthetic Free Energy Transduction

- Nagle J.F. and Dilley R.A. (1986) *J. Bioenerg. Biomembr.* 18, 55-64
- Nelson N. (1981) *Curr. Top. Bioenerg.* 11, 1-33
- Nuijs A.M., Shuvalov V.A., van Gorkom H.J., Plijter J.J. and Duysens L.N.M. (1986) *Biochim. Biophys. Acta* 850, 319-323
- Olsen L.F., Telfer A. and Barber J. (1980) *FEBS Lett.* 118, 11-17
- Ooms J.J.J., Buurmeijer W.F. and Vredenberg W.J. (1987) *FEBS Lett.*, in preparation
- Ort D.R. and Dilley R.A. (1976) *Biochim. Biophys. Acta* 449, 95-107
- Ort D.R., Dilley R.A. and Good N.E. (1976) *Biochim. Biophys. Acta* 449, 108-124
- Ott R.J. and Rys P. (1973) *J. Chem. Soc. Farad. Trans.* 69I, 1694-1704
- Peters A.L.J., van der Pal R.H.M., Peters R.L.A., Vredenberg W.J. and Kraayenhof, R. (1984) *Biochim. Biophys. Acta* 766, 169-178
- Peters R.L.A., Bossen M., van Kooten O. and Vredenberg W.J. (1983) *J. Bioenerg. Biomembr.* 15, 335-346
- Peters R.L.A., van Kooten O. and Vredenberg W.J. (1984a) in: *Advances in Photosynthesis Research* (Sybesma C. ed.) Vol. II, pp. 269-272, Nijhoff & Junk Pub., The Hague
- Peters R.L.A., van Kooten O. and Vredenberg W.J. (1984b) *J. Bioenerg. Biomembr.* 16, 283-294
- Peters R.L.A., van Kooten O. and Vredenberg W.J. (1984c) *FEBS Lett.* 177, 11-16
- Peters R.L.A., van Kooten O. and Vredenberg W.J. (1985) *J. Bioenerg. Biomembr.* 17, 207-216
- Peters R.L.A., van Kooten O. and Vredenberg W.J. (1986) *FEBS Lett.* 202, 361-366
- Peters R.L.A. (1986) Dissertation, Agricultural University Wageningen, the Netherlands
- Polle A. and Junge W. (1984) in: *Advances in Photosynthesis Research* (Sybesma C. ed.) Vol. II, pp. 261-264, Nijhoff & Junk Pub., The Hague
- Polle A. and Junge W. (1986a) *FEBS Lett.* 198, 263-267
- Polle A. and Junge W. (1986b) *Biochim. Biophys. Acta* 848, 257-264
- Polle A. and Junge W. (1986c) *Biochim. Biophys. Acta* 848, 274-278
- Pressman B.C. (1965) *Proc. Natl. Acad. Sci. USA* 53, 1065
- Pressman B.C. (1968) *Fed. Proc.* 27, 1283
- Provencher S.W. (1976) *J. Chem. Phys.* 64, 2772-2777
- Reed P.N. and Lardy H.A. (1972) *J. Biol. Chem.* 247, 6970
- Remis D., Bulychev A.A. and Kurella G.A. (1981) *J. Exp. Bot.* 32, 979-987
- Remis D., Bulychev A.A. and Kurella G.A. (1984) in: *Membrane Transport in Plants* (Cram W.J. et al. eds.), pp. 279-280, Wiley and Sons, New York
- Remis D., Bulychev A.A. and Kurella G.A. (1986a) *Physiologia Rasteniyi* 33, 319-325
- Remis D., Bulychev A.A. and Kurella G.A. (1986b) *Biochim. Biophys. Acta* 852, 68-73
- Renger G. and Schulze A. (1985) *Photobiochem. Photobiophys.* 9, 79-87
- Rich P.R. (1984) *Photosynth Res.* 6, 335-348
- Rich P.R., Heathcote P. and Moss D.A. (1987) in: *Progress in Photosynthesis Research* (Biggins J. ed.), Vol. II, pp. 453-460, M. Nijhoff Pub., Dordrecht
- Rieske J.S. (1971) *Arch. Biochem. Biophys.* 145, 179-193

- Robinson S.P. and Downton W.J.S. (1984) *Archiv. Biochem. Biophys.* 228, 197-206
- Robinson S.P. (1985) *Biochim. Biophys. Acta* 806, 187-184
- Rubin B.T. and Barber J. (1980) *Biochim. Biophys. Acta* 592, 87-102
- Rutherford A.W. and Heathcote P. (1985) *Photosynth. Res.* 6, 295-316
- Schapendonk A.H.C.M. and Vredenberg W.J. (1977) *Biochim. Biophys. Acta* 462, 613-621
- Schapendonk A.H.C.M., Vredenberg W.J. and Tonk W.J.M. (1979) *FEBS Lett.* 100, 325-330
- Schapendonk A.H.C.M. and Vredenberg W.J. (1979) *FEBS Lett.* 106, 257-261
- Schapendonk A.H.C.M., Hemrika-Wagner A.M., Theuvenet A.P.R., Wong Fong Sang H.W., Vredenberg W.J. and Kraayenhof R. (1980) *Biochemistry* 19, 1922-1927
- Schapendonk A.H.C.M. (1980) Dissertation, Agricultural University Wageningen, Wageningen, the Netherlands
- Schlodder E., Gräber P. and Witt H.T. (1982) in: *Electron Transport and Photophosphorylation* (Barber J. ed.), pp. 105-175, Elsevier, the Netherlands
- Schöder H.U. and Lockau W. (1986) *FEBS Lett.* 199, 23-27
- Schönfeld M. and Schickler H. (1984) *FEBS Lett.* 167, 231-234
- Schreiber U. and Rienits K.G. (1982) *Biochim. Biophys. Acta* 682, 115-123
- Schreiber U. and Del Valle-Tascon S. (1982) *FEBS Lett.* 150, 32-37
- Schreiber U. (1983) *Photosynth. Res.* 4, 361-373
- Schreiber U., Schliwa U. and Bilger W. (1986) *Photosynth. Res.* 10, 51-62
- Schultz S.G. (1980) in: *Basic Principles of Membrane Transport*, p. 29, Cambridge University Press, Cambridge
- Schuermans J.J., Peters A.L.J., Leeuwerik, F.J. and Kraayenhof R. (1981) in: *Vectorial Reactions in Electron and Ion Transport in Mitochondria and Bacteria* (Palmieri F. et al. eds.), pp. 359-370, Elsevier, Amsterdam, New York
- Selak M.A. and Whitmarsh J. (1982) *FEBS Lett.* 150, 286-292
- Setif P. and Mathis P. (1986) in: *Encyclopedia of Plant Physiology, Photosynthesis III* (Staehelin L.A. and Arntzen C.J. eds.) vol. 19, pp. 295-316, Springer Verlag, Berlin
- Shahak Y., Crowther D. and Hind G. (1980) *FEBS Lett.* 114, 73-78
- Shahak Y., Crowther D. and Hind G. (1981) *Biochim. Biophys. Acta* 636, 234-243
- Shahak Y. (1982) *Plant Physiol.* 70, 87-91
- Sigalot K., Haraux F., de Kouchkovsky F., Hung S.P.N. and de Kouchkovsky Y. (1985) *Biochim. Biophys. Acta* 809, 403-413
- Siggel U. (1976) *Bioelectrochem. Bioenerget.* 3, 302-318
- Siggel U. (1981a) *Bioelectrochem. Bioenerget.* 8, 327-337
- Siggel U. (1981b) *Bioelectrochem. Bioenerget.* 8, 339-346
- Siggel U. (1981c) *Bioelectrochem. Bioenerget.* 8, 347-354
- Siggel U. (1981d) in: *Photosynthesis* (Akoyunoglou G. ed.) Vol II, pp. 431-441, Balaban Int, Philadelphia
- Skulachev V.P. (1980) *Biochim. Biophys. Acta* 604, 297-320
- Slovacek R.E. and Hind G. (1977) *Plant Physiol.* 60, 538-542
- Slovacek R.E. and Hind G. (1978) *Biochem. Biophys. Res. Commun.* 84, 901-906
- Slovacek R.E., Crowther D. and Hind G. (1979) *Biochim. Biophys. Acta* 547, 137-148

- Snel J.F.H., van Kooten O. and Vredenberg W.J. (1987) in: Progress in Photosynthesis Research (Biggins J. ed.), Vol. II, pp. 617-620, M. Nijhoff Pub., Dordrecht
- Sowers A.E. and Hackenbrock C.R. (1981) Proc. Natl. Acad. Sci. U.S.A. 78, 6246-6250
- Strasser R.J. and Butler W.L. (1980) in: The Blue Light Syndrome (Senger H. ed.), pp. 205-211, Springer Verlag, Berlin
- Strotmann H. and Schumann J. (1983) Physiol. Plant. 57, 375-382
- Strotmann H. and Bickel-Sandkötter S. (1984) Ann. Rev. Plant Physiol. 35, 97-120
- Strotmann H., Niggemeyer S. and Mansy A.R. (1987) in: Progress in Photosynthesis Research (Biggins J. ed.), Vol. III, pp. 29-36, M. Nijhoff Pub., Dordrecht
- Sundby C. and Larsson C. (1985) Biochim. Biophys. Acta 813, 61-67
- Theg S.M. and Homann P.H. (1982) Biochim. Biophys. Acta 679, 221-234
- Theg S.M., Johnson J.D. and Homann P.H. (1982) FEBS Lett. 145, 25-29
- Theg S.M. and Junge W. (1983) Biochim. Biophys. Acta 723, 294-307
- Theg S.M. and Dilley R.A. (1987) in: Progress in Photosynthesis Research (Biggins J. ed.), Vol. III, pp.161-164, M. Nijhoff Pub., Dordrecht
- Trebst A. (1985) in: Coenzyme Q (Lenaz G. ed.) pp. 257-284, John Wiley & Sons Ltd.
- Trissl H.-W. and Kunze U. (1985) Biochim. Biophys. Acta 806, 136-144
- Tornber J.P. (1986) in: Encyclopedia of Plant Physiology, Photosynthesis III (Staehelin L.A. and Arntzen C.J. eds.), vol. 19, pp.98-142, Springer Verlag, Berlin
- Thorne S.W., Horváth G., Kahn A. and Boardman N.K. (1975) Proc. Natl. Acad. Sci. USA 72, 3858-3862
- Van Gorkom H.J. (1985) Photosynth. Res. 6, 97-112
- Van Gorkom H.J. (1986) in: Light Emission by Plants and Bacteria (Govindjee, Ames J. and Fork D.C. eds.) pp. 267-289, Academic Press, Orlando
- Van Kooten O., Gloudemans A.G.M. and Vredenberg W.J. (1983) Photobiochem. Photobiophys. 6, 9-14
- Van Kooten O., Leermakers F.A.M., Peters R.L.A. and Vredenberg W.J. (1984) in: Advances in Photosynthesis Research (Sybesma C. ed.) Vol.II, pp.265-268, M. Nijhoff Pub., The Hague
- Van Kooten O. (1984) Trends Biochem. Sci. 9(5), 221-222
- Van Kooten O., Snel J.F.H. and Vredenberg W.J. (1986) Photosynth. Res. 9, 211-227
- Van Kooten O., Snel J.F.H. and Vredenberg W.J. (1987) in: Progress in Photosynthesis Research (Biggins J. ed.), Vol. II, pp. 621-624, M. Nijhoff Pub., Dordrecht
- Velthuys B.R. (1978) Proc. Natl. Acad. Sci. USA 75, 6031-6034
- Velthuys B.R. (1980) Annu. Rev. Plant Physiol. 31, 545-567
- Vermaas W.J.F. and Govindjee (1981) Photochem. Photobiol. 34, 775-793
- Vredenberg W.J., Homann P.H. and Tonk W.J.M. (1973) Biochim. Biophys. Acta 314, 261-265
- Vredenberg W.J., and Tonk W.J.M. (1975) Biochim. Biophys. Acta 387, 580-587
- Vredenberg W.J. (1976) in: The Intact Chloroplast (Barber J. ed.), Vol.I, pp.53-88, Elsevier, North-Holland

- Vredenberg W.J. and Bulychev A.A. (1976) *Plant Sci. Lett.* 7, 101-107
- Vredenberg W.J. and Schapendonk A.H.C.M. (1978) *FEBS Lett.* 91, 90-93
- Vredenberg W.J. and Schapendonk A.H.C.M. (1981) in: *Photosynthesis* (Akoyunoglou G. ed.) Vol. 1, pp. 489-499, Balaban Int. Sci. Serv., Philadelphia
- Vredenberg W.J. (1981) *Physiol. Plant.* 53, 598-602
- Vredenberg W.J., van Kooten O. and Peters L.A.R. (1984) in: *Advances in Photosynthesis Research* (Sybesma C. ed.) Vol. II, pp. 241-246, Nijhoff & Junk Pub., The Hague
- Vredenberg W.J., Van Kooten O. and Snel J.F.H. (1987) in: *Progress in Photosynthesis Research* (Biggins J. ed.), Vol. II, pp. 613-616, M. Nijhoff Pub., Dordrecht
- Vredenberg W.J., Buurmeijer W.F. and Ooms J.J.J. (1987) *Abstracts Internat. Biophys. Congr. 1987*, Jerusalem, Israel, p. 150
- Walz D., Goldstein L. and Avron M. (1974) *Eur. J. Biochem.* 47, 403-407
- Weis E. (1985) *Biochim. Biophys. Acta* 807, 118-126
- Werdan K., Heldt H.W. and Milovancev M. (1975) *Biochim. Biophys. Acta* 396, 276-292
- Westerhoff (1983) Dissertation, University of Amsterdam, the Netherlands
- Westerhoff H.V., Helgerson S.L., Theg S.M., van Kooten O., Wikström M., Skulachev V.P. and Dancsházy Zs. (1983) *Acta Biochim. Biophys. Acad. Sci. Hung.* 18, 125-149
- Westerhoff H.V., Melandri B.A., Venturoli G., Azzone G.F. and Kell D.B. (1984) *Biochim. Biophys. Acta* 768, 257-292
- Westerhoff H.V. (1985) *Biomed. Biochim. Acta* 44, 929-941
- Westerhoff H.V. and Chen Y. (1985) *Proc. Natl. Acad. Sci. USA* 82, 3222-3226
- Whitmarsh J., Bowyer J.R. and Crofts A.R. (1982) *Biochim. Biophys. Acta* 682, 404-412
- Whitmarsh J. and Ort D.R. (1984) *Arch. Biochem. Biophys.* 231, 276-292
- Wikström M., Krab K. and Saraste M. (1981) *Ann. Rev. Biochem.* 50, 623-655
- Williams R.J.P. (1961) *J. Theor. Biol.* 1, 1-17
- Williams R.J.P. (1975) *FEBS Lett.* 53, 123-125
- Williams R.J.P. (1985) in: *The Enzymes of Biological Membranes* (Martonosi A.N., ed.), Vol. 4, pp. 71-110, Plenum Press, New York
- Witt H.T. (1971) *Quart. Rev. Biophys.* 4, 365-477
- Witt H.T. and Zickler A. (1973) *FEBS Lett.* 37, 307-310
- Witt H.T. (1979) *Biochim. Biophys. Acta* 505, 355-427
- Zickler A., Witt H.T. and Boheim G. (1976) *FEBS Lett.* 66, 142-148
- Zimanyi L. and Garab Gy. (1982) *J. Theor. Biol.* 95, 811-821

Curriculum Vitae

naam: Olaf van Kooten

geboorte datum: 24 maart 1952

geboorte plaats: Lagunillas (Venezuela)

nationaliteit: Nederlandsche

middelbare school: HBS-B Casimir Lyceum te Amstelveen 1971

kandidaats examen: natuurkunde en wiskunde met chemie, Vrije Universiteit
Amsterdam 1976

doctoraal examen: Hoofdvak: natuurkunde

hoofdrichting: experimentele natuurkunde

bijvakken: wiskunde en bioröntgenstructuuronderzoek
Vrije Universiteit Amsterdam 1980

betrekkingen:

maart '79 tot september '80: practicum assistent vakgroep biofysica der Vrije
Universiteit te Amsterdam.

november '80 tot november '84: promotie assistent laboratorium voor planten-
fysiologisch onderzoek (Stichting voor Biofysica,
Z.W.O.) te Wageningen.

januari '85 tot februari '86: assistent onderzoeker op een kort lopend projekt
van de Landbouwniversiteit te Wageningen

maart '86 tot juni '86: toegevoegd onderzoeker bij de Stichting voor Planten-
veredeling (SVP) te Wageningen.

juni '86 tot juni '88: toegevoegd onderzoeker voor het Additioneel Programma
Verzurings Onderzoek (RIVM) en gestationeerd op
het Laboratorium voor Plantenfysiologisch
Onderzoek, Landbouwniversiteit te Wageningen.

